IMPACT OF THE LIGANDS ON LINEAR TRIMETAL CHAINS

A Dissertation

by

PENG LEI

Submitted to the Office of Graduate Studies of
Texas A&M University
in partial fulfillment of the requirements for the degree of

DOCTOR OF PHILOSOPHY

May 2003

Major Subject: Chemistry

IMPACT OF THE LIGANDS ON LINEAR TRIMETAL CHAINS

A Dissertation

by

PENG LEI

Submitted to Texas A&M University
in partial fulfillment of the requirements
for the degree of

DOCTOR OF PHILOSOPHY

Approved as to style and content by:

F. A. Cotton (Chair of Committee)	F. P. Gabbaï (Member)
R. L. Watson (Member)	W. H. Bassichis (Member)
E. A. Schweikert (Head of Department)	

May 2003

Major Subject: Chemistry

ABSTRACT

Impact of the Ligands on Linear Trimetal Chains. (May 2003)

Peng Lei, B.S., Central South University of Technology;

M.S., Wuhan University

Chair of Advisory Committee: Dr. F. Albert Cotton

Increasing attention has been given to the preparation and study of compounds with linear chains of metal atoms surrounded by four ligands. The majority of linear trimetal complexes are supported by dpa, the anion of dipyridylamine, having the general formula $M_3(dpa)_4X_2$, where X is typically a monoanion. It has been shown that the behavior of the trinuclear system is far more complicated than might have been expected. Specifically, both symmetrical and unsymmetrical chains can occur and the interpretation of the magnetic properties of certain compounds has been a challenging task.

Present in this dissertation is the bulk of work completed on an exploration of syntheses and characterizations of linear trichromium and trinickel compounds with different types of tridentate ligands. These ligands include 2,6-bis(phenylamino)pyridine, H_2BPAP, (the corresponding dianion of this is denoted by BPAP) and a set of five unsymmetrical formamidines with different organic substituents ranging from strong electron-donating groups, such as $–OCH_3$, to electron-withdrawing groups, e.g., F.

Ligands impact on the trimetal chain in various ways. In the case of the $M_3(BPAP)_4^{2-}$ ions, there are no axial interactions because these anionic species do not attract electron donating ligands. Thus they have properties which are different from those of $M_3(dpa)_4X_2$ molecules. Most notably, the $Ni_3(BPAP)_4^{2-}$ ion is diamagnetic and all three nickel ions can be described as square-planar, low-spin Ni^{II} centers.

When unsymmetrical formamidines are used to support linear trichromium chains with a Cl anion at each end, the separation between terminal chromium atoms is significantly longer (*ca*. 0.15 - 0.25 Å) than those in trichromium compounds reported earlier. Moreover, the unsymmetrical formamidinates tend to support symmetrical trichromium chains, while the rest of the known tridentate ligands typically yield unsymmetrical Cr_3^{6+} chains.

The synthesis and structural studies of trinickel compounds with unsymmetrical formamidines are also presented.

DEDICATION

To my wife, Liu, for her love and patience.

To my parents and brother, for their care and support.

ACKNOWLEDGMENTS

First I must acknowledge the love, support and patience of my wife Liu. She left her friends and colleagues and accompanied me to a new and challenging environment. Her love and commitment to my work are always the driving force to my success.

My parents have constantly encouraged me to love science, to work hard, and to serve people. My brother, Kai, is always a fountain of support and encouragement. Their love and support are essential to the completion of this degree.

I will always appreciate Dr. Cotton for giving me the chance to work in his lab. I am very grateful for his patience and encouragement. I have learned a lot in College Station.

Of course Carlos Murillo is invaluable to my graduate study. He has offered me some know-how advice from which I will benefit. His friendship enriched my life here. Lee Daniels shared his expertise of crystallography with me, and was always helpful. Xiaoping Wang has been of great help, getting me started in the lab, guiding me while solving my first few structures, and contributing much to my understanding of crystallography. Hongcai Zhou, Daren Timmons, Chun Lin shared their experimental skills with me. John Berry helped me with magnetic measurements for compounds in Chapter IV. I am thankful to all the members in Cotton's group, in particular Jim Donahue, Liz Hillard, Chad Wilkinson. Beverly Moore has shown me much about how to use computer software.

TABLE OF CONTENTS

CHAPTER Page

LIST OF FIGURES

LIST OF TABLES

CHAPTER I

INTRODUCTION

Metal-metal interactions in dinuclear paddlewheel compounds have been intensively investigated and are well understood.[1] Recently, increasing attention has been given to the chemistry of the metal complexes with larger numbers of metal atoms in linear arrays.[2] Thus, a large number of complexes with linear trimetal unit have been synthesized.[2-7] The majority of these complexes characterized to date are supported by the anion of dipyridylamine (dpa) and have the formula $M_3(dpa)_4X_2$ (M = Cr[3], Co,[4] Ni,[5] Cu,[6] Rh,[7] Ru,[7]) where X is usually an anion, such as Cl^-,[2b] Br^-,[2d] CN^-,[8] SCN^-,[8] $N(CN)_2^-$,[8] BF_4^-,[4b] occupying the axial positions. The typical structure of a $M_3(dpa)_4X_2$ molecule is shown in Figure 1.

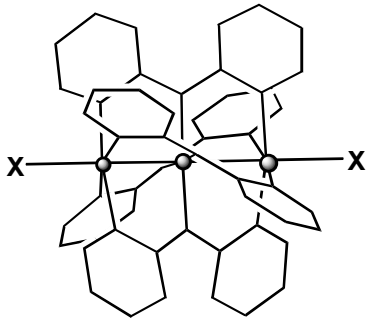

Figure 1. A schematic drawing of the typical structure motif of $M_3(dpa)_4Cl_2$.

This dissertation follows the style and format of *Inorganic Chemistry*.

These species exhibit extraordinary variation in their internal structure, as a consequence of changes in the crystal environment of the molecule in some cases, but also as a result of changes in the axial ligands, X. The M–M separations in both $Cr_3(dpa)_4Cl_2$[3b] and $Co_3(dpa)_4Cl_2$[9] may be symmetrical (*s*) or unsymmetrical (*u*). The bonding in *s*-$M_3(dpa)_4Cl_2$ compounds can be described in terms of the molecular orbitals formed by metal atom *3d* orbitals and spread over the three metal atoms. For M = Co or Cr, there are three or six bonding electrons respectively, for the M_3 unit. For the *u*-$Co_3(dpa)_4Cl_2$ molecule there is one singly bonded Co_2^{4+} unit and an isolated low-spin Co^{2+} ion, while for the *u*-$Cr_3(dpa)_4Cl_2$ molecule, there is a quadruply-bonded Cr_2^{4+} unit and an isolated high-spin Cr^{2+} ion.

In all known $M_3(dpa)_4X_2$ compounds (M = Cr, Co, Ni, Cu, Ru and Rh), the dpa anion is not planar because of the repulsion of two hydrogen atoms on different, but adjacent pyridine rings shown in Figure 2a. This leads to a considerable torsion angle (40 - 50°) and a helical arrangement of the four dpa ligands around the trimetal unit as shown in Figure 1. The configuration can be of either right- or left-handed helicity; chiral crystals containing only one of the two configurations have been isolated.[10] In order to avoid the H···H repulsion and thus obtain a flat ligand that will not demand a helical conformation in the product, there are basically three ways to proceed. First would be using a tridentate ligand having free rotation of two terminal aromatic rings, namely 2,6-bis(phenylamino)pyridine, H_2BPAP, shown in Figure 2b. The second way would be the choice of tridentate unsymmetrical formamidinate ligands as Figure 2c. Such unsymmetrical formamidinates have enough space between two adjacent hydrogen atoms on the different aromatic rings so that a flat conformation is again possible. The third way would be to use a tridentate ligand with a bridged atom, such as O, connecting two terminal aromatic ring as shown in Figure 2d. Thus there is no hydrogen atoms bumping into each other. However, the very low solubility of this ligand

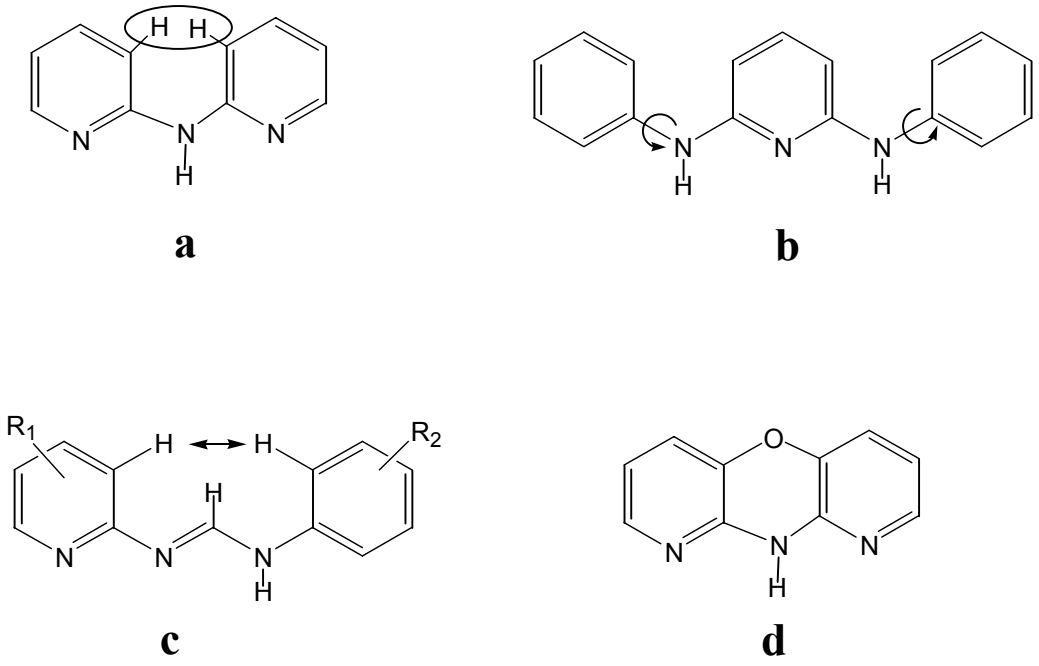

Figure 2. Typical tridentate ligands for a linear trimetal unit.

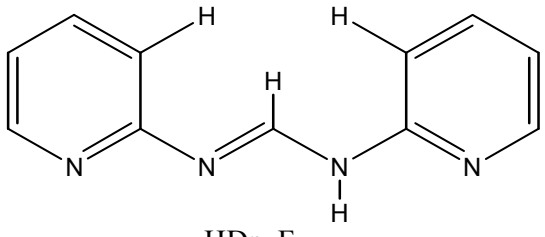

HDpyF

Figure 3. A schematic presentation of dipyridylformamidine.

makes the synthesis of a trimetal analog compound practically impossible in addition to the fact that the preparation of this ligand involves time-comsuming procedures and low yield.[11]

It should also be noted, however, that in the complex $[Cr_3(DPyF)_4](PF_6)_2$,[2a] where DPyF is the anion of dipyridylformamidine (Figure 3), the ligands are three-coordinate and perfectly planar so that there is no torsion angle. Potentially, with four of these ligands a fourth chromium ion could be bound and, in fact, the compound $[Cr_4(DPyF)_4Cl_2](PF_6)_2$ was also obtained, in which the ligands are again planar and there is no torsion.

Therefore, unsymmetrical formamidines are attractive choices to examine the question of torsion and other structural features, while also limiting the chain to a maximum of three metal atoms. The choice of unsymmetrical formamidines offers an additional advantage to study the ligand's impact on the trimetal chain as different organic groups are introduced into the supporting ligand. Thus, five unsymmetrical formamidines of the type ArNC(H)NPy, shown in Figure 4, with substituents ranging from strong electron-donating groups, such as –OCH3, to electron-withdrawing groups, e.g., –F are proposed.

A very detailed study of $Ni_3(dpa)_4Cl_2$[5b] from this laboratory led to the conclusion that there is no metal-metal bonding even though the nickel-nickel separations are relatively short (*ca*. 2.43 Å). Instead, there is antiferromagnetic coupling between the terminal five-coordinated nickel atoms, each of which has two unpaired electrons. The central nickel atom is d^8, square-planar and diamagnetic. S.-M. Peng and coworkers[12] have done extensive work on the preparation of multinuclear nickel compounds with five, seven, nine nickel atoms in a linear array using oligo-pyridyl amino ligands. Their results indicate that antiferromagnetic interactions are similar to those in the trinickel unit and they decrease as might be expected with increasing chain length.

More recently, the one-electron oxidation of $Ni_3(dpa)_4Cl_2$ was reported.[13] The Ni—Ni

distances in the oxidized compound $Ni_3(dpa)_4(PF_6)_3$ (~2.28 Å) are much shorter than those in the unoxidized species (~2.43 Å), and are consistent with three-center metal-metal bonding and a formal bond order of 0.5. This exiting result naturally leads to an exploration of the trinickel compounds with unsymmetrical formamidinates

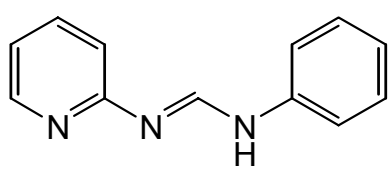

HPhPyF

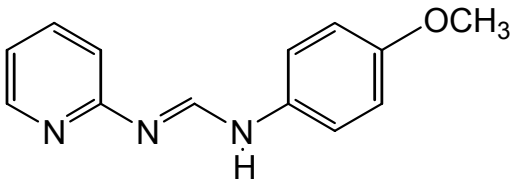

HAniPyF

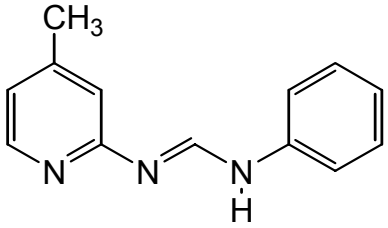

HPcPyF

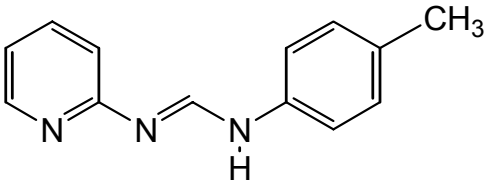

HTolPyF

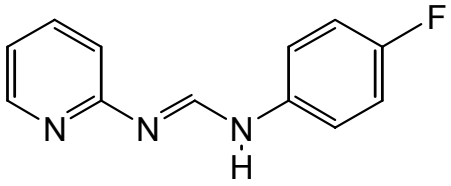

HPh^{F}PyF

Figure 4. Five types of unsymmetrical formamidines with different organic substituents.

CHAPTER II

COMPLEXES WITH THE MONO- AND DIANION OF 2,6–BIS(PHENYLAMINO)PYRIDINE*

In order to avoid the H···H repulsion in $M_3(dpa)_4X_2$ as mentioned in Chapter I and thus obtain a flat ligand that will not demand a helical conformation in the product, a tridentate ligand having free rotation of two terminal aromatic rings was considered desirable. We have prepared one such ligand, namely 2,6-bis(phenylamino)pyridine, H_2BPAP. Moreover, since a recent study in our group had shown that electron-donating atoms in appended groups near the axial positions of a dichromium core can greatly affect the Cr—Cr distance,[14] we felt that preparing dinuclear complexes with this tridentate ligand could also be of interest. Finally, since the BPAP ligand is a dianion, the resulting trimetal complexes, $M_3(BPAP)_4^{2-}$, must be anionic when M is a divalent ion and would not therefore be expected for have axial anionic ligands. We hoped, therefore, to see if the absence of axial ligands would have a significant effect on the electronic structure of the trimetal chain.

Reported here are the preparation and structural characterization of four species, two dinuclear and two trinuclear. They are $Cr_2(HBPAP)_4$ (**1**), $Mo_2(HBPAP)_4$ (**2**), $(Bu^n{}_4N)_2Cr_3(BPAP)_4$ (**3**) and $(Bu^n{}_4N)_2Ni_3(BPAP)_4$ (**4**).

---

* Reproduced in part with permission from "Di- and Trinuclear Complexes with the Mono- and Dianion of 2,6–bis(phenylamino)pyridine: High Field Displacement of Chemical Shifts Due to the Magnetic Anisotropy of Quadruple Bonds " Cotton, F. A.; Daniels, L. M.; Lei, P.; Murillo, C. A.; Wang, X. *Inorg. Chem*, **2002**, *40*, 2778. Copyright 2002, American Chemical Society.

EXPERIMENTAL

All manipulations were carried out under nitrogen using standard Schlenk techniques. Solvents were dried by conventional methods, and were freshly distilled under nitrogen before use. Anhydrous $CrCl_2$ and $NiCl_2$, as well as 2,6-dibromopyridine, were purchased from Strem Chemicals and stored in a N_2 dry-box; MeLi, Bu^n_4NBr and aniline hydrochloride were purchased from Aldrich and used as received; $Mo_2(O_2CCF_3)_4$ was prepared as reported earlier.[15] The ^1H NMR spectra were recorded on a Varian XL-300 instrument at 300 MHz. Cyclic voltammetry was performed in dichloromethane for compound **1** and in THF for compound **3** with a BAS model 100 scanning potentiostat using Pt working and auxiliary electrodes and 0.1 M TBAH ($Bu^n_4NPF_6$) as the supporting electrolyte. Potentials are referenced to the ferrocene/ferrocenium (Fc/Fc^+) couple, which occurs at $E_{1/2}$ = +0.44 V versus Ag/AgCl. The values of $E_{1/2}$ were taken as $(E_{pa} + E_{pc})/2$, where E_{pa} and E_{pc} are the anodic and cathodic peak potentials, respectively, for the quasi-reversible peaks. Elemental analyses were performed by Canadian Microanalytical Service Ltd.

Preparation of 2,6-bis(phenylamino)pyridine. This was prepared according to the literature[16] with some modifications: 2,6-dibromopyridine (12.5 g, 50.0 mmol) and aniline hydrochloride (23.5 g, 250 mmol) were added to a 500 mL three-neck flask fitted with a stirring bar and a condenser. The mixture was heated to 200 °C. As the mixture melted, it turned dark orange. After 4 h of stirring under N_2, 100 mL of aqueous 10% sodium carbonate solution was added to the mixture to neutralize the acid. Chloroform (2×150 mL) was added to extract the product from the aqueous solution. The volume was reduced to *ca.* 40 mL under reduced pressure, then 100 mL of ethanol was added. Further addition of a large amount of water into the $EtOH/CHCl_3$ solution precipitated a yellow product, which was recrystallized twice from water-ethanol, and then from an

ethyl acetate–hexanes mixture. Yield: 16.5 g (65%, based on 2,6–dibromopyridine). Anal. Calcd for $C_{17}N_3H_{15}$: C, 78.16; H, 5.75; N, 16.09. Found: C, 78.11; H, 5.70; N, 16.02 . ^{1}H NMR (300 MHz, CD_2Cl_2, δ): 8.04 (broad, 2H), 7.63 (d, 4H), 7.45 (t,1H), 7.20 (t, 4H), 6.88 (t,2H) 6.28(d,2H).

Preparation of Li(HBPAP). Methyllithium (1.05 mmol) was added to a 15 mL THF solution containing H_2BPAP (0.267 g, 1.00 mmol) at –78 °C. After allowing the THF solution to warm up slowly to room temperature, the volume was reduced to *ca.* 7 mL and some yellow precipitate formed. Addition of 35 mL of hexanes increased the amount of solid. This was collected by filtration and washed with 10 mL of hexanes, and then dried under vacuum. Yield: 0.256 g (95%). ^{1}H NMR (300 MHz, CD_2Cl_2, δ): 7.38 (d, 4H), 7.29 (m, 5H), 7.02 (t, 2H), 6.44 (broad, 1H) and 6.31(d, 2H).

Preparation of 1·toluene and 1·C_6H_{14}. The compound H_2DPAP (0.522 g, 2.00 mmol) was dissolved in 15 mL THF and then deprotonated by adding MeLi (2.1 mmol) at –78 °C. The THF solution was allowed to return slowly to room temperature, and transferred into a flask containing $CrCl_2$ (0.135 g, 1.10 mmol). After stirring the mixture at room temperature overnight, a red orange solid formed, and was separated by filtration. This solid was found to be slightly soluble in toluene and dichloromethane. The solid was added 20 mL of toluene. The mixture was filtered, the layer of hexanes was added to the toluene solution. After 2 weeks, crystals of **1**·toluene suitable for X-ray studies formed. The filtrate from the original mixture was dried under vacuum. The solid was washed with ether 2×20 mL; It was dissolved in THF, and the solution was layered with hexanes. Red crystals **1**·C_6H_{14} suitable for X-ray study were obtained after nine days. The overall yield was 0.430 g (87%). ^{1}H NMR (300 MHz, CD_2Cl_2, δ): 7.23 (m, 12H), 7.02 (m, 12H), 6.75 (m, 12H), 5.95 (d, 4H), 6.78 (t,12H), 3.4 (d, 4H). Anal. Calcd for $C_{68}H_{56}N_{12}Cr_2$: C, 71.32; H, 4.92; N, 14.68. Found: C, 69.75; H, 5.41; N, 13.84. CV: one quasireversible wave at 0.32 V in the scan range of 0.00 V

to +0.06 V and two irreversible waves at 0.38 V and 0.86 V in the scan range 0.00 V to +1.00 V.

Preparation of 2·toluene. The ligand precursor H_2BPAP (0.522 g, 2.00 mmol) was dissolved in 15 mL THF, and deprotonated with one equivalent of MeLi at -78 °C. After the temperature of the solution had slowly risen to room temperature, it was added to a flask containing $Mo_2(O_2CCF_3)_4$(0.32 g, 0.50 mmol). The reaction mixture was stirred overnight, and the solvent was then removed under vacuum. The remaining solid was washed with 2×20 mL hexanes, then dissolved in toluene, and layered with hexanes. Red crystals suitable for X-ray study were obtained after two weeks. Yield: 0.320 *g* (78%). ^{1}H NMR (300 MHz, CD_2Cl_2, δ): 7.43 (d, 16H), 7,40(t, 4H), 7.35 (t, 16H), 7.05 (t, 8H), 6,34 (d, 8H), 3.04 (broad, 4H). Anal. Calcd for $C_{68}H_{56}N_{12}Mo_2$: C, 66.23; H, 4.58; N, 13.63. Found: C, 66.18; H, 4.33; N, 13.32. CV: one quasireversible wave at 0.56 V in the scan range of 0.00 V to +1.00 V.

Preparation of 3·2THF. The compound H_2BPAP (0.267 g, 1.00 mmol) was dissolved in THF (15 mL), and deprotonated at -78 °C by adding two equivalents of MeLi (1.5 mL of 1.4 M MeLi in ether.) After the THF solution had slowly warmed to room temperature, it was transferred to a flask containing a mixture of $CrCl_2$ (0.10 g, 0.85 mmol) and tetrabutylammonium bromide (0.16 g, 0.50 mmol). The reaction mixture was stirred for 2 h at room temperature, and then refluxed overnight. After cooling, the solvent was removed under vacuum and the remaining solid was washed with 2×20 mL ether and 20 mL of a 10:1 ether-THF solution. The remaining solid was redissolved in THF, and layered with hexanes. Dark red crystals formed after six days. Yield: 0.144 g (25%) Anal. Calcd for $C_{100}H_{126}N_{14}Cr_3$: C, 71.40; H, 7.67; N, 11.66. Found: C, 71.81; H, 7.62; N, 11.46. CV: one quasireversible wave at 0.03 V with scanning between -0.50 V and 0.40 V, which is likely to correspond to oxidation of the separated Cr^{II} atom (see structure) to Cr^{III}. In the extended scan range -0.5 V to 1.4 V, three irreversible peaks were seen at +0.03 V, 0.69 V, and 1.08 V.

Preparation of 4·2THF. The compound H_2BPAP (0.267 g, 1.00 mmol) was dissolved in 15 mL THF, and deprotonated at -78 °C with two equivalents of MeLi (1.5 mL of 1.4 M MeLi in ether.) After the THF solution had slowly warmed to room temperature, it was transferred into a flask which contained $NiCl_2$ (0.11 g, 0.85 mmol) and tetrabutylammonium bromide (0.16 g, 0.50 mmol). The reaction mixture was stirred for 2 h at room temperature, and then refluxed overnight. After cooling, the solvent was removed under vacuum. The dark red solid was washed with 2×20 mL ether and 20 mL of a 10:1 ether-THF solution and then dissolved in THF and layered with hexanes. Dark-red crystals were obtained after five days. Yield: 0.268 g (56%). ^{1}H NMR (300 MHz, CD_3CN, δ): 8.54 (d, 16H), 8.39 (t, 4H), 8.26 (t, 16), 7.96 (t, 8H), 7.24 (d, 8H), 2.92 (t, 16H), 2.55(q, 16H), 2.36 (m, 16H), 2.01 (t, 24H). Anal. Calcd for $C_{100}H_{128}N_{14}Ni_3$: C, 70.56; H, 7.58; N, 11.52. Found: C, 70.20; H, 7.68; N,11.86. CV: no reversible or quasireversible waves between +0.1 V and +1.2 V.

CRYSTALLOGRAPHIC STUDIES

Crystals of **1**·toluene, **1**·C_6H_{14} and **2**·toluene were used for data collection at 213 K on a Nonius FAST area detector system, utilizing the software MADNES.[17] Each crystal was mounted on a quartz fiber with a small amount of silicone grease and transferred to a goniometer head. Cell parameters for FAST data were obtained from an auto-indexing routine and were refined using 250 strong reflections. Cell dimensions and Laue symmetry were confirmed by axial photography. All data were corrected for Lorentz and polarization effects.

Data for **3**·2THF and **4**·2THF were collected on a Bruker SMART 1000 CCD area detector system. Cell parameters were obtained using SMART[18] software. Data were corrected for Lorentz

and polarization effects using the program SAINTPLUS.[19] Absorption corrections were applied using SADABS.[20]

The positions of the heavy atoms were found by the direct methods program in SHELXS-97.[21] Subsequent cycles of least-squares refinement followed by difference Fourier syntheses revealed the positions of the non-hydrogen atoms. All aromatic hydrogen atoms were added in idealized positions. The hydrogen atoms attached to N were refined for $Cr_2(HBPAP)_4$ and $Mo_2(HBPAP)_4$.

Crystallographic data for **1**·toluene, **1**·C_6H_{14}, **2**·toluene, **3**·2THF, and **4**·2THF are given in Tables I, II, III, IV, V repectively; selected bond distances and angles for **1**·toluene, **2**·toluene, **3**·2THF, and **4**·2THF are listed in Tables VI, VII, VIII and IX, receptively.

RESULTS AND DISCUSSION

Synthetic considerations. The ligand precursor, H_2BPAP, can be made easily according to the equation shown in Figure 5.[16]

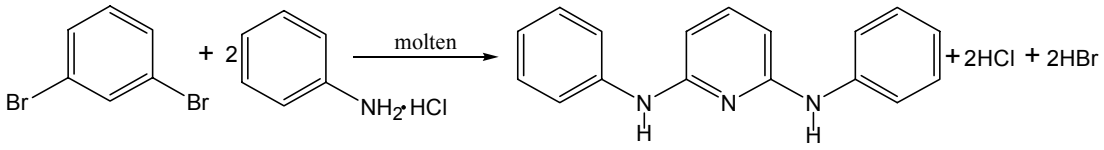

Figure 5. A strategy to prepare 2,6-bis(phenylamino)piridine.

Aniline hydrochloride must be present in great excess in order to obtain a satisfactory yield because it readily sublimes during the reaction. The analytically pure compound can be obtained by recrystallization of the crude product from an ethanol-water mixture. An additional recrystallization from a mixture of ethyl acetate and hexanes is necessary to obtain anhydrous crystals. Elemental analysis and ^{1}H NMR indicated that the purity was satisfactory. The ligand is fairly soluble in organic solvents, such as ether and hexanes.

The compound H_2BPAP has two N—H groups, each of which can be sequentially deprotonated by methyllithium to give the corresponding mono- and dianion. The second K_a is very small and weaker deprotonating agents such as K^+OBu^- will not eliminate the second proton. For example, when two equivalents of K^+OBu^- were added to one equivalent of H_2BPAP along with $CrCl_2$ and TBA^+ in THF, under reflux condition, the red orange dinuclear compound **1** was the only isolated product. The formation of the trinuclear chromium compound **3** required the use of MeLi; **3** is extremely sensitive to moisture and it is slowly decomposed by CH_2Cl_2. Single crystals containing the trinuclear anion were obtained only after addition of the large tetrabutylammonium counterion.

Table I. Crystal Data and Structure Refinement for **1**·toluene

Empirical formula	$C_{75}H_{64}Cr_2N_{12}$	
Formula weight	1237.38	
Temperature	213(2) K	
Wavelength	0.71073 Å	
Crystal system	Monoclinic	
Space group	$P2_1/n$	
Unit cell dimensions	a = 10.460(1) Å	α= 90˚
	b = 32.32(3) Å	β= 105.94(2)˚
	c = 18.798(1) Å	γ = 90˚
Volume	6110.8(7) Å^3	
Z	4	
Density (calculated)	1.345 g/mm^3	
Absorption coefficient	0.412 mm^{-1}	
Crystal size	0.48 x 0.27 x 0.18 mm	
Instrument for data collection for	Nonius-FAST data detector	
Theta range for data collection	2.10 to 24.41˚	
Reflections collected	24885	
Independent reflections	7919 [R(int) = 0.0460]	
Scan Method	ω-scan	
Refinement method	Full-matrix least-squares on F^2	
Data / restraints / parameters	7891 / 3 / 788	
Goodness-of-fit on F^2	1.145	
Final R^{22} indices [$I > 2\sigma(I)$]	$R1$ = 0.0608, $wR2$ = 0.1357	
R indices (all data)	$R1$ = 0.0784, $wR2$ = 0.1550	
Largest Shift / esd, final cycle	-0.005	
Largest diff. peak and hole	0.585 and -0.570 e/Å^3	

Table II. Crystal Data and Structure Refinement for **1**·C_6H_{14}

Empirical formula	C74 H70 Cr2 N12	
Formula weight	1231.42	
Temperature	213(2) K	
Wavelength	0.71073 Å	
Crystal system	Monoclinic	
Space group	*C2/c*	
Unit cell dimensions	a = 14.521(5) Å	α = 90˚
	b = 25.003(5) Å	β = 108.03(3)˚
	c = 17.664(4) Å	γ = 90˚
Volume	6098(3) Å^3	
Z	4	
Density (calculated)	1.341 g/mm^3	
Absorption coefficient	0.413 mm^{-1}	
Crystal size	0.33 x 0.22 x 0.16 mm	
Instrument for data Collection	Nonius-FAST data detector	
Theta range for data collection	2.33 to 25.16˚	
Reflections collected	16600	
Independent reflections	5337 [*R*(int) = 0.1118]	
Scan Method	ω-scan	
Refinement method	Full-matrix least-squares on F^2	
Data / restraints / parameters	5319 / 1 / 415	
Goodness-of-fit on F^2	1.122	
Final *R* indices [$I>2\sigma(I)$]	*R*1 = 0.0802, *wR*2 = 0.2033	
R indices (all data)	*R*1 = 0.1099, *wR*2 = 0.2425	
Largest Shift / esd, final cycle	-0.032	
Largest diff. peak and hole	0.585 and -0.535 e/Å^3	

Table III. Crystal Data and Structure Refinement for **2**·toluene

Empirical formula	$C_{75}H_{64}Mo_2N_{12}$	
Formula weight	1325.26	
Temperature	213(2) K	
Wavelength	0.71073 Å	
Crystal system	Monoclinic	
Space group	$P2_1/n$	
Unit cell dimensions	a = 10.601(2) Å	α = 90˚
	b = 32.432(2) Å	β =.106.149(9)˚
	c = 18.809(4) Å	γ = 90˚
Volume	6211.6(18) Å^3	
Z	4	
Density (calculated)	1.417 g/mm^3	
Absorption coefficient	0.460 mm^{-1}	
Crystal size	0.4 x 0.32 x 0.28 mm	
Instrument for data Collection	Nonius-FAST data detector	
Theta range for data collection	2.10 to 24.41˚	
Reflections collected	24817	
Independent reflections	8377 [R(int) = 0.0525]	
Scan Method	ω-scan	
Refinement method	Full-matrix least-squares on F^2	
Data / restraints / parameters	8348 / 3 / 796	
Goodness-of-fit on F^2	1.135	
Final R indices [$I > 2\sigma(I)$]	$R1$ = 0.0485, $wR2$ = 0.1202	
R indices (all data)	$R1$ = 0.0605, $wR2$ = 0.1384	
Largest Shift / esd, final cycle	-0.056	
Largest diff. peak and hole	1.363 and -0.471 e/Å^3	

Table IV. Crystal Data and Structure Refinement for **3**·2THF

Empirical formula	$C_{108}H_{140}Cr_3N_{14}O_2$
Formula weight	1822.34
Temperature	213(2) K
Wavelength	0.71073 Å
Crystal system	Monoclinic
Space group	*C2/c*
Unit cell dimensions	a = 31.483(6) Å α = 90˚
	b = 14.080(2) Å β = 123.385(3)˚
	c = 26.842(4) Å γ = 90˚
Volume	9934.7(30) $Å^3$
Z	4
Density (calculated)	1.218 g/m^3
Absorption coefficient	0.379 mm^{-1}
Crystal size	0.33 x 0.20 x 0.19 mm
Instrument for data Collection	Bruker SMART 1000
Theta range for data collection	1.82 to 25.51˚
Reflections collected	27427
Independent reflections	9220 [*R*(int) = 0.0300]
Scan Method	ω-scan
Refinement method	Full-matrix least-squares on F^2
Data / restraints / parameters	9213 / 0 / 577
Goodness-of-fit on F^2	1.169
Final *R* indices [$I>2\sigma(I)$]	*R*1 = 0.0764, *wR*2 = 0.1873
R indices (all data)	*R*1 = 0.1090, *wR*2 = 0.2162
Largest Shift / esd, final cycle	-0.002
Largest diff. peak and hole	0.892 and -0.878 e/$Å^3$

Table V. Crystal Data and Structure Refinement for **4**·2THF

Empirical formula	$C_{108}H_{140}N_{14}Ni_3O_2$	
Formula weight	1842.47	
Temperature	213(2) K	
Wavelength	0.71073 Å	
Crystal system	Monoclinic	
Space group	*C2/c*	
Unit cell dimensions	a = 31.729(2) Å	α = 90˚
	b = 13.7505(8) Å	β = 125.104(1)˚
	c = 27.167(2) Å	γ = 90˚
Volume	9696(1) $Å^3$	
Z	4	
Density (calculated)	1.262 g/mm^3	
Absorption coefficient	0.634 mm^{-1}	
Crystal size	0.41 x 0.31 x 0.14 mm	
Instrument for data Collection	Bruker SMART 1000	
Theta range for data collection	1.68 to 27.53˚	
Reflections collected	28971	
Independent reflections	11020 [*R*(int) = 0.0721]	
Scan Method	ω-scan	
Refinement method	Full-matrix least-squares on F^2	
Data / restraints / parameters	10994 / 0 / 575	
Goodness-of-fit on F^2	1.334	
Final *R* indices [$I > 2\sigma(I)$]	*R*1 = 0.1120, *wR*2 = 0.2393	
R indices (all data)	*R*1 = 0.1741, *wR*2 = 0.2788	
Largest Shift / esd, final cycle	-0.002	
Largest diff. peak and hole	1.359 and -1.040 e/$Å^3$	

Table VI. Selected Bond Lengths (Å) and Angles (˚) for **1**·toluene[a]

Cr(1)—Cr(2)	1.873(2)	Cr(1)···N(7)	3.148(5)
Cr(1)—N(11)	2.043(4)	Cr(1)—N(6)	2.063(3)
Cr(1)—N(9)	2.065(4)	Cr(2)—N(5)	2.039(3)
Cr(2)—N(8)	2.045(4)	Cr(2)—N(10)	2.071(4)
Cr(2)—N(1)	2.088(4)	Cr(1)—N(2)	2.027(4)
Cr(1)···N(12)	3.136(4)	Cr(1)···N(3)	3.066(5)
Cr(2)···N(4)	3.110(4)		
Cr(2)—Cr(1)—N(2)	99.2(1)	Cr(2)—Cr(1)—N(11)	99.3(1)
N(2)—Cr(1)—N(11)	161.4(1)	Cr(2)—Cr(1)—N(6)	92.8(1)
N(2)—Cr(1)—N(6)	90.4(1)	N(11)—Cr(1)—N(6)	89.1(1)
Cr(2)—Cr(1)—N(9)	92.8(1)	N(2)—Cr(1)—N(9)	87.1(1)
N(11)—Cr(1)—N(9)	91.6(1)	N(6)—Cr(1)—N(9)	174.2(1)
Cr(1)—Cr(2)—N(5)	98.7(1)	Cr(1)—Cr(2)—N(8)	98.6(1)
N(5)—Cr(2)—N(8)	162.8(1)	Cr(1)—Cr(2)—N(10)	92.2(1)
N(5)—Cr(2)—N(10)	89.1(1)	N(8)—Cr(2)—N(10)	89.8(1)
Cr(1)—Cr(2)—N(1)	92.1(1)	N(5)—Cr(2)—N(1)	89.1(1)
N(8)—Cr(2)—N(1)	90.7(1)	N(10)—Cr(2)—N(1)	175.6(1)
C(7)—N(1)—Cr(2)	118.9(3)	C(1)—N(1)—Cr(2)	124.1(3)

[a] The Cr—Cr distances are 1.875(2) in **1**·C_6H_{14}. All other interatomic distances are also similar to those for **1**·tolene.

Table VII. Selected Bond Lengths (Å) and Angles (˚) for **2**·toluene

Mo(1)—Mo(2)	2.0813(5)	Mo(2)—N(10)	2.153(4)
Mo(1)—N(5)	2.137(4)	Mo(2)—N(8)	2.137(4)
Mo(1)—N(11)	2.148(4)	Mo(2)—N(2)	2.143(4)
Mo(1)—N(1)	2.174(4)	Mo(2)—N(4)	2.144(4)
Mo(1)—N(7)	2.178(4)		
Mo(2)—Mo(1)—N(5)	94.1(1)	N(5)—Mo(1)—H(7N)	55.1(1)
Mo(2)—Mo(1)—N(11)	94.01(9)	N(11)—Mo(1)—H(7N)	117.4(1)
N(5)—Mo(1)—N(11)	171.9(2)	N(1)—Mo(1)—H(7N)	105.6(1)
Mo(2)—Mo(1)—N(1)	90.8(1)	N(7)—Mo(1)—H(7N)	72.0(1)
N(5)—Mo(1)—N(1)	89.7(2)	Mo(2)—Mo(1)—H(9N)	145.1(1)
N(11)—Mo(1)—N(1)	89.8(2)	N(5)—Mo(1)—H(9N)	115.4(1)
Mo(2)—Mo(1)—N(7)	91.3(1)	N(11)—Mo(1)—H(9N)	56.8(1)
N(5)—Mo(1)—N(7)	88.9(2)	N(1)—Mo(1)—H(9N)	72.2(1)
N(11)—Mo(1)—N(7)	91.2(2)	N(7)—Mo(1)—H(9N)	106.6(1)
N(1)—Mo(1)—N(7)	177.5(1)	Mo(1)—Mo(2)—N(8)	94.5(1)

Table VIII. Selected Bond Lengths (Å) and Angles (°) for **3**·2THF [a, b]

Cr(1)—Cr(2)	1.904(3)	Cr(2')···Cr(1)	2.589(2)
Cr(1)—N(1A)	2.050(4)	Cr(2')—N(2A)	2.031(6)
Cr(1)—N(4)	2.059(4)	Cr(2')—N(7)	2.044(4)
Cr(1)—N(6)	2.062(4)	Cr(2')—N(3)	2.071(6)
Cr(1)—N(1)	2.082(4)	Cr(2')—N(5)	2.076(4)
Cr(2)—N(3A)	2.029(6)	Cr(2)—N(2)	2.071(6)
Cr(2)—N(5A)	2.036(4)	Cr(2)—N(7A)	2.079(4)
Cr(2)—Cr(1)—N(1A)	94.0(2)	N(6)—Cr(1)—N(1)	88.8(1)
N(1A)—Cr(1)—N(4)	90.7(1)	Cr(1)—Cr(2)—N(5A)	95.9(1)
Cr(2)—Cr(1)—N(6)	94.00(8)	N(3A)—Cr(2)—N(5A)	90.9(2)
N(1A)—Cr(1)—N(6)	89.7(1)	Cr(1)—Cr(2)—N(2)	95.8(2)
N(4)—Cr(1)—N(6)	172.7(1)	N(3A)—Cr(2)—N(2)	168.4(2)
Cr(2)—Cr(1)—N(1)	93.4(2)	N(5A)—Cr(2)—N(2)	89.7(2)
N(1A)—Cr(1)—N(1)	172.5(1)	Cr(1)—Cr(2)—N(7A)	95.0(1)
N(4)—Cr(1)—N(1)	89.8(1)	N(3A)—Cr(2)—N(7A)	89.6(2)
N(5A)—Cr(2)—N(7A)	169.0(2)	N(3)—Cr(2')—N(5)	88.7(2)
N(2)—Cr(2)—N(7A)	87.6(2)	N(2A)—Cr(2')—N(7)	89.6(2)
N(2A)—Cr(2')—N(5)	89.7(2)	N(2A)—Cr(2')—N(3)	168.1(2)
N(7)—Cr(2')—N(5)	167.6(2)	N(7)—Cr(2')—N(3)	89.4(2)

[a] Atomic label with ' denotes the disordered atoms counterparts of the unprimed atoms.

[b] Atomic labels with "A" denote symmetry related atoms.

Table IX. Selected Interatomic Separations (Å) and Angles (°) for **4**·2THF [a]

Ni(2)···Ni(1)	2.368(1)		
Ni(2)—N(6)	1.897(8)	Ni(1)—N(3A)	1.916(5)
Ni(2)—N(4)	1.907(7)	Ni(1)—N(7)	1.917(5)
Ni(2)—N(2)	1.910(5)	Ni(1)—N(5)	1.919(6)
Ni(2)—N(2A)	1.910(5)	Ni(1)—N(1)	1.919(5)
N(6)—Ni(2)—N(4)	180.00(1)	N(2A)—Ni(2)···Ni(1)	90.1(2)
N(6)—Ni(2)—N(2)	89.8(2)	Ni(1A)—Ni(2)···Ni(1)	179.93(7)
N(4)—Ni(2)—N(2)	90.2(2)	N(3A)—Ni(1)—N(7)	90.8(2)
N(6)—Ni(2)—N(2A)	89.8(2)	N(3A)—Ni(1)—N(5)	88.9(2)
N(4)—Ni(2)—N(2A)	90.2(2)	N(7)—Ni(1)—N(5)	173.0(2)
N(2)—Ni(2)—N(2A)	179.5(3)	N(3A)—Ni(1)—N(1)	173.1(2)
N(6)—Ni(2)···Ni(1A)	90.04(4)	N(7)—Ni(1)—N(1)	89.0(2)
N(4)—Ni(2)···Ni(1A)	89.96(4)	N(5)—Ni(1)—N(1)	90.5(2)
N(2)—Ni(2)···Ni(1A)	90.1(2)	N(3A)—Ni(1)···Ni(2)	86.6(2)
N(2A)—Ni(2)···Ni(1A)	89.9(2)	N(7)—Ni(1)···Ni(2)	86.4(2)
N(6)—Ni(2)···Ni(1)	90.04(4)	N(5)—Ni(1)···Ni(2)	86.5(2)
N(4)—Ni(2)···Ni(1)	89.96(4)	N(1)—Ni(1)···Ni(2)	86.5(2)

[a] Atoms labeled with "A" are symmetry related atoms.

Structures of the dinuclear compounds. Two crystal forms of compound **1**, namely **1**·toluene and **1**·C_6H_{14}, were obtained by slow diffusion of hexanes into the corresponding solutions of **1** in toluene and THF. Crystal data and structure refinement parameters are listed in Table I and II, repectively, and some important bond distances and angles are shown in Table VI. The idealized D_{2d} core structure in the two crystals is essentially the same, having two chromium atoms, each surrounded by nitrogen atoms. If the phenyl groups are neglected, the structure is essentially eclipsed as shown in Figures 6 and 7. The Cr—Cr distances of 1.873(2) Å in **1**·toluene and 1.875(2) Å in **1**·C_6H_{14} are similar to that, 1.870(3) Å, in Cr_2(6-Me,2-NH-$C_6H_3N)_4$, where the ligand is very similar to the coordinated part of HBPAP.[23] However, the Cr—Cr distance is very short when compared with those in other dichromium compounds with somewhat similar tridentate nitrogen ligands. For example, the distances between chromium atoms in Cr_2(DPhIP)·2THF (DPhIP is the anion of 2,6-di(phenylimino)piperide anion) and $Cr_2(dpa)_4$ are 2.155(1) Å and 1.943(2) Å, respectively.[14] While the average distance of 3.114[4] Å[24] from a pendent N to a metal atom in **1** is not much greater than the corresponding distances of 2.901[3] Å[24] and 2.920[6] Å[24] in $Cr_2(DPhIP)_4$·2THF and $Cr_2(dpa)_4$, respectively,[14] there is a significant chemical difference between these ligands. Because of the sp^3-hybridization and the proton present in the anilido nitrogen atom in $Cr_2(HBPAP)_4$, the donor ability of the pendent N atom from the anilido group is far inferior to that of the sp^2 N-atoms found at the axial positions of $Cr_2(DPhIP)_4$ and $Cr_2(dpa)_4$. Thus the dichromium distance in $Cr_2(HDPAP)_4$ falls into the typical range of dichromium quadruple bonds.

The dimolybdenum complex , **2**·toluene, is isomorphous to the dichromium complex,

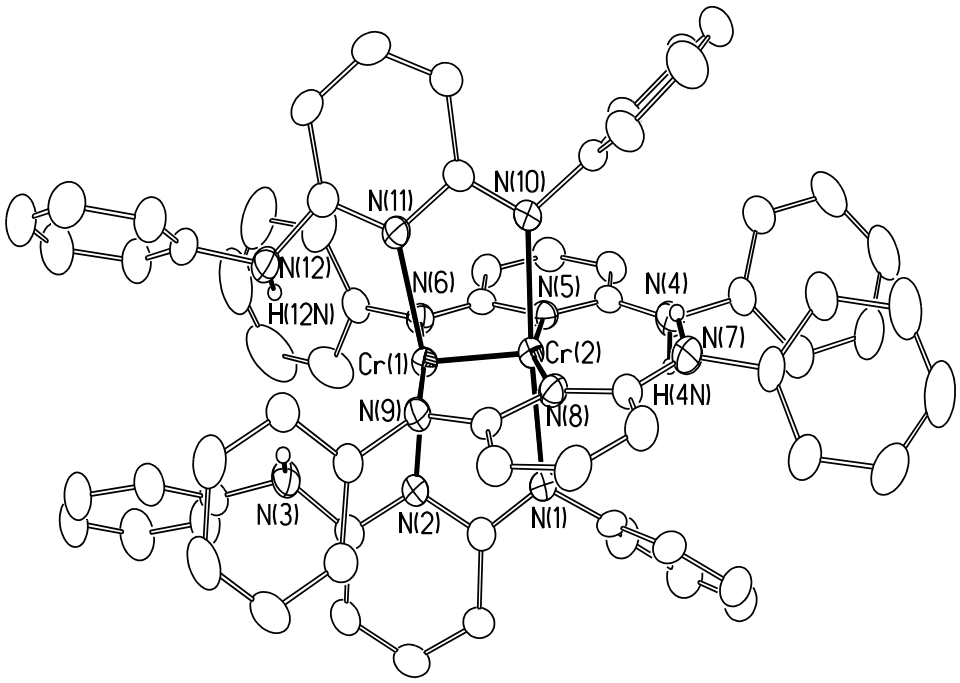

Figure 6. Perspective view of $Cr_2(HBPAP)_4$ in **1**·toluene. Atoms are drawn at the 40% probability level and aromatic hydrogen atoms are omitted for clarity.

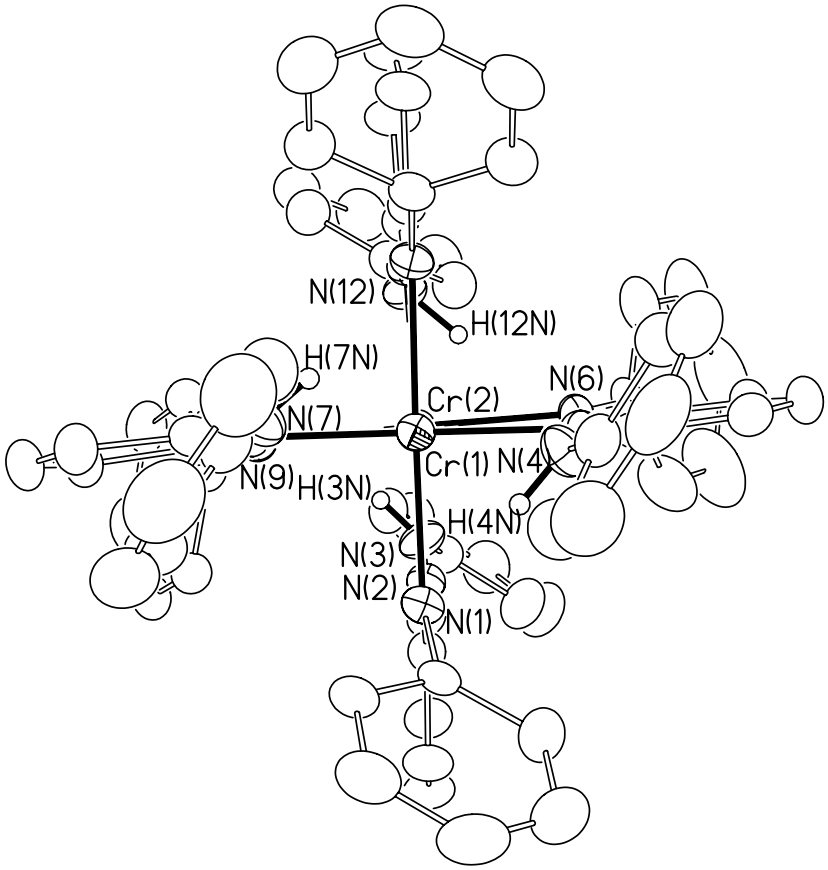

Figure 7. A view down the Cr—Cr vector in **1**·toluene.

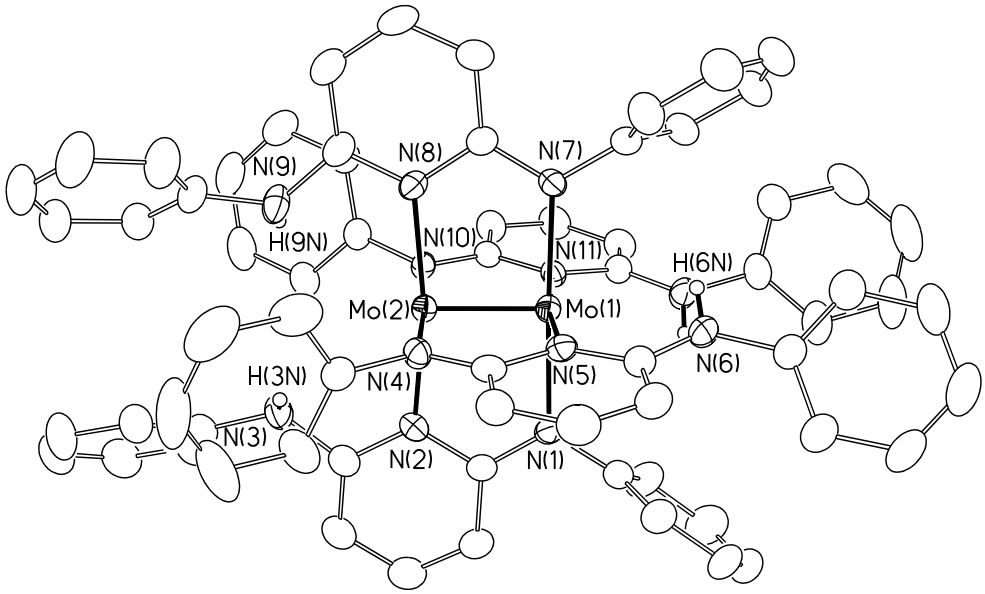

Figure 8. Perspective view of $Mo_2(HBPAP)_4$ in **2**·toluene. Atoms are drawn at the 40% probability level and aromatic hydrogen atoms are omitted for clarity.

1·toluene, and, as shown in Figure 8, the molecular structure is very similar. The Mo—Mo distance of 2.0812(5) Å is typical of a quadruply-bonded Mo_2 unit. The Mo—Mo and Mo—N distances and the angles in the metal core are very similar to those found in $Mo_2(PhNPy)_4$,[25] where PhNPy stands for the anion of 2-anilinopyridine.

^{1}H NMR studies of $Cr_2(HDPAP)_4$ and $Mo_2(HDPAP)_4$. The ^{1}H-NMR spectra showed that the purity of **1** and **2** was good. All signals corresponding to the aromatic C—H protons were sharp, as expected from a diamagnetic species. However, the signals associated with the amine hydrogen atoms on each of the pendant N atoms were slightly broader and were found at 3.46 ppm for **1** and 3.04 ppm for **2**. The corresponding signal in the neutral H_2BPAP is at 8.04 ppm and for the lithium salt of $HBPAP^-$ it is at 6.44 ppm. This displacement is significantly larger than that of the aromatic hydrogen atoms which change by less than 1 ppm from the neutral molecule to the monoanionic species to those of the metal-metal bound complexes. The small downfield displacement, 1.6 ppm, of the signals corresponding to the amine hydrogen atoms of the monoanionic species compared to that of the neutral one is not surprising and can be attibuted to the negative charge on the monoanion as well as possible pairing of ions by formation of intermolecular hydrogen bonds between N—H units and deprotonated nitrogen atoms in the monoanionic species, as shown in Figure 9. The much greater displacement of the N—H signals of **1** and **2** toward higher field is quite remarkable. When compared to those of LiHBPAP, these signals are displaced by 2.98 and 3.40 ppm upfield for **1** and **2**, respectively. There are many previous examples of relatively large shifts in the opposite direction. For example, the methine hydrogen atoms of bridging formamidinate groups, ArN—C(H)—NAr, in $M_2(DArF)_4$ complexes is well documented[26] for compounds containing M—M multiple bonds. These signals are found at *ca.* 8.53 ppm in quadruply-bonded dimolybdenum complexes and at *ca.* 6.28 ppm in the

corresponding non-metal-metal bound dinickel complexes.[18] Familiar also are the differences of *ca.* 1 ppm observed for proximal and distal protons in complexes of the type $M_2Cl_4(PR)_4$,[27] $M_2Cl_4(diphos)_2$[28], or $M_2(NR_2)_6$[29] where again there are metal-metal bonds.

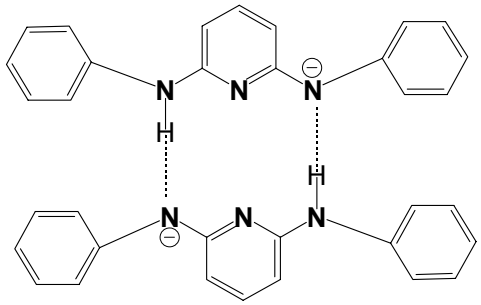

Figure 9. A schematic drawing of the possible dimer of the monoanion of 2,6-bis(phenylamino)pyridine.

High and low field displacements share a common origin. In a semiclassical way, the angular momentum of electrons in the M—M multiple bond about the bond axis induces a magnetic field which is highly anisotropic. This magnetic anisotropy has also been found in many organic compounds and is mainly responsible for the significantly different shifts found in benzene and alkyne systems. For example, in acetylene the protons have signals at δ 2.35 ppm, more shielded than those in ethylene (δ 4.60 ppm).[30] In acetylene, the triple bond is along the molecular axis. When this axis is aligned with the applied magnetic field, the circulation of the π-electrons

of the bond gives rise to an opposing magnetic field and the NMR peak is found further upfield than that predicted from electronegativity considerations alone. Clearly, similar behavior must occur for triple and quadruple bonds between metal atoms.

For metal-metal multiply-bound systems, the theoretical considerations of McConnell[31] can be used to explain long range shielding or deshielding. This simple mathematical model relates the chemical shift change, $\Delta\delta$, and the molar diamagnetic anisotropy, χ. The magnitude of the magnetic anisotropy, given by the difference between the parallel and perpendicular components along the metal-metal bond, has been demonstrated [18] to be correlated to the chemical shift of a given hydrogen atom by the following equation:

$$\Delta\chi = \chi_{\parallel} - \chi_{\perp} = \frac{12\pi R^3 \Delta\delta}{1 - 3\cos^2\theta}$$

where R is the length of the vector from the center of the bond to the proton in question (e.g. the N—H proton on the hanging N atom of a ligand in **1** and **2**) and θ is the angle subtended by R and the M—M axis. The value, $\Delta\delta$, is the displacement of the resonance from where it would be in the absence of the anisotropy. Because of the angular dependence of this relationship, the value of the function for an axially symmetrical bond changes sign at 55 ˚44'. Thus one would expect protons above the M—M bond to be deshielded (e.g. the methine protons of a formamidinate ligand) and thus shifted downfield, or shielded if they are more or less along the M—M axis, as shown schematically in Figure 10 and thus shifted upfield. Since the amine protons in **1**and **2** fall in the positive shielding zone, one would expect an upfield displacement, relative to that of the non-coordinated ligands, exactly as observed here. To our knowledge, this is the first time an upfield

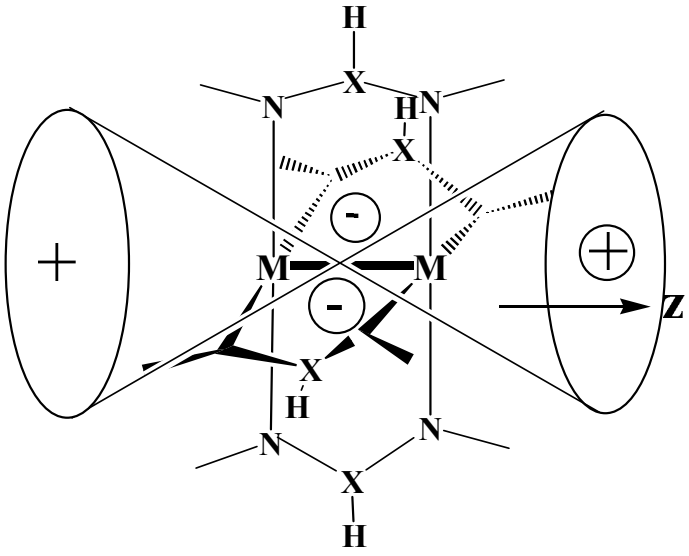

a

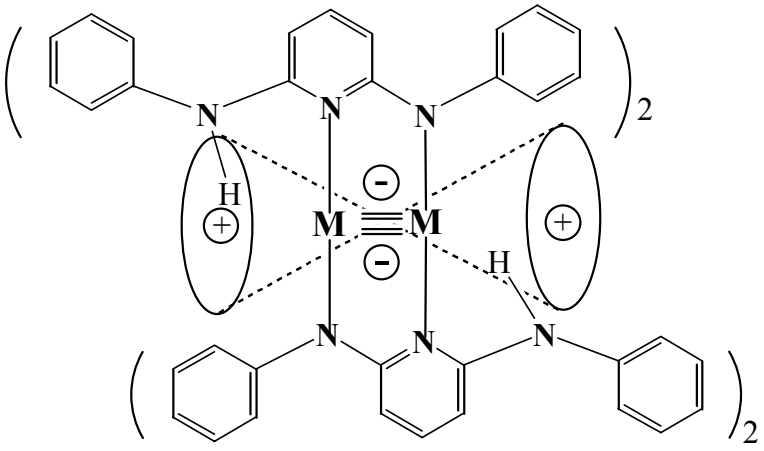

b

Figure 10. Shielding and deshielding caused by magnetic anisotropy of the M—M multiple bond in dinuclear paddlewheel compounds. Positive signs (+) indicate shielding zones, while negative signs (-) represent deshielding zones.

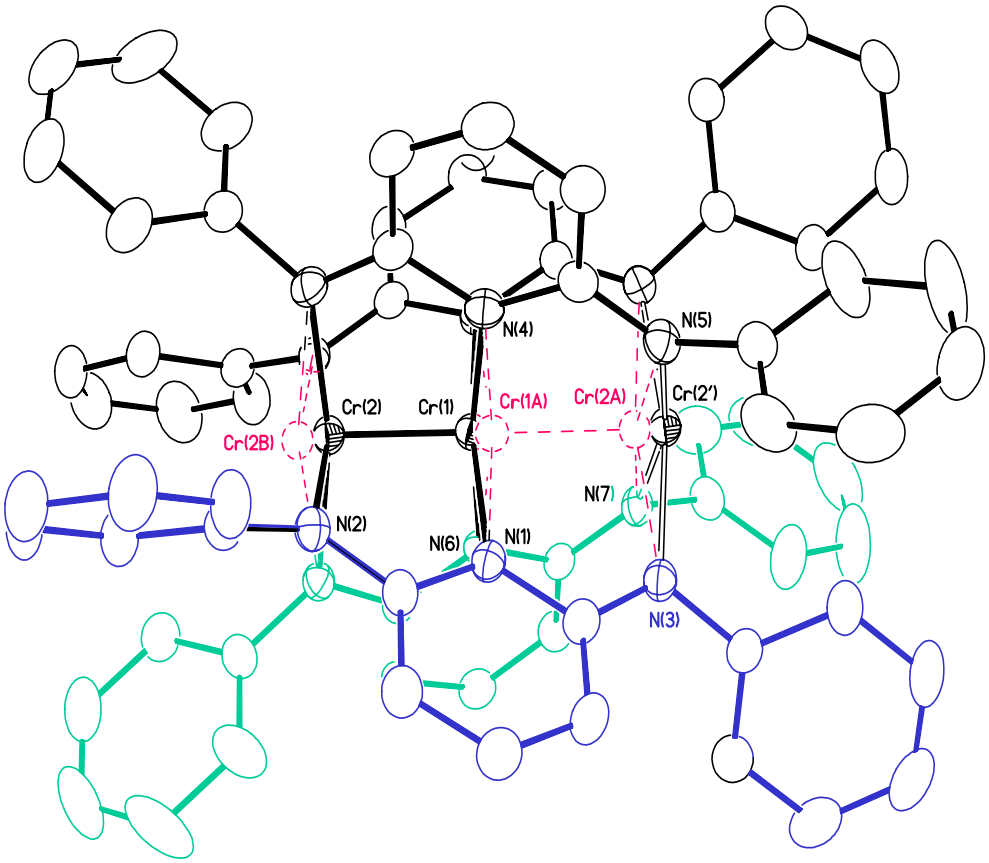

Figure 11. Perspective view of $Cr_3(BPAP)_4^{2-}$ in **3**·2THF. Atoms are drawn at 40% probability level and hydrogen atoms are omitted for clarity. One set of disordered chromium atoms is represented by broken circles.

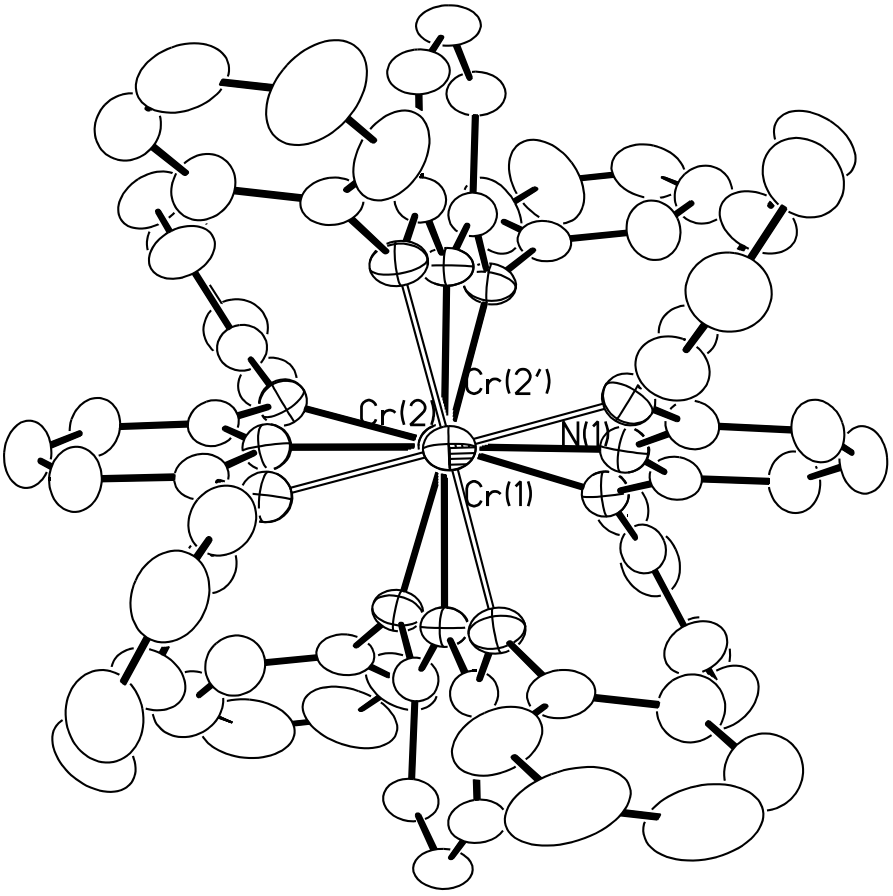

Figure 12. A view looking down the Cr_3 unit in **3**·2THF.

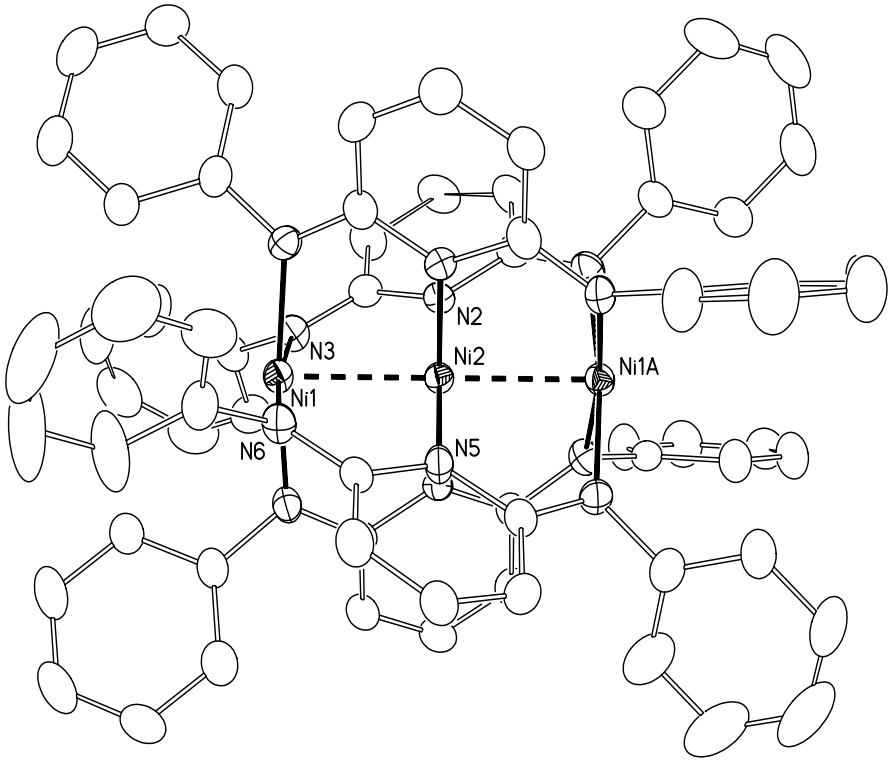

Figure 13. Perspective view of the anion $Ni_3(BPAP)_4^{2-}$ in **4**·2THF. Atoms are drawn at the 40% probability level and hydrogen atoms are omitted for clarity.

displacement has been documented in the chemistry of multiply-bonded complexes. More descriptions about magnetic anisotropy of multiple bond can be found in Appendix II.

Using the above equation, many calculations have been performed using the methine protons as probes for metal-metal bonded paddlewheel compounds having four formamidinate ligands. For these rigid groups, the angle θ is essentially 90° and the distance R is easily calculated using the structural parameters. Unfortunately for the $M_2(HBPAP)_4$ compounds **1** and **2**, this type of calculation is not reliable. One could obtain all the necessary values from the solid state structure, but since the N—H groups of the pendant HBPAP ligand are restrained to fixed protons in solution;[32] no correlation between the solid state and the solution structures, in this respect, is possible.

Structures of compounds 3 and 4. Compound **3** crystallized in the space group *C2/c* with two interstitial THF molecules. Here, a linear chain of three chromium atoms is surrounded by four BPAP dianions, as shown in Figure 11. The trinuclear anion resides on a crystallographic site of two-fold symmetry with the 2-fold axis perpendicular to the Cr—Cr—Cr chain. However, the trinuclear chromium chain is actually very unsymmetrical. The initial appearance of equality of the Cr—Cr distances is due to crystallographic disorder. This type of disorder has been encountered also in other species containing linear Cr_3^{6+} cores.[3a] Full anisotropic refinement of the chromium atoms in the chain was not possible because of disorder but the two Cr to Cr distances were found to be quite different, namely, 1.904(3) Å for Cr(1)—Cr(2) and 2.589(3) Å for Cr(1)···Cr(2'). Therefore, the bonding in this trinuclear chromium chain should be considered to consist of a Cr—Cr quadruple bond and an isolated Cr^{II} unit, with the latter having approximately square planar geometry. The countercations, $Bu^n_4N^+$, reside on general positions in the unit cell.

Figure 12 shows an end view of the trinuclear anion of **3**. The torsion angle N(2)

···Cr(2)···Cr(1)···(N1) is 15.3°; the total torsion angle in the molecule is 30.6°. This is smaller than that in the similar trinuclear dpa complex (45.4°).[3a] Thus, the idea that simply eliminating H···H interactions such as those in the dpa anion (in Chapter I) would produce a trinuclear species without a torsion angle did not prove correct. The reason for this is not readily evident.

The trinuclear nickel compound, **4**·2THF, is isomorphous with **3**·2THF, crystallizing in space group *C2/c*, with $Z = 4$. The anion therefore has crystallographic symmetry C_2 and in this case the metal atom chain is symmetrical; there is no disorder. Again, there is no axial ligation and there is an overall twist of about 30°. The structure is depicted in Figure 13 and metrical parameters are listed in Table IX. The end nickel atoms as well as the central one are coordinated by an essentially square planar array of nitrogen atoms and the Ni—N distances to the end nickel atoms, with an average value of 1.917[6] Å,[24] are scarcely different from those to the central nickel atom, 1.906[6] Å.[24] From this structure it would be expected that all three nickel atoms would be in a low-spin (i.e., diamagnetic) state, and this is indeed the case as shown by the ^{1}H NMR spectrum.

The two Ni···Ni separations are 2.368(1) Å, which is much shorter than those in $Ni_3(dpa)_4Cl_2$,[5] 2.433[8] Å.[24] However, in $Ni_3(dpa)_4Cl_2$ as well as in all nickel compounds in this class with more extended chains,[12] i.e., Ni_5, Ni_7, Ni_9, the nickel atoms at the ends are different from those inside the chain. The end nickel atoms have a fifth ligand atom (e.g., Cl^-, NCS^-), and are high spin. Thus, while the inner nickel atom(s) is(are) square-planar, low-spin atoms with relatively short (*ca.* 1.90 Å) Ni—N bonds, those on the ends are five-coordinate, high-spin atoms, with longer Ni—N bonds (*ca.* 2.1 Å) and the Ni···Ni separations to the terminal nickel atoms are long. It is the absence of axial ligation in the present case leading to the end nickel atoms being square-planar, low-spin atoms that allows for their closer approach to the central nickel atom.

Compound **4** is not the first compound with a chain of nickel atoms having no axial ligation. The compound shown in Figure 14 was reported in 1999.[2f] It is diamagnetic, like **4,** but has Ni···Ni separations that are appreciably shorter than those in **4**, namely 2.3269[6], 2.3010[6] and 2.3280[6] Å,[24] as compared to 2.368(1) Å in **4**. The Ni—N distances in both this compound and **4** are quite similar, all being in the range of 1.90-1.93 Å. It seems clear that unless there are axial ligands present, chains of nickel(II) atoms simply consist of stacked square, diamagnetic NiN_4 units. In both compounds the stacks are twisted, however.

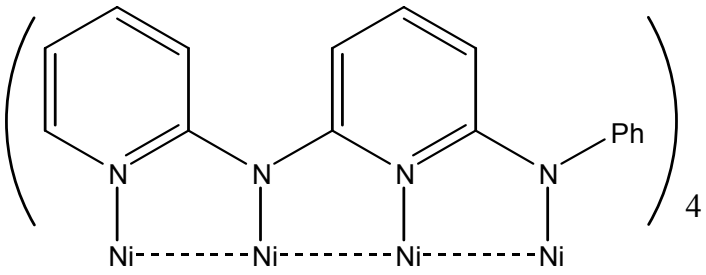

Figure 14. A schematic drawing of a tetranickel compound with a short Ni–Ni separation.

CHAPTER III

SYNTHESIS OF UNSYMMETRICAL FORMAMIDINES*

The development of multidentate ligands to support linear chains of three or more metal atoms is being actively pursued by both this laboratory[2a-d] and elsewhere.[2e,f] Depending on the number of donor atoms on the ligands, compounds with three, four, five, seven, nine atoms in a linear arrays have been synthesized.[12] Generally, the ligands are symmetrical. Examples are dpa (the anion of 2,6-dipyridylamine),[2] DPhIP (the anion of 2,6-di(phenylimino)-piperidine) [33], BPAP (the dianion of 2,6-bisphenylaminopyridine),[34] DPyF (the anion of dipyridylformamidine).[2a] As part of our ongoing study of complexes containing extended metal atoms in linear arrays, we investigated the effects of other functionalized ligands on the metal–metal interactions. Amidinate and formamidinate ligands are attractive choices since dimetal paddlewheel complexes with such ligands have been intensively investigated and are well-understood,[1] and the synthesis of functionalized, symmetrical amidine and formamidine ligands is not a difficult task [35].

Here we report the synthesis of a series of unsymmetrical amidines and formamidines and their transition metal complexes. The ligands (Figure 4 in Chapter I) include five unsymmetrical formamidines with substituents ranging from strong electron-donating groups, such as $-OCH_3$, to electron-withdrawing groups, e.g., F. The metal complexes include mainly mononuclear complexes for this chapter. A large group of linear trinuclear species is described in the following chapters.

---

* Taken in part from *Inorg. Chim. Acta,* Cotton, F. A.; Lei, P.; Murillo, C. A.; Wang, L. "Synthesis of unsymmetrical formamidines and benzamidines: structural studies of copper, cobalt and chromium complexes", accepted for publication.

EXPERIMENTAL

General procedures. Ethyl orthoformate, aniline, *p*-anisidine, *p*-toluidine, *p*-fluroaniline, and 2-aminopyridine, were obtained from Aldrich. Cobalt dichloride, $CrCl_2$ and $CuCl_2 \cdot 3H_2O$ were purchased from Strem Chemicals Inc. All solvents were freshly distilled from appropriate drying agents under nitrogen. All routine operations were carried out under N_2 unless otherwise noted. ^{1}H NMR spectra were obtained on XL-300 spectrometers.

Preparation of ethyl pyridylformimidate, 5. 2-aminopyridine (18.8 g, 0.200 mol), triethylorthoformate (50 ml, excess) and two drops of 2 M HCl were charged into a 200 ml flask. The flask was heated slowly using a heating mantle. At *ca.* 110 °C, ethanol began to distill. When 95% of the theoretical amount of ethanol had been collected, the flask was allowed to cool slowly. The excess of triethyl orthoformate was removed by vacuum distillation at 115 - 120 °C using a water aspirator (*ca.* 25 mm Hg). Upon further heating the final product, a pale yellow liquid, distilled at 177 - 180 °C. Yield, 14.1 g, 60%. ^{1}H NMR (300 MHz, acetone-d_6, δ): 8.52 (s, 1 H), 8.35 (d, 1 H), 7.81 (s, 1 H), 7.42 (m, 2 H), 4.26 (q, 2 H), 1.33 (t, 3 H).

Preparation of N,N′-phenylpyridylformamidine, HPhPyF, 6. A 50 ml acid-free flask were charged with ethyl pyridylformimidate (4.62 g, 30.0 mmol) and freshly distilled aniline (2.79 g, 30.0 mmol). The mixture solidified upon stirring for 5 min generating heat. White needle crystals, were obtained by recrystallization from toluene. Yield > 85%. ^{1}H NMR (300 MHz, acetone-d_6, δ): 9.05 (broad, 1 H), 8.52 (s, 1 H), 8.38 (d, 1 H), 7.64 (m, 1 H), 7.45 (m, 2 H), 7.01 (m, 2 H), 6,52 (m, 3 H). Low resolution mass spectrum (FAB+): m/z 198 $[M+1]^+$ (100%).

Preparation of N,N′-anisylpyridylformamidine, HAniPyF, 7. This was made similarly to **6** by using anisidine instead of aniline as white needle-like crystals with a yield greater than

80%. ^{1}H NMR (300 MHz, acetone-d_6, δ): 9.08 (broad, 1 H), 8.56 (s, 1 H), 8.30 (d, 1 H), 7.64 (m, 1 H), 7.45 (m, 2 H), 6.82 (d, 2 H), 6.36 (d, 2 H), 2.38 (s, 3 H). Low resolution mass spectrum (FAB+): m/z 228 $[M+1]^+$(100%).

Preparation of N,N′ -tolylpyridylformamidine, HTolPyF, 8. This was prepared similarly to **6** by substituting aniline by toluidine. Yield: 82% (after recrystallization from toluene). ^{1}H NMR (300 MHz, acetone-d_6, δ): 9.10 (broad, 1 H), 8.48(s, 1 H), 8,25 (d, 1 H), 7.68 (m, 1 H), 7.50 (m, 2 H), 6.79 (d, 2 H), 6.31 (d, 2 H), 2.35 (s, 3 H). Low resolution mass spectrum (FAB+): m/z 212 $[M+1]^+$(100%).

Preparation of N,N′ -4-fluorophenylpyridylformamidine, HPh^{F}PyF, 9. This was synthesized similarly to **6** by reacting 4-fluoroaniline with ethyl pyridylformamidinate. The final product was recrystallized from toluene. Yield 76%. ^{1}H NMR (300 MHz, acetone-d_6, δ): 9.12 (broad, 1 H), 8.30 (s, 1 H), 8.19 (d, 1 H), 7.68 (m, 1 H), 7.48 (m, 2 H), 6.72 (d, 2 H), 6.44 (d, 2 H). Low resolution mass spectrum (FAB+): m/z 216 $[M+1]^+$ (100%).

Preparation of ethyl 4-picolylformimidate, 10. The preparation was similar to that of **5**. Ethyl 4-picolylformimidate was distilled at 168 - 171 °C under reduced pressure. Yield 44%. ^{1}H NMR (300 MHz, acetone-d_6, δ): 8.35 (d, 1 H), 7.80 (s, 1 H), 7.42 (m, 2 H), 4.28 (q, 2 H), 2.37 (s, 3 H), 1.33 (t, 3 H).

Preparation of N,N′ -phenylpicolylformamidine, HPhPcF, 11. This was prepared similarly to **6** by reacting freshly distilled aniline with ethylpicolylformamidine. The product was recrystallized in toluene. Yield: 80%. ^{1}H NMR (300 MHz, acetone-d_6, δ): 9.04 (broad, 1 H), 8.34 (s, 1 H), 8.25 (d, 1 H), 7.44 (m, 2 H), 7.05 (m, 2 H), 6.62 (t, 1 H), 6.46 (d, 2 H). Low resolution mass spectrum (FAB+): m/z 212 $[M+1]^+$ (100%).

Preparation of Co(HPhPyF)Cl_2, 12. To a flask charged with **6** (210 mg, 1.10 mmol) and

$CoCl_2$ (130 mg,1.00 mmol) was added 20 ml of THF. After stirring for 2 h the mixture was bright blue. The solid was collected by filtration, and it was washed with 2×20 ml of THF. This was dried under vacuum for 1 h. Yield: 82%. Blue crystals were obtained by slow diffusion of ether into a methanol solution of the compound.

Preparation of Cu(HPhPyF)Cl_2, 13. The ligand **6** was dissolved in 15 ml of THF. This was slowly added to a methanol solution of $CuCl_2 \cdot 3H_2O$ (170 mg, 1.00 mmol). A brown-red precipitate formed immediately. The mixture was stirred for 1 h. The solid was collected by filtration and was washed with 20 ml THF. This was dried under vacuum for 1 h. Yield: 72%. Red crystals were obtained by slow diffusion of ether into a methanol/MeCN (1:1) solution of the compound.

Preparation of Cu(PhPyF)$_2$, 14. To a flask charged with $CuCl_2 \cdot 3H_2O$ (170 mg, 1.00 mmol), HPhPyF (197 mg, 1.00 mmol) and an excess of copper wire (1.00 g) was added 40 ml MeCN. The mixture was refluxed under air for 8 h, forming a yellow solution over the copper wire, and then it was allowed to cool slowly to room temperature. After 24 h, the color changed to deep purple and a lot of deep-purple, block-shaped crystals deposited on the glass walls. From these crystals, one suitable for X-ray crystallographic study was selected. The crystals were separated manually from the unreacted copper wire. Yield: 44%.

Table X. Crystal Data and Structure Refinement for **12**

Empirical formula	$C_{12}H_{11}Cl_2CoN_3$	
Formula weight	327.07	
Temperature	213(2) K	
Wavelength	0.71073 Å	
Crystal system	Monoclinic	
Space group	$P2_1/c$	
Unit cell dimensions	a = 13.338(2) Å	α = 90˚
	b = 12.795(2) Å	β = 95.067(3)˚
	c = 7.9981(13) Å	γ = 90˚
Volume	1359.7(4) Å^3	
Z	4	
Density (calculated)	1.598 g/mm^{-3}	
Absorption coefficient	1.639 mm^{-1}	
Crystal size	0.39 x 0.12 x 0.08 mm	
Instrument for data collections	Bruker SMART 1000	
Theta range for data collection	2.21 to 27.52˚	
Reflections collected	4699	
Independent reflections	2308 [R(int) = 0.0208]	
Scan Method	ω-scan	
Refinement method	Full-matrix least-squares on F^2	
Data / restraints / parameters	2307 / 0 / 163	
Goodness-of-fit on F^2	1.097	
Final R indices [$I > 2\sigma(I)$]	$R1$ = 0.0342, $wR2$ = 0.0822	
R indices (all data)	$R1$ = 0.0428, $wR2$ = 0.0876	
Largest Shift / esd, final cycle	-0.001	
Largest diff. peak and hole	0.440 and -0.387 e./Å^{-3}	

Table XI. Crystal Data and Structure Refinement for **13**

Empirical formula	$C_{12}H_{11}Cl_2CuN_3$	
Formula weight	331.68	
Temperature	213(2) K	
Wavelength	0.71073 Å	
Crystal system	Monoclinic	
Space group	$P\bar{1}$	
Unit cell dimensions	a = 7.5991(7) Å	α = 97.642(2)˚
	b = 9.6871(9) Å	β = 111.090(2)˚
	c = 10.0425(9) Å	γ = 105.646(2)˚
Volume	642.1(1) Å^3	
Z	2	
Density (calculated)	1.716 g/mm^3	
Absorption coefficient	2.099 mm^{-1}	
Crystal size	0.28 x 0.21 x 0.04 mm	
Theta range for data collection	2.25 to 27.50˚	
Reflections collected	4136	
Independent reflections	2837 [R(int) = 0.0172]	
Scan Method	ω-scan	
Refinement method	Full-matrix least-squares on F^2	
Data / restraints / parameters	2837 / 0 / 163	
Goodness-of-fit on F^2	1.052	
Final R indices [$I > 2\sigma(I)$]	$R1$ = 0.0298, $wR2$ = 0.0742	
R indices (all data)	$R1$ = 0.0400, $wR2$ = 0.0799	
Largest Shift / esd, final cycle	0.001	
Largest diff. peak and hole	0.355 and -0.280 e./Å^3	

Table XII. Crystal Data and Structure Refinement for **14**

Empirical formula	$C_{24}H_{20}CuN_6$	
Formula weight	456.00	
Temperature	213(2) K	
Wavelength	0.71073 Å	
Crystal system	Triclinic	
Space group	$P\bar{1}$	
Unit cell dimensions	a = 9.0546(7) Å	α = 90.894(1)˚
	b = 10.3920(8) Å	β = 98.220(2)˚
	c = 12.102(1) Å	γ = 110.891(1)˚
Volume	1050.2(1) Å^3	
Z	2	
Density (calculated)	1.442 g/mm^3	
Absorption coefficient	1.064 mm^{-1}	
Crystal size	0.52 x 0.45 x 0.25 mm	
Instrument for data collections	Bruker SMART 1000	
Theta range for data collection	1.70 to 27.51˚	
Reflections collected	6707	
Independent reflections	4617 [R(int) = 0.0116]	
Scan Method	ω-scan	
Refinement method	Full-matrix least-squares on F^2	
Data / restraints / parameters	4617 / 0 / 280	
Goodness-of-fit on F^2	1.048	
Final R indices [$I > 2\sigma(I)$]	$R1$ = 0.0274, $wR2$ = 0.0728	
R indices (all data)	$R1$ = 0.0301, $wR2$ = 0.0752	
Largest Shift / esd, final cycle	0.003	
Largest diff. peak and hole	0.350 and -0.370 e/Å^3	

Table XIII. Selected Bond Lengths (Å) and Angles (˚) for **12**

Co(1)—N(3)	1.982(2)	Co(1)—Cl(2)	2.2172(11)
Co(1)—N(1)	2.015(2)	Co(1)—Cl(3)	2.2471(9)
N(1)—C(5)	1.333(4)	C(2)—C(3)	1.394(5)
N(1)—C(1)	1.361(3)	C(3)—C(4)	1.365(4)
N(2)—C(6)	1.346(3)	C(4)—C(5)	1.405(4)
N(2)—C(5)	1.393(3)	C(7)—C(8)	1.380(5)
N(3)—C(6)	1.291(4)	C(7)—C(12)	1.381(5)
N(3)—C(7)	1.438(3)	C(8)—C(9)	1.391(5)
C(1)—C(2)	1.368(4)	C(9)—C(10)	1.375(6)
C(11)—C(12)	1.386(4)	C(10)—C(11)	1.365(6)
N(3)—Co(1)—N(1)	93.21(9)	C(5)—N(1)—C(1)	117.7(2)
N(3)—Co(1)—Cl(2)	116.73(9)	C(5)—N(1)—Co(1)	123.7(2)
N(1)—Co(1)—Cl(2)	110.19(8)	C(1)—N(1)—Co(1)	118.5(2)
N(3)—Co(1)—Cl(3)	112.10(8)	C(6)—N(2)—C(5)	130.1(2)
N(1)—Co(1)—Cl(3)	109.48(8)	C(6)—N(3)—C(7)	117.9(2)
C(3)—C(4)—C(5)	119.1(3)	C(6)—N(3)—Co(1)	121.4(2)
N(1)—C(5)—N(2)	120.0(2)	C(7)—N(3)—Co(1)	120.7(2)
N(1)—C(5)—C(4)	122.2(3)	N(1)—C(1)—C(2)	123.0(3)
N(2)—C(5)—C(4)	117.8(3)	C(1)—C(2)—C(3)	118.7(3)
N(3)—C(6)—N(2)	126.5(3)	C(4)—C(3)—C(2)	119.2(3)
C(8)—C(7)—C(12)	120.7(3)	C(12)—C(7)—N(3)	121.2(3)
C(8)—C(7)—N(3)	118.1(3)	C(7)—C(8)—C(9)	119.4(3)

Table XIV. Selected Bond Lengths (Å) and Angles (˚) for **13**

Cu(1)—N(3)	1.961(2)	Cu(1)—Cl(3)	2.2292(7)
Cu(1)—N(1)	2.000(2)	Cu(1)—Cl(2)	2.2482(7)
N(1)—C(5)	1.347(3)	C(7)—C(8)	1.386(3)
N(1)—C(1)	1.360(3)	C(7)—C(12)	1.394(4)
N(2)—C(6)	1.347(3)	C(8)—C(9)	1.393(3)
N(2)—C(5)	1.388(3)	C(9)—C(10)	1.378(4)
N(3)—C(6)	1.296(3)	C(10)—C(11)	1.381(4)
N(3)—C(7)	1.440(3)	C(11)—C(12)	1.388(3)
C(1)—C(2)	1.367(3)	C(3)—C(4)	1.370(4)
C(2)—C(3)	1.390(4)	C(4)—C(5)	1.392(3)
N(3)—Cu(1)—N(1)	93.10(8)	C(5)—N(1)—C(1)	117.1(2)
N(3)—Cu(1)—Cl(3)	138.41(7)	C(5)—N(1)—Cu(1)	125.55(16)
N(1)—Cu(1)—Cl(3)	99.80(6)	C(1)—N(1)—Cu(1)	117.26(16)
N(3)—Cu(1)—Cl(2)	98.44(6)	C(6)—N(2)—C(5)	130.8(2)
N(1)—Cu(1)—Cl(2)	135.50(6)	C(6)—N(3)—C(7)	116.6(2)
C(6)—N(3)—Cu(1)	124.17(17)	C(4)—C(3)—C(2)	119.4(2)
C(7)—N(3)—Cu(1)	119.27(15)	C(3)—C(4)—C(5)	119.0(2)
N(1)—C(1)—C(2)	123.4(2)	N(1)—C(5)—N(2)	120.0(2)
C(1)—C(2)—C(3)	118.5(3)	N(1)—C(5)—C(4)	122.5(2)
N(3)—C(6)—N(2)	126.1(2)	N(2)—C(5)—C(4)	117.5(2)

Table XV. Selected Bond Lengths (Å) and Angles (˚) for **14**

Cu(1)—N(6)	1.921(1)	Cu(1)—N(3)	1.985(1)
Cu(1)—N(1)	1.926(1)	Cu(1)—N(4)	1.989(1)
N(1)—C(7)	1.332(2)	N(5)—C(18)	1.318(2)
N(1)—C(5)	1.421(2)	N(5)—C(17)	1.373(2)
C(8)—N(3)	1.361(2)	N(6)—C(18)	1.330(2)
C(8)—N(2)	1.366(3)	N(6)—C(24)	1.425(2)
C(8)—C(9)	1.416(2)	C(1)—C(2)	1.376(4)
N(3)—C(12)	1.357(2)	C(1)—C(6)	1.395(3)
N(4)—C(17)	1.363(2)	C(2)—C(3)	1.377(3)
N(4)—C(13)	1.364(2)	C(3)—C(4)	1.382(3)
C(9)—C(10)	1.358(3)	C(4)—C(5)	1.394(3)
N(6)—Cu(1)—N(1)	141.77(6)	C(12)—N(3)—Cu(1)	117.28(12)
N(6)—Cu(1)—N(3)	101.21(6)	C(8)—N(3)—Cu(1)	123.81(12)
N(1)—Cu(1)—N(3)	92.92(6)	C(17)—N(4)—C(13)	118.24(15)
N(6)—Cu(1)—N(4)	93.19(6)	C(17)—N(4)—Cu(1)	123.39(11)
N(1)—Cu(1)—N(4)	102.05(6)	C(13)—N(4)—Cu(1)	118.23(11)
N(3)—Cu(1)—N(4)	134.18(6)	C(18)—N(5)—C(17)	124.66(14)
C(7)—N(1)—C(5)	117.94(14)	C(18)—N(6)—C(24)	117.36(13)
C(7)—N(1)—Cu(1)	123.01(12)	C(18)—N(6)—Cu(1)	123.20(11)
C(5)—N(1)—Cu(1)	118.92(11)	C(24)—N(6)—Cu(1)	119.40(10)
N(3)—C(8)—N(2)	124.75(16)	C(1)—C(2)—C(3)	119.8(2)

CRYSTALLOGRAPHIC STUDIES

For compounds **12, 13** and **14**, data were collected on a Bruker SMART 1000 CCD area detector system. Cell parameters were obtained using SMART software.[18] The data were corrected for Lorentz and polarization effects using SAINT[19] and then further corrected for absorption using SADABS.[20] The positions of heavy atoms were found by the direct methods using SHELXS-97.[21] Subsequent cycles of least-squares refinement followed by difference Fourier syntheses revealed the positions of the non-hydrogen atoms. All hydrogen atoms were placed in idealized positions. Important crystallographic and refinement data for **12**, **13** and **14** are given in Tables X, XI, and XII respectively. Selected bond lengths and angles for **12**, **13** and **14** are listed in Tables XIII, XIV and XV.

RESULTS AND DISCUSSION

Synthetic considerations. Five unsymmetrical formamidines were synthesized in two steps with excellent yield and facile separations. First, reactions of aminopyridine derivatives with ethyl orthoformate form pyridyl formimidate (Figure 15a); then the unsymmetrical formamidines are obtained by reacting the formimidate with the corresponding aniline derivatives, as shown in Figure 15b. For the first reaction, the use of a catalytic amount of acid and an excess of ethyl orthoformate are critical for the success of the reaction. However, the second reaction must be carried out in an acid-free environment as trace amounts of acid cause the unsymmetrical formamidines to disproportionate into the corresponding symmetrical formamidines, as shown in Figure 16. For comparison, when ethyl phenylformimidate was used as a starting material instead

of ethyl pyridylformimidate, there is no reaction at room temperature. At higher temperatures such as those that were used to distill out ethanol, a mixture of unsymmetrical and symmetrical formamidines were obtained as evidenced by the mass spectrum. The separation was extremely difficult since the unsymmetrical formamidines decompose in contact with silica gel. Therefore, the method described in Figure 15b is the only good way to prepare the unsymmetrical formamidines.

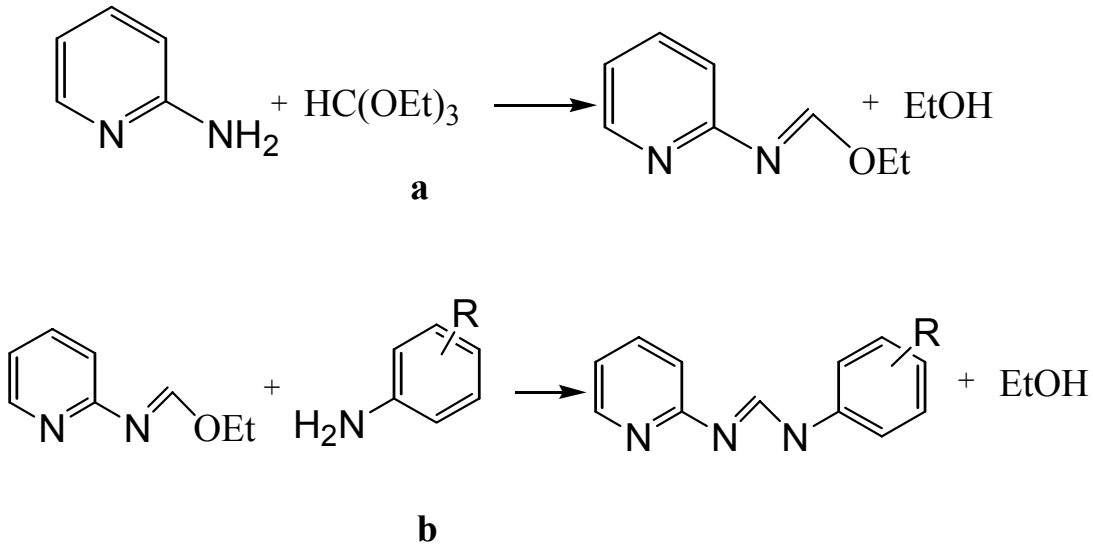

Figure 15. A typical methodology for the preparation of an unsymmetrical formamidine.

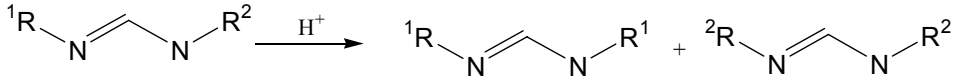

Figure 16. A schematic drawing shows the disproportionation of an unsymmetrical formamidine.

Compound **14** was synthesized by mixing $CuCl_2$, copper metal and the neutral ligand HPhPyF in MeCN under reflux. The reaction condition here was chosen to be very similar to the one used in the preparation of $Cu_3(dpa)_4Cl_2$[6] with the hope of making a tricopper analogue. However, the reaction yielded only a mononuclear species.

Structural studies. Compounds **12** and **13** have similar structures with a 1:1 metal/ligand ratio. The crystal structures for these three compounds display a distorted tetrahedral metal center chelated by a neutral ligand through two nitrogen atoms to form a six-member ring, and two chloride atoms. The molecular structure of **12** is shown in Figure 17 as an example. In both compounds, the M–N distances (*ca.* 2.00 Å) and N–M–N angles (*ca.* 93°) are comparable. The observed N–M–N angles are substantially smaller than those in the ideal geometry possibly due to the backbone constraint of the ligand but similar to those in $Co(Hdpa)Cl_2$ (Hdpa = dipyridylamine).[36] Individual values are listed in Tables XIII and XIV. The C–N distances of the formamidinate (in **12** and **13**) groups should not be equivalent as one would expect for a neutral ligand. Indeed they are not. For example, in compound **12**, the distance of a C–N single bond, C(6)–N(2), is long, 1.346(3) Å, and the distance for a carbon-nitrogen double bond, C(6)–N(3) is short, 1.291(4) Å.

The structure of **14** (Figure 18) shows two PhPyF ligands chelating a heavily distorted tetrahedral copper(II) center, like that found in $Cu(dpa)_2$.[37] Three nitrogen atoms in a plane indicating that the ligand is anionic. Evidence of the anionic nature of the ligand also comes from the equivalence of C–N distances in the formamidinate. In compound **14**, those distances are almost equal, 1.332(2) and 1.308(2) Å, which strongly suggest the existence of a delocalized system.

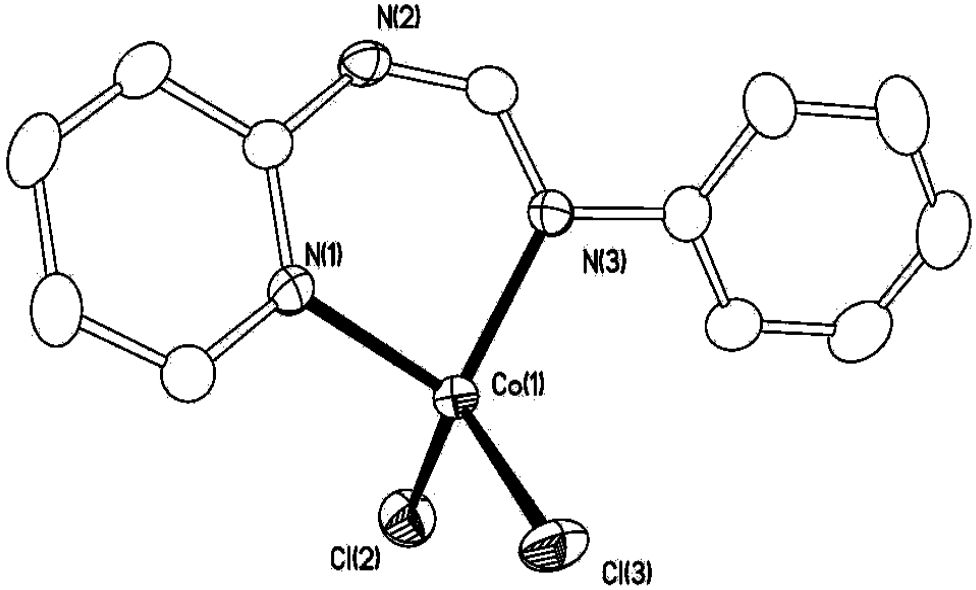

Figure 17. The molecular structure of **12** with ellipsoids drawn at the 45% probability level. The hydrogen atoms are omitted.

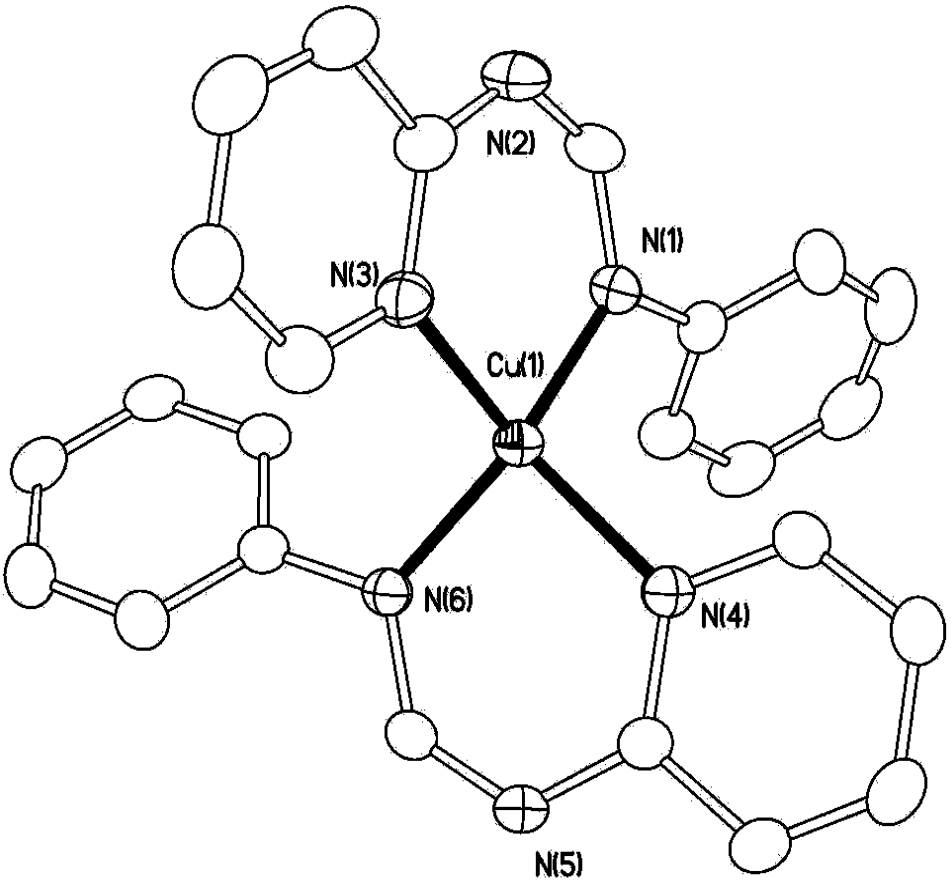

Figure 18. A drawing of the molecular structure of **14** with ellipsoids drawn at the 45% probability level and hydrogen atoms omitted.

CHAPTER IV

LINEAR TRICHROMIUM (II) CHAINS WRAPPED BY UNSYMMETRICAL FORMAMIDINATES*

In Chapter III, a reliable methodology of preparing the unsymmetrical formamidines with excellent yield and facile separation has been established. To examine further the question of torsion and other structural features, while also limiting the chain to a maximum of three metal atoms, we decided to explore five unsymmetrical formamidinates of the type ArNC(H)NPy, shown in Figure 4 in Chapter I, with substituents ranging from strong electron-donating groups, such as $–OCH_3$, to electron-withdrawing groups, e.g., –F. Here reported are the preparation, structural and magnetic studies of six compounds formed by these five ligands.

EXPERIMENTAL

General procedures. All manipulations were carried out under nitrogen using standard Schlenk techniques. Solvents were dried by conventional methods and were freshly distilled under nitrogen before use. Anhydrous chromium dichloride was purchased from Strem Chemicals and stored in an Argon dry box. Methyllithium with low chloride content, 1.6 M solution in Et_2O, was purchased from Acros. All five unsymmetrical formamidines were prepared according the methods in Chapter III, and dried under vacuum at 70 - 75 °C for at least 12 h before use. Magnetic susceptibility data on crystals that have been under vacuum overnight were collected on

* Taken in part from *Inorg. Chim. Acta,* Cotton, F. A.; Lei, P.; Murillo, C. A.; "Linear trichromium(II) chains wrapped by unsymmetrical formamidinates", accepted for publication.

a Quantum Design SQUID (Superconducting Quantum Interference Device) Magnetometer MPMS-XL, with a field a 1000 Gauss as temperature was increased from 2 K to 300 K, or 400 K. A correction was made for the diamagnetic contribution prior to data analysis. Elemental analyses were performed by Canadian Microanalytical Service, Ltd., Canada.

Preparation of $Cr_3(PhPyF)_4Cl_2 \cdot CH_2Cl_2$, 15·$CH_2Cl_2$. The formamidine HPhPyF (394 mg, 2.00 mmol) was dissolved in 15 ml THF and placed in an acetone and dry ice cold bath. Then, 1.3 ml of 1.6 M MeLi was added slowly. The THF solution was allowed to warm up to ambient temperature after being stirred for 30 min in a cold bath. The solution was then transferred into a 100 ml flask charged with $CrCl_2$ (196 mg, 1.60 mmol), and the mixture was stirred for 1 h at room temperature. During this period, the color of the mixture changed from yellow to brown finally to dark-red. Refluxing was continued overnight, and after cooling, a precipitate was collected by filtration. This was washed with 3×15 ml ether, briefly dried under vacuum, and then 20 ml of CH_2Cl_2 were added. After filtration, hexanes (40 ml) were carefully layered on the top of CH_2Cl_2 solution. Dark-red crystals suitable for X-ray study were obtained after 6 days. Yield: 280 mg, 48%. Anal. Calcd for $C_{48}H_{40}Cl_2N_{12}Cr_3$: C, 56.98; H, 3.98; N, 16.61. Found: C, 56.63; H, 4.26; N, 16.22.

Preparation of $Cr_3(AniPyF)_4Cl_2$, 16. To HAniPyF (454 mg, 2.00 mmol) was added 15 ml of THF. The solution was cooled in an acetone and dry ice bath and neutralized by methyllithium (1.3 ml of 1.6 M MeLi solution). The solution was allowed to warm up to room temperature and then it was transferred via cannula to a flask with $CrCl_2$ (196 mg, 1.6 mmol). The mixture was stirred at room temperature for 1.5 h, then refluxed overnight given a dark-red solution. After cooling, 60 ml of hexanes was added to the THF solution with rapid stirring. A precipitate formed and it was collected by filtration, washed with 2×20 ml of hexanes, 3×20 ml

of ether, and dried under vacuum for 30 min. The solid then was washed with 2×2 ml of ethanol, and dried again under vacuum for 1 h. Then 15 ml of toluene was added to the solid, then filtered with the aid of Celite. Dark-red crystals suitable for crystallographic study formed by slow diffusion 40 ml of hexanes into the toluene solution. Yield: 290 mg, 48%. Anal. Calcd for $C_{52}H_{48}N_{12}O_4Cr_3Cl_2$: C, 55.18; H, 4.27; N,14.85. Found C, 55.49; H, 4.52; N,15.23.

Preparation of $Cr_3(TolPyF)_4Cl_2 \cdot 2H_2O$, 17·$2H_2O$. A solution of HTolPyF (422 mg, 2.00 mmol) in 15 ml of THF was deprotonated at -76 °C by addition of 1.3 ml of 1.6 M MeLi solution. After allowing the solution to warm up to the ambient temperature, it was transferred into another flask containing $CrCl_2$ (209 mg, 1.70 mmol). The mixture was stirred at room temperature for 1 h, then refluxed overnight. The THF was removed under vacuum. The remaining solid was washed with 30 ml of hot hexanes, 2×20 ml of ether, then briefly dried under vacuum. Then, 20 ml of toluene was added to the solid, and the mixture was filtered through a 2 cm column packed with Celite. Then 40 ml of hexanes was carefully layered on top of the toluene solution. After one week, dark-red crystals formed. Yield: 276 mg, 45%. Anal. Calcd for $C_{52}H_{48}N_{12}Cr_3Cl_2$: C, 58.48; H, 4.53; N, 15.74. Found: C, 58.02; H, 4.34; N, 15.46.

Preparation of $Cr_3(Ph^FPyF)_4Cl_2$, 18. A solution of MeLi (1.3 ml of 1.6 M) was slowly added to HPh^FPyF (410 mg, 2.00 mmol) in 15 ml of THF at −76 °C. After stirring for 30 min the solution was allowed to warm up. The deprotonated ligand was transferred to a 100 ml flask with $CrCl_2$ (209 mg, 1.70 mmol). The mixture was stirred for 1 h, then refluxed overnight. The solvent was removed under vacuum and the solid was washed with 30 ml of hexanes, 2×20 ml of ether, 2×5 ml of EtOH, then dried under vacuum. To this solid 20 ml of CH_2Cl_2 was added. Diffusion of 40 ml of hexanes into the CH_2Cl_2 solution produced dark-red crystals suitable for X-ray study after 2 weeks. Yield: 160 mg, 28%.

Preparation of $Cr_3(PhPcF)_4Cl_2$ (19a and 19b). A solution of HPhPcF (422 mg, 2.00 mmol) in 15 ml THF at −78 °C was added 1.3 ml of 1.6 M MeLi solution. After the temperature raised to ambient temperature, the resulting solution was transferred to a flask charged with $CrCl_2$ (209 mg, 1.70 mmol). Then the mixture was stirred for 1.5 h at room temperature and refluxed overnight. After cooling to room temperature, there was a solid present and a dark red solution. After filtration, the filtrate was saved and the solid was washed with 2×20 ml of ether, and briefly dried under vacuum. Then 20 ml of toluene was added to the solid, and the mixture was filtered. Dark red crystals of unsymmetrical $Cr_3(PhPcF)_4Cl_2$ (**19a**·THF·$(C_6H_{14})_{0.5}$) were obtained by slow diffusion of 40 ml of hexanes into toluene for 8 days. Yield: 170 mg, 39%. Anal. Calcd. for $C_{52}H_{48}N_{12}Cr_3Cl_2$: C, 58.48; H, 4.53; N, 15.74. Found: C, 59.03; H, 4.72; N, 16.05. To the filtrate, 15 ml of ether was slowly added. The solution was concentrated by allowing some solvent to evaporate slowly under N_2. Dark red crystals of symmetrical $Cr_3(PhPcF)_4Cl_2$ (**19b**·THF·$(Et_2O)_{0.61}$) formed after 2 weeks. Yield: 38 mg, 5%.

CRYSTALLOGRAPHIC STUDIES

For the X-ray structural studies, each crystal was mounted on a quartz fiber with a small amount of grease and transferred to a goniometer head. Data were collected on a Bruker SMART 1000 CCD area detector system. Cell parameters were obtained using SMART[18] software. Data were corrected for Lorentz and polarization effects using the program SAINTPLUS.[19] Absorption corrections were applied using SADABS.[20] The position of the heavy atoms were found by the direct methods program in SHELXTL.[21] Subsequent cycles of least-squares refinements followed by difference Fourier syntheses revealed the positions of the non-hydrogen atoms. All hydrogen

atoms were included in idealized positions.

Crystallographic data for **15**·CH_2Cl_2, **16**, **17**·$2H_2O$, **18**, **19a**·THF·$(C_6H_{14})_{0.5}$ and **19b**·THF·$(Et_2O)_{0.61}$ are given in Tables XVI, XVII, XVIII, XIX, XX and XXI receptively; selected bond distances and angles for **15**·CH_2Cl_2, **16**, **17**·$2H_2O$, **18**, **19a**·THF·$(C_6H_{14})_{0.5}$ and **19b**·THF·$(Et_2O)_{0.61}$ are listed in Tables XXII, XXIII, XXIV, XXV, XXVI and XXVII, respectively.

RESULTS AND DISCUSSION

Synthetic considerations. The strategy involved in the preparation of these linear trichromium compounds with unsymmetrical formamidines was straightforward, and consisted in reacting anhydrous $CrCl_2$ with the lithium salts of the corresponding unsymmetrical formamidine in THF under reflux according to the following equation..

$$3CrCl_2 + 4LiArPyF \longrightarrow Cr_3(ArPyF)_4Cl_2 + 4LiCl$$

Since the substituents on the formamidines changed the solubility of the trinuclear species, distinct separation procedures for different compounds, as described in experimental section, were needed. For example, $Cr_3(PhPyF)_4Cl_2$ was precipitated from THF while $Cr_3(AniPyF)_4Cl_2$ was very soluble in THF.

Table XVI. Crystal Data and Structure Refinement for **15**·CH_2Cl_2

Empirical formula	$C_{49}H_{42}Cl_4Cr_3N_{12}$	
Formula weight	1096.75	
Temperature	213(2) K	
Wavelength	0.71073 Å	
Crystal system	Tetragonal	
Space group	$P4_32_12$	
Unit cell dimensions	a = 15.0065(6) Å	α = 90˚
	b = 15.0065(6) Å	β = 90 ˚
	c = 43.425(3) Å	γ = 90 ˚
Volume	9779.1(8) Å^3	
Z	8	
Density (calculated)	1.490 g/mm^3	
Absorption coefficient	0.923 mm^{-1}	
Crystal size	0.43 x 0.37 x 0.35 mm	
Instrument for data collections	Bruker SMART 1000	
Theta range for data collection	3.30 to 27.21˚	
Reflections collected	49613	
Independent reflections	10154 [R(int) = 0.0415]	
Scan Method	ω-scan	
Refinement method	Full-matrix least-squares on F^2	
Data / restraints / parameters	10154 / 0 / 629	
Goodness-of-fit on F^2	1.130	
Final R indices [$I > 2\sigma(I)$]	$R1$ = 0.0463, $wR2$ = 0.1036	
R indices (all data)	$R1$ = 0.0537, $wR2$ = 0.1073	
Absolute structure parameter	0.01(2)	
Largest Shift / esd, final cycle	0.012	
Largest diff. peak and hole	0.572 and -0.606 e/Å^3	

Table XVII. Crystal Data and Structure Refinement for **16**

Empirical formula	$C_{52}H_{48}Cl_2Cr_3N_{12}O_4$
Formula weight	1131.92
Temperature	213(2) K
Wavelength	0.71073 Å
Crystal system	Monoclinic
Space group	$P2_1/c$
Unit cell dimensions	a = 13.1076(9) Å α = 90˚
	b = 13.5283(9) Å β = 95.070(1)˚
	c = 28.566(2) Å γ = 90˚
Volume	5045.6(6) $Å^3$
Z	4
Density (calculated)	1.490 g/mm^3
Absorption coefficient	0.800 mm^{-1}
Crystal size	0.36 x 0.30 x 0.24 mm
Instrument for data collections	Bruker SMART 1000
Theta range for data collection	2.02 to 27.56˚.
Reflections collected	31797
Independent reflections	11529 [R(int) = 0.0319]
Scan Method	ω-scan
Refinement method	Full-matrix least-squares on F^2
Data / restraints / parameters	11516 / 0 / 658
Goodness-of-fit on F^2	1.079
Final R indices [$I > 2\sigma(I)$]	$R1$ = 0.0431, $wR2$ = 0.1057
R indices (all data)	$R1$ = 0.0732, $wR2$ = 0.1305
Largest Shift / esd, final cycle	0.001
Largest diff. peak and hole	0.728 and -0.387 e/$Å^3$

Table XVIII. Crystal Data and Structure Refinement for **17**·2H_2O

Empirical formula	$C_{52}H_{52}Cl_2Cr_3N_{12}O_2$
Formula weight	1103.96
Temperature	213(2) K
Wavelength	0.71073 Å
Crystal system	Orthombic
Space group	*Pccn*
Unit cell dimensions	a = 16.271(2) Å α = 90˚
	b = 16.554(2) Å β = 90˚
	c = 19.266(2) Å γ = 90˚
Volume	5189.3(11) $Å^3$
Z	4
Density (calculated)	1.413 g/mm^3
Absorption coefficient	0.773 mm^{-1}
Crystal size	0.34 x 0.15 x 0.10 mm
Instrument for data collections	Bruker SMART 1000
Theta range for data collection	1.75 to 25.00˚
Reflections collected	25856
Independent reflections	4572 [*R*(int) = 0.0825]
Scan Method	ω-scan
Refinement method	Full-matrix least-squares on F^2
Data / restraints / parameters	4249 / 0 / 321
Goodness-of-fit on F^2	1.061
Final *R* indices [$I > 2\sigma(I)$]	*R*1 = 0.0626, *wR*2 = 0.1601
R indices (all data)	*R*1 = 0.1080, *wR*2 = 0.2181
Largest Shift / esd, final cycle	0.000
Largest diff. peak and hole	1.254 and -0.423 e/$Å^3$

Table XIX. Crystal Data and Structure Refinement for **18**

Empirical formula	$C_{48}H_{36}Cl_2Cr_3F_4N_{12}$	
Formula weight	1083.79	
Temperature	213(2) K	
Wavelength	0.71073 Å	
Crystal system	Triclininc	
Space group	$P\bar{1}$	
Unit cell dimensions	a = 9.467(2) Å	α = 85.757(5)˚
	b = 12.808(3) Å	β = 81.403(4)˚
	c = 19.948(5) Å	γ = 80.891(4)˚
Volume	2358.1(10) Å^3	
Z	2	
Density (calculated)	1.526 g/mm^3	
Absorption coefficient	0.858 mm^{-1}	
Crystal size	0.59 x 0.35 x 0.19 mm	
Instrument for data collections	Bruker SMART 1000	
Theta range for data collection	1.87 to 25.04˚	
Reflections collected	10282	
Independent reflections	7549 [R(int) = 0.0318]	
Scan Method	ω-scan	
Refinement method	Full-matrix least-squares on F^2	
Data / restraints / parameters	7545 / 0 / 657	
Goodness-of-fit on F^2	1.057	
Final R indices [$I > 2\sigma(I)$]	$R1$ = 0.0902, $wR2$ = 0.2322	
R indices (all data)	$R1$ = 0.1225, $wR2$ = 0.2692	
Largest Shift / esd, final cycle	- 0.099	
Largest diff. peak and hole	1.716 and -1.265 e/Å^3	

Table XX. Crystal Data and Structure Refinement for **19a**·THF·$(C_6H_{14})_{0.5}$

Empirical formula	$C_{59}H_{63}Cl_2Cr_3N_{12}O$
Formula weight	1183.11
Temperature	213(2) K
Wavelength	0.71073 Å
Crystal system	*C2/c*
Space group	Monoclinic
Unit cell dimensions	a = 45.771(3) Å α = 90˚
	b = 11.1140(7) Å β = 99.464(1)˚
	c = 22.7263(14) Å γ = 90˚
Volume	11403.5(12) $Å^3$
Z	8
Density (calculated)	1.378 g/mm^3
Absorption coefficient	0.707 mm^{-1}
Crystal size	0.22 x 0.12 x 0.12 mm
Instrument for data collections	Bruker SMART 1000
Theta range for data collection	1.80 to 25.05˚
Reflections collected	29261
Independent reflections	10053 [*R*(int) = 0.0489]
Scan Method	ω-scan
Refinement method	Full-matrix least-squares on F^2
Data / restraints / parameters	10053 / 0 / 695
Goodness-of-fit on F^2	1.066
Final *R* indices [$I > 2\sigma(I)$]	*R*1 = 0.0703, *wR*2 = 0.1934
R indices (all data)	*R*1 = 0.1251, *wR*2 = 0.2332
Largest Shift / esd, final cycle	- 0.07
Largest diff. peak and hole	1.193 and -0.502 $e.Å^{-3}$

Table XXI. Crystal Data and Structure Refinement for **19b**·THF·$(Et_2O)_{0.61}$

Empirical formula	$C_{58.44}H_{66.10}Cl_2Cr_3N_{12}O_{1.61}$	
Formula weight	1188.14	
Temperature	213(2) K	
Wavelength	0.71073 Å	
Crystal system	Monoclinic	
Space group	*P2/n*	
Unit cell dimensions	a = 11.338(1) Å	α = 90˚
	b = 11.194(1) Å	β = 99.569(2)˚
	c = 22.262(2) Å	γ = 90˚
Volume	2785.9(5) $Å^3$	
Z	2	
Density (calculated)	1.311 g/mm^3	
Absorption coefficient	0.720 mm^{-1}	
Crystal size	0.45 x 0.38 x 0.36 mm	
Instrument for data collections	Bruker SMART 1000	
Theta range for data collection	1.90 to 27.52˚	
Reflections collected	17120	
Independent reflections	6324 [*R*(int) = 0.0417]	
Scan Method	ω-scan	
Refinement method	Full-matrix least-squares on F^2	
Data / restraints / parameters	6324 / 6 / 348	
Goodness-of-fit on F^2	1.044	
Final *R* indices [$I > 2\sigma(I)$]	*R*1 = 0.0763, *wR*2 = 0.2095	
R indices (all data)	*R*1 = 0.1357, *wR*2 = 0.2561	
Largest Shift / esd, final cycle	0.0918	
Largest diff. peak and hole	1.157 and -1.239 e/$Å^3$	

Table XXII. Selected Bond Lengths (Å) and Angles (˚) for **15**·CH_2Cl_2

Cr(3)—Cr(2)	2.4602(8)	Cr(1)—Cr(2)	2.4380(8)
Cr(3)—Cl(2)	2.485(1)	Cr(1)—Cl(1)	2.473(1)
Cr(3)—N(9)	2.132(3)	Cr(3)—N(6)	2.112(3)
Cr(3)—N(3)	2.160(3)	Cr(3)—N(12)	2.119(3)
Cr(1)—N(7)	2.103(3)	Cr(2)—N(2)	2.015(3)
Cr(1)—N(1)	2.132(3)	Cr(2)—N(5)	2.018(3)
Cr(1)—N(10)	2.147(3)	Cr(2)—N(11)	2.030(3)
Cr(1)—N(4)	2.166(3)	Cr(2)—N(8)	2.038(3)
N(3)—Cr(3)—Cr(2)	84.52(8)	N(9)—Cr(3)—Cl(2)	96.69(8)
N(6)—Cr(3)—Cl(2)	96.47(8)	N(3)—Cr(3)—Cl(2)	94.36(8)
N(12)—Cr(3)—Cl(2)	97.71(9)	Cr(2)—Cr(3)—Cl(2)	177.7(4)
N(1)—Cr(1)—Cl(1)	96.34(9)	N(7)—Cr(1)—N(10)	88.4(1)
N(6)—Cr(3)—N(12)	89.9(1)	N(1)—Cr(1)—N(10)	166.9(1)
N(6)—Cr(3)—N(9)	166.8(1)	N(7)—Cr(1)—N(4)	167.8(1)
N(12)—Cr(3)—N(9)	89.0(1)	N(1)—Cr(1)—N(4)	92.7(1)
N(6)—Cr(3)—N(3)	90.8(1)	N(10)—Cr(1)—N(4)	87.0(1)
N(12)—Cr(3)—N(3)	167.8(1)	N(7)—Cr(1)—Cr(2)	83.39(9)
N(9)—Cr(3)—N(3)	87.6(1)	N(1)—Cr(1)—Cr(2)	82.46(8)
N(6)—Cr(3)—Cr(2)	81.52(8)	N(10)—Cr(1)—Cr(2)	84.49(8)
N(12)—Cr(3)—Cr(2)	83.50(8)	N(4)—Cr(1)—Cr(2)	84.92(8)
N(9)—Cr(3)—Cr(2)	85.31(8)	N(7)—Cr(1)—Cl(1)	97.28(9)

Table XXIII. Selected Bond Lengths (Å) and Angles (˚) for **16**

Cr(1)—Cr(2)	2.4789(7)	Cr(2)—Cr(3)	2.4759(7)
Cr(1)—Cl(1)	2.4814(9)	Cr(3)—Cl(2)	2.4814(9)
Cr(1)—N(1)	2.149(3)	Cr(1)—N(6)	2.092(2)
Cr(1)—N(10)	2.164(2)	Cr(1)—N(9)	2.109(2)
Cr(2)—N(8)	2.014(2)	Cr(3)—N(12)	2.105(2)
Cr(2)—N(11)	2.016(2)	Cr(3)—N(3)	2.115(2)
Cr(2)—N(2)	2.035(2)	Cr(3)—N(4)	2.148(2)
Cr(2)—N(5)	2.037(2)	Cr(3)—N(7)	2.183(2)
N(6)—Cr(1)—N(9)	88.95(9)	N(6)—Cr(1)—Cl(1)	97.40(7)
N(6)—Cr(1)—N(1)	89.35(9)	N(9)—Cr(1)—Cl(1)	97.78(7)
N(9)—Cr(1)—N(1)	168.0(1)	N(1)—Cr(1)—Cl(1)	94.27(7)
N(6)—Cr(1)—N(10)	167.35(9)	N(10)—Cr(1)—Cl(1)	95.24(7)
N(9)—Cr(1)—N(10)	88.95(9)	Cr(2)—Cr(1)—Cl(1)	178.73(3)
N(1)—Cr(1)—N(10)	90.11(9)	N(8)—Cr(2)—N(11)	88.9(1)
N(6)—Cr(1)—Cr(2)	83.49(7)	N(8)—Cr(2)—N(2)	178.5(1)
N(9)—Cr(1)—Cr(2)	83.12(7)	N(11)—Cr(2)—N(2)	89.7(1)
N(1)—Cr(1)—Cr(2)	84.84(7)	N(8)—Cr(2)—N(5)	90.0(1)
N(10)—Cr(1)—Cr(2)	83.87(7)	N(11)—Cr(2)—N(5)	178.9(1)
N(2)—Cr(2)—Cr(3)	89.12(7)	N(2)—Cr(2)—N(5)	91.5(1)
N(5)—Cr(2)—Cr(3)	89.32(7)	N(8)—Cr(2)—Cr(3)	91.28(7)
N(8)—Cr(2)—Cr(1)	90.46(7)	N(11)—Cr(2)—Cr(3)	90.98(7)

Table XXIV. Selected Bond Lengths (Å) and Angles (˚) for **17**·2H_2O [a]

Cr(1)—Cr(2)	2.4298(9)	Cr(2)—Cr(1)#1	2.4298(9)
Cr(1)—Cl(1)	2.524(2)	Cr(1)—N(5)	2.149(4)
Cr(1)—N(4)	2.125(4)	Cr(2)—N(6)#1	2.014(4)
Cr(1)—N(2)	2.133(4)	Cr(2)—N(6)	2.014(4)
Cr(1)—N(3)	2.141(4)	Cr(2)—N(1)	2.026(4)
N(4)—Cr(1)—N(2)	166.4(2)	Cr(2)—Cr(1)—Cl(1)	177.44(5)
N(4)—Cr(1)—N(3)	93.5(2)	N(6)—Cr(2)—N(1)	90.6(2)
N(2)—Cr(1)—N(3)	90.8(2)	N(6)—Cr(2)—Cr(1)	91.2(1)
N(4)—Cr(1)—N(5)	84.4(2)	N(1)—Cr(2)—Cr(1)	89.7(1)
N(2)—Cr(1)—N(5)	88.7(2)	C(1)—N(1)—C(2)	120.8(4)
N(3)—Cr(1)—N(5)	168.3(2)	C(1)—N(1)—Cr(2)	119.0(3)
N(4)—Cr(1)—Cr(2)	83.2(1)	C(2)—N(1)—Cr(2)	120.3(3)
N(2)—Cr(1)—Cr(2)	84.3(1)	C(21)—N(6)—C(22)	121.7(4)
N(3)—Cr(1)—Cr(2)	85.4(1)	C(21)—N(6)—Cr(2)	118.4(3)
N(5)—Cr(1)—Cr(2)	82.9(1)	C(22)—N(6)—Cr(2)	118.7(3)
N(4)—Cr(1)—Cl(1)	96.5(1)	C(14)—N(4)—Cr(1)	119.8(3)
N(2)—Cr(1)—Cl(1)	95.7(1)	N(2)—C(2)—N(1)	115.9(4)
N(3)—Cr(1)—Cl(1)	97.2(1)	N(2)—C(2)—C(3)	119.6(5)
N(5)—Cr(1)—Cl(1)	94.5(1)	N(1)—C(2)—C(3)	124.4(5)
C(26)—N(5)—Cr(1)	116.4(3)	C(26)—N(5)—C(22)	118.9(4)

[a] Symmetry transformations used to generate equivalent atoms: #1 -x+1/2,-y+3/2,z.

Table XXV. Selected Bond Lengths (Å) and Angles (˚) for **18**

Cr(1)—Cr(3)	2.500(1)	Cr(1)—Cr(2)	2.460(1)
Cr(3)—Cl(2)	2.498(2)	Cr(2)—Cl(1)	2.498(2)
Cr(1)—N(5)	2.029(6)	Cr(2)—N(12)	2.120(6)
Cr(1)—N(2)	2.034(6)	Cr(2)—N(4)	2.138(7)
Cr(1)—N(11)	2.038(6)	Cr(2)—N(1)	2.146(6)
Cr(1)—N(8)	2.045(6)	Cr(2)—N(9)	2.102(6)
Cr(3)—N(3)	2.107(7)	Cr(3)—N(10)	2.116(6)
Cr(3)—N(6)	2.110(7)	Cr(3)—N(7)	2.128(7)
N(5)—Cr(1)—N(2)	179.3(3)	N(5)—Cr(1)—Cr(3)	89.8(2)
N(5)—Cr(1)—N(11)	90.4(3)	N(2)—Cr(1)—Cr(3)	90.2(2)
N(2)—Cr(1)—N(11)	88.9(3)	N(11)—Cr(1)—Cr(3)	88.6(2)
N(5)—Cr(1)—N(8)	91.0(3)	N(8)—Cr(1)—Cr(3)	88.6(2)
N(2)—Cr(1)—N(8)	89.7(3)	Cr(2)—Cr(1)—Cr(3)	179.08(6)
N(11)—Cr(1)—N(8)	176.9(2)	N(9)—Cr(2)—N(12)	167.5(2)
N(5)—Cr(1)—Cr(2)	89.3(2)	N(9)—Cr(2)—N(4)	90.1(3)
N(2)—Cr(1)—Cr(2)	90.7(2)	N(12)—Cr(2)—N(4)	89.6(3)
N(11)—Cr(1)—Cr(2)	91.1(2)	N(9)—Cr(2)—N(1)	87.7(3)
N(8)—Cr(1)—Cr(2)	91.7(2)	N(12)—Cr(2)—N(1)	90.5(3)
N(12)—Cr(2)—Cr(1)	84.1(2)	N(4)—Cr(2)—N(1)	170.8(2)
N(4)—Cr(2)—Cr(1)	85.9(2)	N(9)—Cr(2)—Cr(1)	83.4(2)

Table XXVI. Selected Bond Lengths (Å) and Angles (˚) for **19a**·THF·$(C_6H_{14})_{0.5}$

Cr(1)—Cr(3)	2.216(1)	Cr(1)—Cr(2)	2.646(1)
Cr(3)—Cl(4)	2.493(2)	Cr(2)—Cl(5)	2.467(2)
Cr(1)—N(2)	2.020(5)	Cr(2)—N(9)	2.105(5)
Cr(1)—N(5)	2.026(4)	Cr(2)—N(6)	2.134(4)
Cr(1)—N(11)	2.035(5)	Cr(2)—N(12)	2.161(5)
Cr(1)—N(8)	2.051(5)	Cr(2)—N(1)	2.163(5)
Cr(3)—N(3)	2.096(5)	Cr(3)—N(7)	2.132(5)
Cr(3)—N(10)	2.128(5)	Cr(3)—N(4)	2.167(5)
N(2)—Cr(1)—N(5)	89.3(2)	N(2)—Cr(1)—Cr(2)	86.6(1)
N(2)—Cr(1)—N(11)	175.1(2)	N(5)—Cr(1)—Cr(2)	87.2(1)
N(5)—Cr(1)—N(11)	89.0(2)	N(11)—Cr(1)—Cr(2)	88.7(1)
N(2)—Cr(1)—N(8)	90.9(2)	N(8)—Cr(1)—Cr(2)	85.1(1)
N(5)—Cr(1)—N(8)	172.3(2)	Cr(3)—Cr(1)—Cr(2)	177.50(5)
N(11)—Cr(1)—N(8)	90.2(2)	N(9)—Cr(2)—N(6)	164.5(2)
N(2)—Cr(1)—Cr(3)	93.6(1)	N(9)—Cr(2)—N(12)	86.3(2)
N(5)—Cr(1)—Cr(3)	95.3(1)	N(6)—Cr(2)—N(12)	91.9(2)
N(11)—Cr(1)—Cr(3)	91.2(1)	N(9)—Cr(2)—N(1)	88.8(2)
N(8)—Cr(1)—Cr(3)	92.4(1)	N(6)—Cr(2)—N(1)	87.9(2)

Table XXVII. Selected Bond Lengths (Å) and Angles (˚) for **19b**·THF·$(Et_2O)_{0.61}$ [a]

Cr(1)—Cr(2)	2.4743(8)	Cr(1)—Cr(2)#1	2.4743(8)
Cr(2)—N(6)#1	2.116(5)	Cr(1)—N(2)	2.020(4)
Cr(2)—N(3)#1	2.118(4)	Cr(1)—N(2)#1	2.020(4)
Cr(2)—N(4)	2.129(5)	Cr(1)—N(5)#1	2.026(4)
Cr(2)—N(1)	2.164(4)	Cr(1)—N(5)	2.026(4)
Cr(2)—Cl(1)	2.480(1)		
N(2)—Cr(1)—N(5)	89.30(18)	C(14)—N(4)—Cr(2)	119.6(4)
N(2)—Cr(1)—Cr(2)	90.00(11)	C(18)—N(4)—Cr(2)	123.0(4)
N(5)—Cr(1)—Cr(2)	87.85(12)	C(19)—N(5)—Cr(1)	117.0(4)
N(4)—Cr(2)—N(1)	84.59(17)	C(18)—N(5)—Cr(1)	123.2(3)
N(4)—Cr(2)—Cr(1)	85.71(12)	N(1)—Cr(2)—Cl(1)	95.30(11)
N(1)—Cr(2)—Cr(1)	84.80(11)	Cr(1)—Cr(2)—Cl(1)	178.16(5)
N(4)—Cr(2)—Cl(1)	96.12(12)	C(1)—N(1)—Cr(2)	119.2(3)
C(6)—N(2)—Cr(1)	116.2(3)	C(5)—N(1)—Cr(2)	123.1(3)
C(5)—N(2)—Cr(1)	123.7(3)		

[a] Symmetry transformations used to generate equivalent atoms: #1 -x+3/2,y,-z+1/2

Structural studies. All compounds have a linear trichromium chain wrapped by four supporting ligands with two chloride ions on each end. These have much in common except for small differences in distances between the Cr atoms and the ligand conformations. All Cr–N distances for the central nitrogen atoms are slightly shorter (2.02 - 2.04 Å) than those for the end nitrogen atoms (2.12 - 2.14 Å). All Cr–Cl distances are long and about the same length, ranging between 2.47 Å and 2.52 Å. The ligands are non-planar in all six cases, even though they do not have to. A summary of important structural results for six compounds is presented in Table XXVIII. We shall now discuss the results individually.

$Cr_3(PhPyF)_4Cl_2$. This compound crystallized in space group *$P4_32_12$*. The molecular structure, shown in Figure 19, reveals that the Cr_3^{6+} core is wrapped by four formamidinate ligands with one chloride ion on each end. The surrounding ligands have a *cisoid* relationship to each other. The distances between chromium atoms, 2.4380(8) Å and 2.4602(8) Å, do not differ by a chemically significant amount. The possibility of a disordered metal chain was carefully excluded. Thus, the Cr_3^{6+} unit is essentially symmetrical. The end-view down the metal chain, shown in Figure 20, indicates that there is still a considerable torsion angle of 34.9°.

$Cr_3(AniPyF)_4Cl_2$. This compound crystallized from a mixture of hexanes and toluene in space group *$P2_1/c$*, with all atoms occupying general positions. The Cr···Cr separations are 2.4789(7) Å and 2.4759(7)) Å; considering the standard deviations, those distances are in fact the same. The four surrounding ligands again adopt a *cisoid* relationship, as shown in Figure 21. The ligands are not flat, and the molecule has an overall torsion angle of 29.3°.

$Cr_3(TolPyF)_4Cl_2$. This compound crystallized in space group *Pccn*. There is a two-fold bisecting the molecule, and the trichromium chain is rigorously symmetrical with Cr···Cr separations of 2.4298(8) Å. Again, disorder was carefully excluded. The four supporting ligands

have a *cisoid* relationship and they are twisted by *ca.* 37.5° between terminal chromiums atom. The interstitial water molecules found in these crystals have an adventitious origin.

$Cr_3(Ph^FPyF)_4Cl_2$. This compound crystallized in space group $P\bar{1}$. It has a linear, nearly symmetrical trichromium chain. The distances between chromium atoms are 2.460(1) Å and 2.500(1) Å, and the ligands are in *transoid* relation to each other. The overall torsion angle is *ca.* 27.9°.

$Cr_3(PhPcF)_4Cl_2$. Two types of crystals were obtained when $CrCl_2$ was treated with the lithium salt of *N,N′*-phenylpicolylformamidine (its anion is abbreviated as PhPcF). The most abundant type were in space group *C2/c,* and the molecules are the 3-1 regioisomer, with three picoline groups on the one end and the fourth picoline group at the other end as shown in Figure 22. The structure of the other crystal was determined in space group *P2/n,* and the molecules are the 2:2 *cisoid* regioisomer with four ligands *cis* to each other, as shown in Figure 23. The difference between the two structures goes beyond the ligand configuration. Actually, the distances between the chromium atoms in the two structures are very different. In the 3:1 regioisomer, the separations between chromium atoms are 2.216(1) Å and 2.646(1) Å. The bonding can be interpreted as two chromium atoms being paired together to form a long quadruple bond with a separate chromium atom at a distance of 2.646(1) Å. However, in the *cisoid* isomer of $Cr_3(PhPcF)_4Cl_2$, the chromium chain is symmetrical with Cr–Cr separations of 2.4743(8) Å. In both cases, there are considerable torsion angles of 30.0 and 33.6°.

Table XXVIII. Selected Structural Parameters for All Compounds with Cr_3^{6+} Wrapped by Unsymmetrical Formamidine [a]

	$Cr_3(PhPyF)_4Cl_2$	$Cr_3(AniPyF)_4Cl_2$	$Cr_3(TolPyF)_4Cl_2$	$Cr_3(Ph^FPyF)_4Cl_2$	$Cr_3(PhPcF)_4Cl_2$	$Cr_3(PhPcF)_4Cl_2$
Conformation	2:2, *cisoid*	2:2, *cisoid*	2:2, *cisoid*	2:2, *transoid*	2:2, *cisoid*	3:1
Cr_3^{6+} chain[b]	*s*	*s*	*s*	*s*	*s*	*u*
Cr–Cr, Å	2.4380(8) 2.4602(8)	2.4789(7) 2.4759(7)	2.4298(9) 2.4298(9)	2.460(1) 2.500(1)	2.4743(8) 2.4743(8)	2.216(1) 2.646(1)
Cr–Cl, Å	2.473(1) 2.485(1)	2.4814(9) 2.4814(9)	2.524(2) 2.524(2)	2.498(2) 2.498(2)	2.480(1) 2.480(1)	2.467(2) 2.493(2)
$Cr–N_{central}$, Å	2.025[3]	2.2026[3]	2.020[4]	2.037[6]	2.024[4]	2.034[5]
$Cr–N_{end}$, Å	2.134[3]	2.134[4]	2.137[4]	2.121[7]	2.132[4]	2.137[6]
Torsion angle, °	34.9	29.3	37.5	27.9	30.0	33.6

[a]The values in square parentheses are esds for average values. [b]*s* = symmetrical, *u* = unsymmetrical.

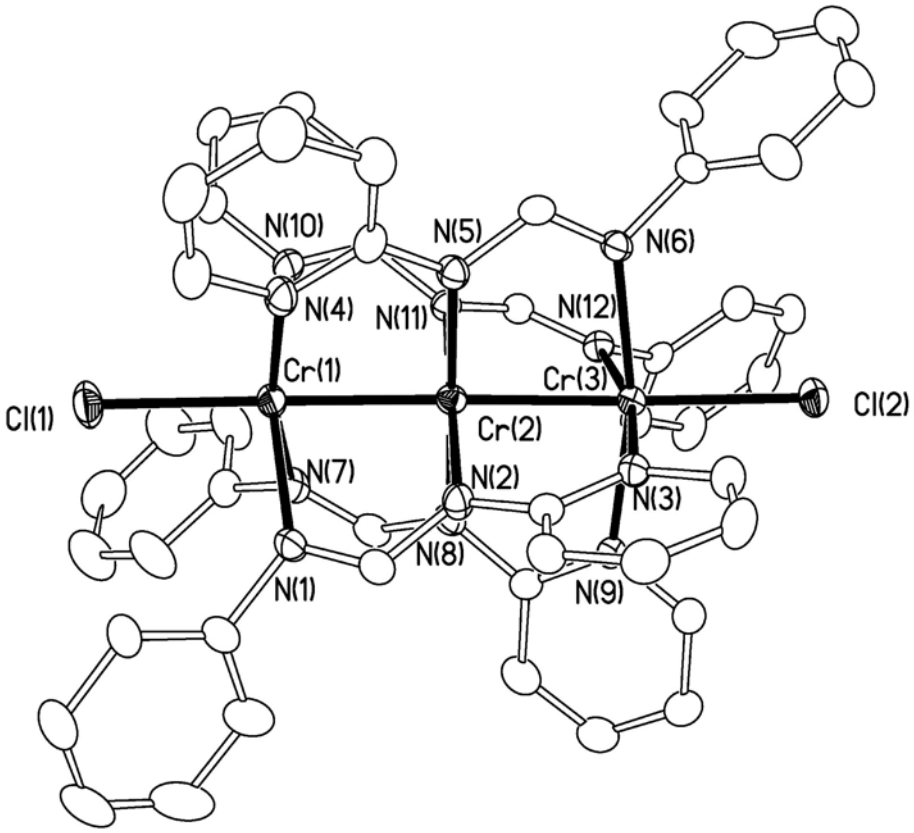

Figure 19. Perspective view of $Cr_3(PhPyF)_4Cl_2$ in **15**·CH_2Cl_2. Atoms are drawn at the 45% probability level and hydrogen atoms are omitted for clarity.

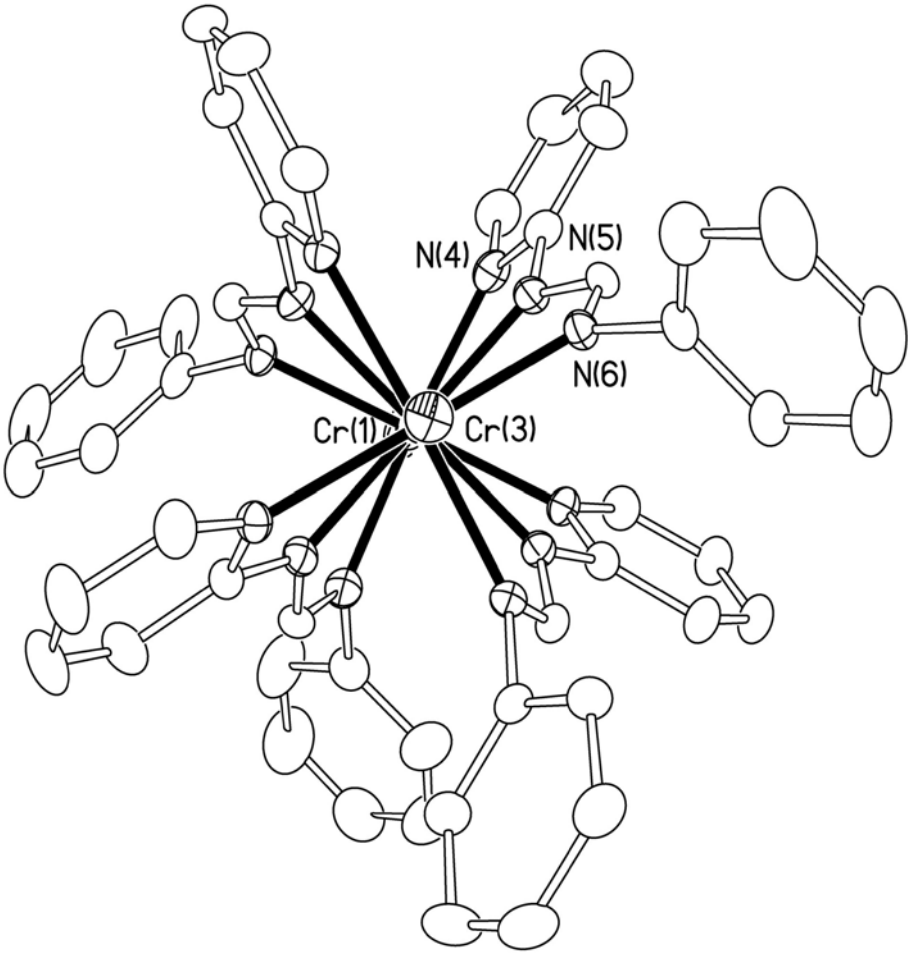

Figure 20. A view of $Cr_3(PhPyF)_4Cl_2$ looking down the Cr_3 axis. Atoms are at the 45% probability level and hydrogen atoms are omitted.

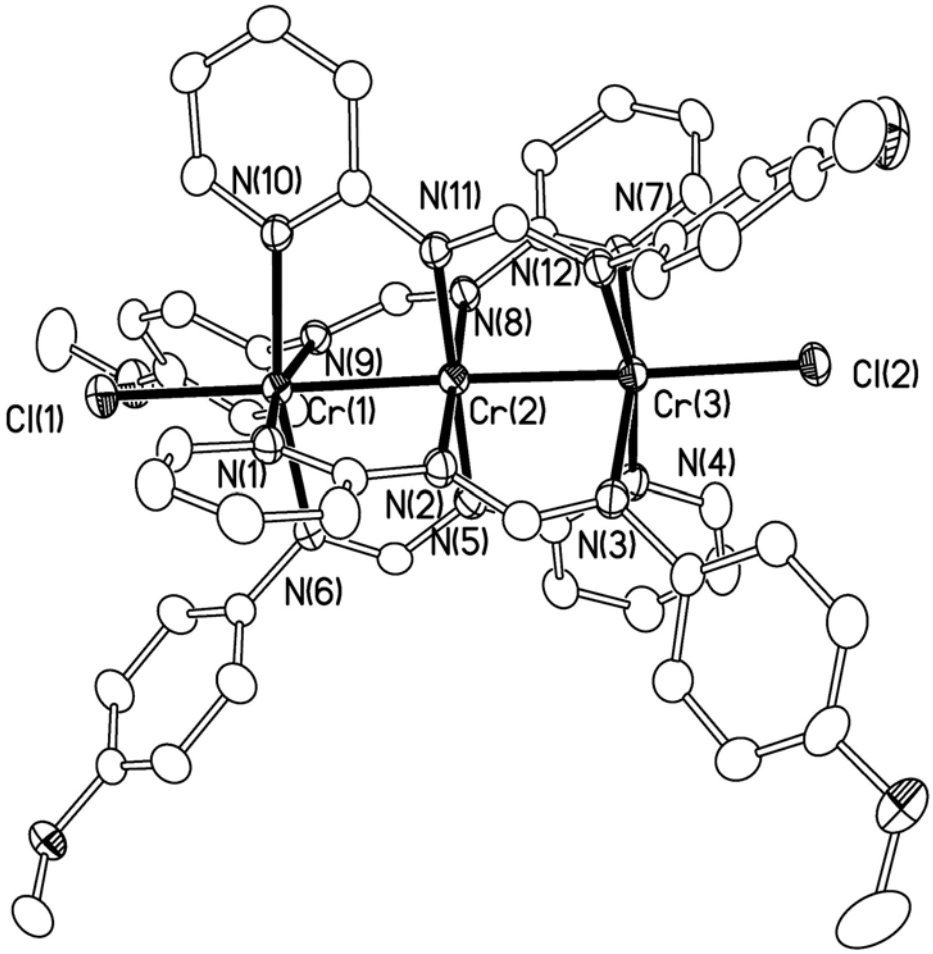

Figure 21. Perspective view of $Cr_3(AniPyF)_4Cl_2$ with ellipsoids drawn at the 45% probability level.

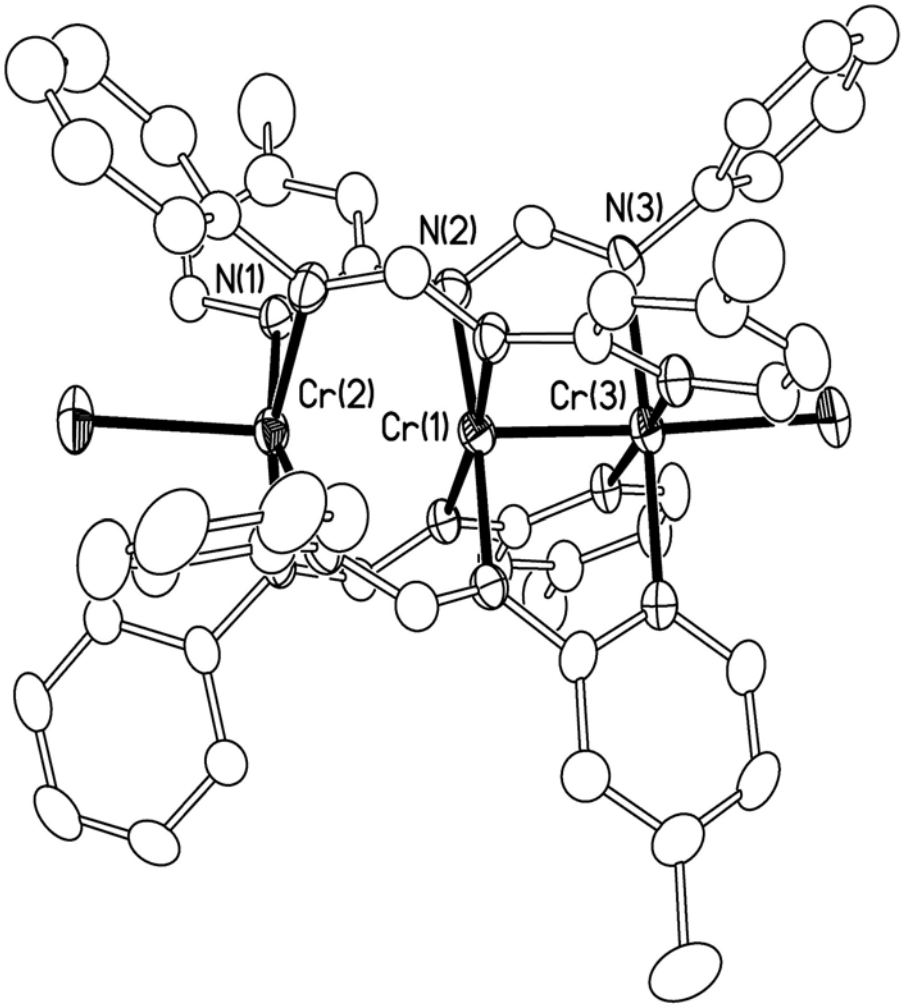

Figure 22. A representation of the 3:1 regioisomer of $Cr_3(PhPcF)_4Cl_2$ showing the unsymmetrical trichromium chain. Atoms are drawn with the 40% probability ellipsoids and hydrogen atoms are omitted.

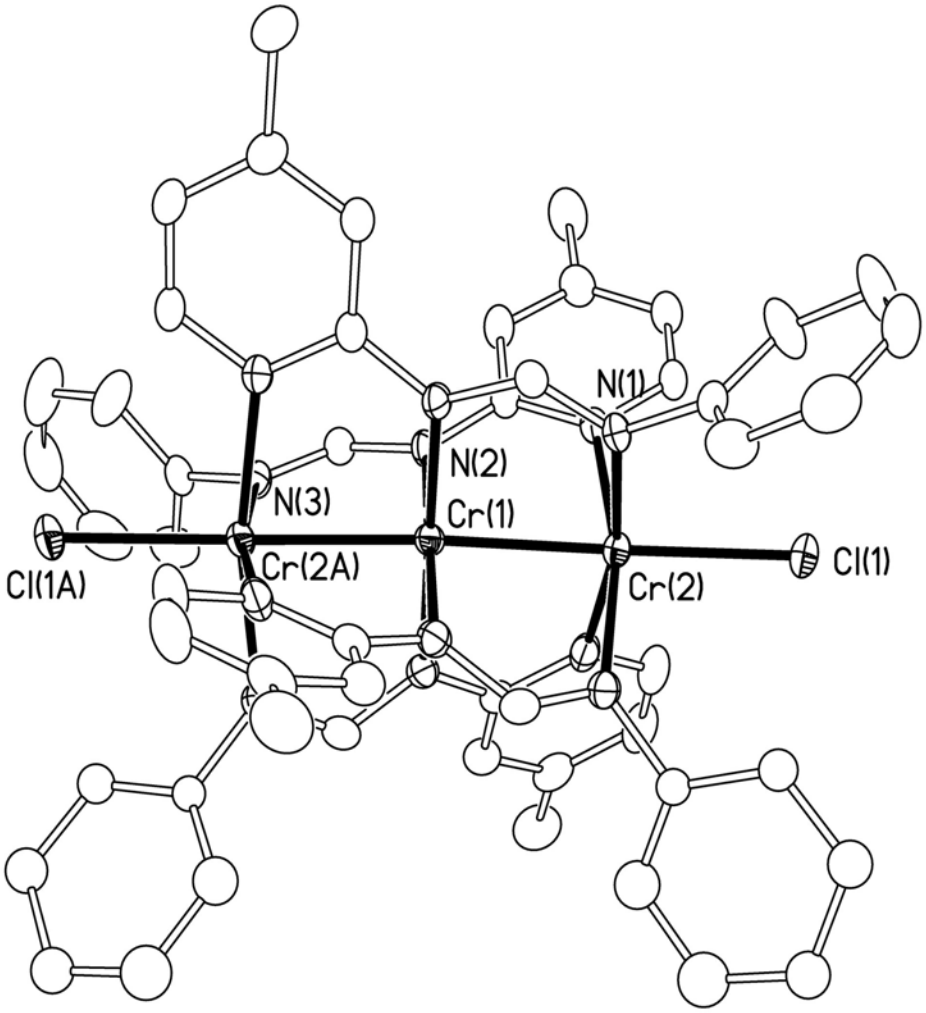

Figure 23. Perspective view of *cisoid* isomer of $Cr_3(PhPcF)_4Cl_2$ showing a symmetrical chromium chain with atoms drawn at the 40% probability level. Hydrogen atoms are omitted for clarity.

Magnetism. The magnetism of four compounds, $Cr_3(PhPyF)_4Cl_2$, $Cr_3(AnsiPyF)_4Cl_2$, as well as both isomers of $Cr_3(PhPcF)_4Cl_2$ has been measured. These include three symmetrical and the only unsymmetrical unit in this series. We show the results in Figure 24 for both forms of $Cr_3(PhPcF)_4Cl_2$; the other magnetic results are available Appendix I. All these compounds obey the Curie-Weiss law in the measured temperature range and display simple paramagnetism. For example, for the compound $Cr_3(PhPyF)_4Cl_2$, the experimental data were taken from 2 K to 400 K (the limits of the apparatus), and were fitted very closely to the Curie-Weiss equation after a diamagnetic contribution was included. The Curie constant is 2.90 emu*K*mol^{-1} and the Weiss constant is -1.4 K. The value of μ_{eff}, which is constant from 10 K to 400 K, is 4.78(2) μ_B; the corresponding *g* value is 1.97. All these clearly indicate that this and the other symmetrical compounds have a ground state with four unpaired electrons. All magnetic data are collected in Table XXIX. Although not measured, we feel confident that the magnetic behavior of the other two compounds, $Cr_3(TolPyF)_4Cl_2$ and $Cr_3(Ph^FPyF)_4Cl_2$, should be very similar to those of the three symmetrical ones, in view of the close structural similarities.

Table XXIX. Magnetic Data

Compound	μ_{eff} (μ_B)	Curie constant (emu*K*mol^{-1})	Weiss constant (K)	*g*
$Cr_3(PhPy)_4Cl_2$	4.78(2)	2.90	-1.4	1.97
$Cr_3(AniPy)_4Cl_2$	4.69(1)	2.76	-0.037	1.92
$Cr_3(PhPc)_4Cl_2$ (*cisoid)*	4.65(2)	2.64	0.44	1.88
$Cr_3(PhPy)_4Cl_2$ (3:1)	4.70(1)	2.76	0.44	1.92

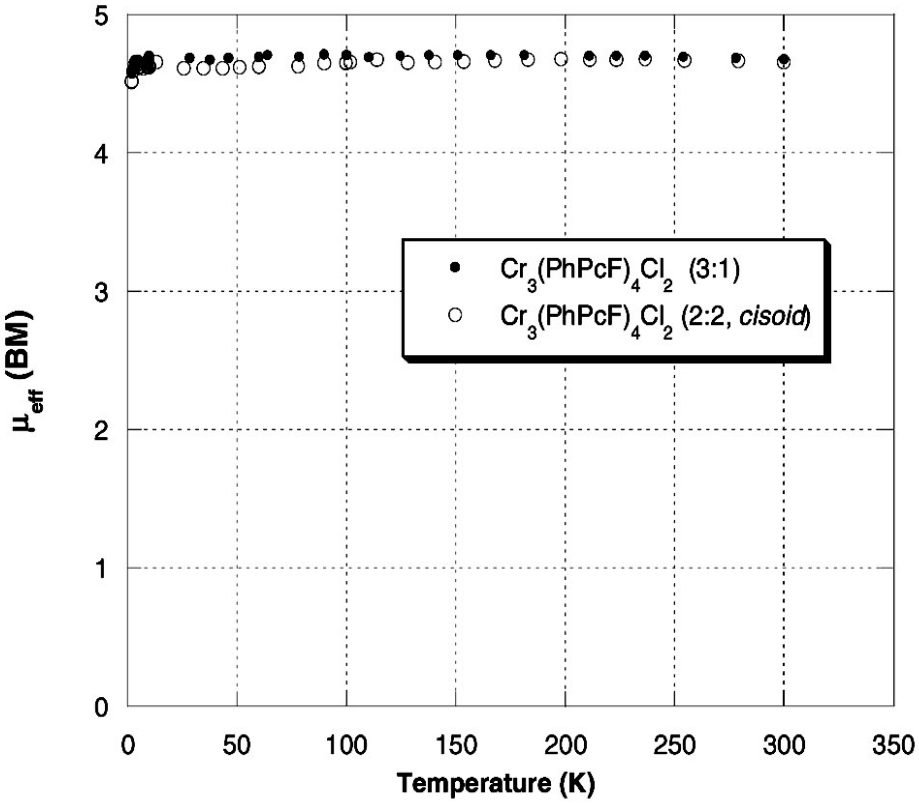

Figure 24. Plots of μ_{eff} vs T for the symmetrical (2:2, *cisoid*) **19a** and unsymmetrical (3:1) **19b**.

The magnetic behavior of the unsymmetrical compound $Cr_3(PhPcF)_4Cl_2$, in which the Cr–Cr distances are 2.216(1) and 2.647(1) Å, and the ligands have a 3-1 configuration, also showed there are four unpaired electrons in the molecule. However, in view of the relatively short distance between two of the chromium atoms, they are assumed to be quadruply bonded and the paramagnetism thus arise entirely from the remaining Cr^{II} unit. The least-squares fit of data with Curie-Weiss equation leads to C = 2.76 emu*K*mol^{-1}, θ = 0.44 K. The resultant *g* value is 1.92. From 28 K to 300 K, the μ_{eff} is 4.70(1) μ_B.

Discussion. The results reported here bring to 9 the number of symmetrical Cr_3^{6+} compounds and to 8 the number of unsymmetrical Cr_3^{6+} compounds that have been structurally characterized.[2a, 3b, 33, 34] These are listed in Table XXX, where Cr–Cr distances, mean inner and outer Cr–N distances, magnetic moments and overall torsion angles for the molecules are given.

Structural studies on this series of trichromium compounds with unsymmetrical formamidines clearly indicate that the unsymmetrical formamidines tend to support a symmetrical trichromium chain with Cr–Cr distances of *ca.* 2.46 Å and Cr–Cl distances of *ca.* 2.49 Å. The only unsymmetrical trichromium chain $Cr_3(PhPcF)_4Cl_2$ (**19a**) may be attributed to the uneven ligand arrangement that has a 3 to 1 conformation. Almost all other linear trichromium complexes with different wrapping ligands such as dpa$^-$,[3] BPAP^{2-} [34] and DPhIP$^-$ (DPhIP is the anion of 2,6-di(phenylimino)piperide),[14] and various axial ligand are unsymmetrical, in which two of the chromium atoms are paired by a quadruple bond with short distance while an isolated chromium has a longer distance to the central chromium atom. $Cr_3(PhPyF)_4Cl_2$ is not the first example of a symmetrical chain of chromium atoms. Very recently, the observation of a symmetrical chain of three chromium atoms in $Cr_3(dpa)_4Cl_2\cdot THF$ was reported.[3a] The most striking difference between these compounds with unsymmetrical formamidines and those reported earlier is the large

difference in the separations between the terminal metal atoms. The Cr–Cr distance in the symmetrical $Cr_3(dpa)_4Cl_2$·THF is considerably shorter than that in Cr_3(unsymmetrical-formamidine)$_4Cl_2$, namely, 2.36 Å, as compared to *ca.* 2.46 Å in Cr_3(unsymmetrical-formamidine)$_4Cl_2$. Moreover, different substitutes have no noticeable influence on Cr–Cr distances in the symmetrical chain, neither shorting nor elongating the distances.

For all trichromium compounds reported here, the ligands are not planar. The torsion angles from one terminal chromium atom to the other terminal chromium atom range from 27.9 ° to 34.9°. Individual values are given in Table XXVIII. These values are smaller than those in the similar trichromium dpa complexes (> 45°).[3a] Thus, the idea of that elongating the H···H distance such as those in the dpa anion (Figure 2a in Chapter I) does not always produce a trinuclear species without a torsion angle. However, as mentioned earlier, the very similar ligand, dipyridylformamidine does yield a trichromium compound, $[Cr_3(DPyF)_4](PF_6)_2$, without any torsion angle. In this compound the PF_6 anions are occupying crystal interstices. Thus, the axial positions are vacant, which allows the free pyridyl rings on each terminal Cr atom to be positioned almost in the same plane (Figure 25). This arrangement is impossible upon substitution of the N atom of the pyridyl group by a C–H group, as in **15 - 19** which have Cl anions in the axial positions. We believe that this makes an important contribution towards the torsion angles in **15 - 19** or lack of such distortion in the $[Cr_3(DPyF)_4]^{2+}$ cations. This effect also contributes to the elongated $Cr_{terminal}\cdots Cr_{terminal}$ distances, whereas those in $[Cr_3(DPyF)_4]^{2+}$ are shorted by *ca.* 0.25 Å and are very similar to those in $Cr_3(dpa)_4Cl_2$ compounds.

Finally, it is clear that in every case where the magnetic measurements have been made, whether the Cr_3^{6+} chain is symmetrical or unsymmetrical and regardless of any other molecular dimensions, the molecules have four unpaired electrons. (See Appendix III)

Table XXX. Comparison of Structural and Magnetic Data for All Known Compounds Containing Linear Cr_3^{6+} Cores [a]

Compound	Cr_1–Cr_2 (Å)	Cr_2–Cr_3 (Å)	Total Cr···Cr (Å)[b]	Cr_1–N (Å)	Cr_2–N (Å)	Cr_3–N (Å)	Cr_1–X (Å)[b]	Cr_1–Y (Å)[b]	Torsion angle (°)	μ_{eff}, 300K (μ_B)	Ref.
$Cr_3(dpa)_4Cl(BF_4)\cdot 2CH_2Cl_2$	1.995(1)	2.643(1)	4.638(1)	2.080[2]	2.030[2]	2.148[2]	2.374(3)	2.530(1)	37.7		3b
$Cr_3(dpa)_4Cl(PF_6)\cdot 2CH_2Cl_2$	2.008(1)	2.614(1)	4.622(1)	2.072[4]	2.024[3]	2.148[4]	2.536(4)	2.521(2)	38.4		3b
$Cr_3(dpa)_4Cl_2\cdot C_6H_6$[d]	2.296(2)	2.414(2)	4.710(2)	2.117[5]	2.025[5]	2.120[5]	2.539(2)	2.525(2)	43.9		3b
$Cr_3(dpa)_4Cl_2\cdot C_7H_8$	2.353(2)	2.365(2)	4.718(2)	2.112[6]	2.028[6]	2.123[6]	2.560(2)	2.533(2)	42.3	4.62	3b
$Cr_3(dpa)_4Cl_2\cdot C_4H_8O$	2.366(1)	2.366(1)	4.732(1)	2.113[5]	2.024[6]	2.109[5]	2.549(2)	2.549(2)	43.8	5.10	3b
$Cr_3(dpa)_4Cl_2\cdot CH_2Cl_2$	2.365(2)	2.365(2)	4.730(2)	2.133[8]	2.027[7]	2.133[8]	2.561(4)	2.561(4)	41.5		3b
$Cr_3(dpa)_4(CCPh)_2$	2.415(2)	2.422(2)	4.837(2)	2.135[5]	2.044[5]	2.137[6]	2.326(6)	2.307(6)	41.7		3b
$[Cr_3(DPhIP)_4Cl]Cl$	1.932(2)	2.659(2)	4.591(2)	2.056[6]	2.037[6]	2.129[6]	—	2.425(2)	31.2		33
$[Cr_3(DPhIP)_4MeCN](PF_6)_2$	1.907(2)	2.633(2)	4.540(2)	2.063[3]	2.051[3]	2.110[3]	—	2.220(7)[e]	38.4	4.30	33
$(Bu^n{}_4N)_2Cr_3(BPAP)_4$	1.904(3)	2.589(2)	4.493(5)	2.063[4]	2.056[6]	2.054[6]	—	—	30.6		34
$Cr_3(PhNC(Ph)NPy)_4Cl_2$	2.269(1)	2.513(1)	4.782(1)	2.123[5]	2.041[5]	2.134[5]	2.499(2)	2.456(2)	42.1	5.2	38
$Cr_3(DpyF)_4(PF_6)_2$	1.949(7)	2.738(7)	4.687(2)	2.057[5]	2.082[5]	2.073[6]	—	—	0		2a
$Cr_3(PhPyF)_4Cl_2$	2.4380(8)	2.4602(8)	4.8982(8)	2.131[3]	2.025[3]	2.137[3]	2.473(1)	2.485(1)	34.9	4.78(2)	Chapter IV
$Cr_3(AniPyF)_4Cl_2$	2.4789(7)	2.4759(7)	4.9548(9)	2.129[3]	2.026[3]	2.138[2]	2.4814(9)	2.4814(9)	29.3	4.69(1)	Chapter IV
$Cr_3(TolPyF)_4Cl_2$	2.4289(9)	2.4189(9)	4.8478(9)	2.137[4]	2.020[4]	2.137[4]	2.524(2)	2.524(2)	37.5		Chapter IV
$Cr_3(Ph^FPyF)_4Cl_2$	2.460(1)	2.500(1)	4.960(1)	2.126[7]	2.037[6]	2.126[7]	2.498(2)	2.498(2)	27.9		Chapter IV
cis-$Cr_3(PhPcF)_4Cl_2$	2.4743(8)	2.4743(8)	4.9486(8)	2.132[4]	2.024[4]	2.132[4]	2.480(1)	2.480(1)	30.0	4.65(2)	Chapter IV
$Cr_3(PhPcF)_4Cl_2$ (3:1)	2.216(1)	2.646(1)	4.862(1)	2.141[5]	2.034[5]	2.131[5]	2.467(2)	2.493(2)	33.6	4.70(1)	Chapter IV

[a]The values in square parentheses are average values.
[b]These are the separation between terminal Cr atoms.
[c]X and Y are typically monoanions unless otherwise noted.
[d]There are two independent molecules in the asymmetric unit.
[e]For this compound, there is a MeCN molecule occupying one axial position.

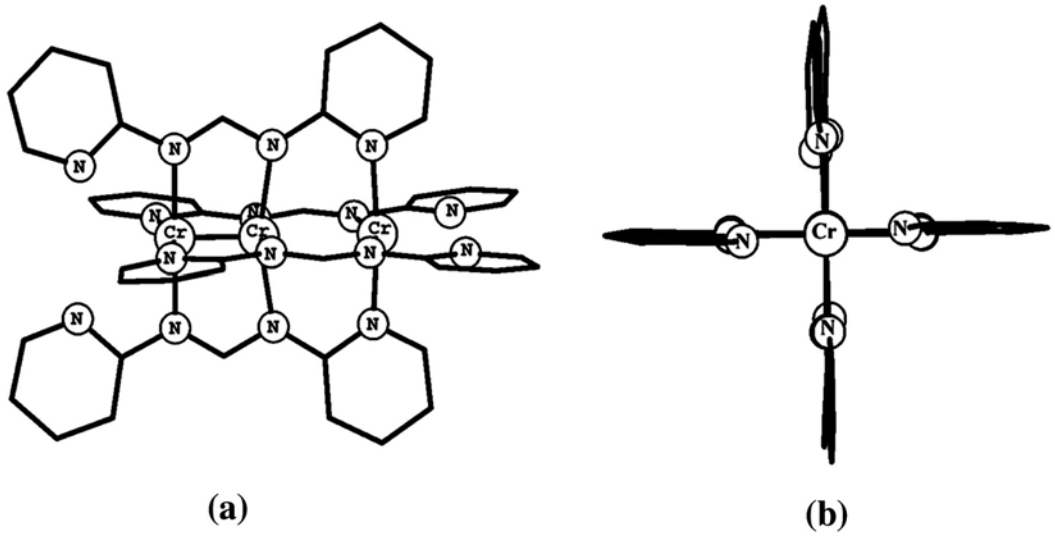

Figure 25. Drawings showing that the two free pyridine rings *trans* to each other in $Cr_3(DPyF)_4^{2+}$ cation are in a plane. **b** shows an end view of the cation along the Cr_3^{6+} vector

CHAPTER V

NICKEL COMPLEXES OF N-PHENYL-N-(2-PYRIDYL)FORMAMIDIME*

A very detailed study of $Ni_3(dpa)_4Cl_2$[5c] from this laboratory led to the conclusion that there is no metal-metal bonding even though the nickel-nickel separations are relatively short (*ca.* 2.43 Å). Instead, there is antiferromagnetic coupling between the terminal five-coordinated nickel atoms, each of which has two unpaired electrons. The central nickel atom is d^8, square-planar and diamagnetic. S.-M. Peng and coworkers[12] have done extensive work on the preparation of multinuclear nickel compounds with five, seven, nine nickel atoms in a linear array using oligo-pyridyl amino ligands. Their results indicate that antiferromagnetic interactions are similar to those in the trinickel unit and they decrease as might be expected with increasing chain length.

More recently, the one-electron oxidation of $Ni_3(dpa)_4Cl_2$ was reported.[13] The Ni—Ni distances in the oxidized compound $Ni_3(dpa)_4(PF_6)_3$ (~2.28 Å) are much shorter than those in the unoxidized species (~2.43 Å), and are consistent with three-center metal-metal bonding and a formal bond order of 0.5. (See Appendix IV)

In this Chapter, we are presenting syntheses and structural studies of a series of nickel complexes including mononickel, dinickel and trinickel complexes supported by the anion of the unsymmetrical *N,N'*-phenylpyridylformamidine HPhPyF.

---

* Taken in part from *Inorg. Chim. Acta,* Cotton, F. A.; Lei, P.; Murillo, C. A.; "Structural studies of nickel complexes of the unsymmetrical tridentate ligand *N*-phenyl-*N*-(2-pyridyl)formamidinate", accepted for publication.. Copyright 2003, with permission from Elsevier Science

EXPERIMENTAL

General procedures. All manipulations were carried out under an atmosphere of dry nitrogen using standard Schlenk techniques. Solvents were purified prior to use by distillation over appropriate drying agents in a nitrogen atmosphere. The compounds HPhPyF,[38] $Ni(py)_4Cl_2$ [39] and $Ni(PPh_3)_2Br_2$ [40] were synthesized as previously described. Anhydrous $NiCl_2$, $NiBr_2$ and $AgBF_4$ were purchased from Strem. The former was refluxed in thionyl chloride prior to use. Methyllithium (1.6 M in ether) was obtained from Acros. Magnetic measurements were done at room temperature on a magnetic susceptibility balance (Johnson Matthey Chemicals Limited).

Preparation of $Ni_2(PhPyF)_4$, 20. A flask was charged with HPhPyF (396 mg, 2.00 mmol) dissolved in 30 ml of THF. The solution was cooled to -78 °C, and 1 equiv of MeLi was added slowly. The solution was removed from the cold bath, stirred until it reached room temperature. The mixture was then added via cannula to a flask containing anhydrous $Ni(py)_4Cl_2$ (670 mg, 1.50 mmol). The reaction mixture was refluxed for 12 h. The volume was then reduced to *ca.* 10 ml, and upon addition of 40 ml of hexanes a deep-brown precipitate formed. The solid was collected by filtration, and washed thoroughly with ether. After drying, the solid was dissolved in 15 ml of CH_2Cl_2, and then 40 ml of hexanes was added to precipitate the product. The mixture was filtered, and the solid was briefly dried under vacuum. Finally, the product was dissolved in 15 ml of CH_2Cl_2, and layered with 40 ml of hexanes. Large, dark-blue crystals of $Ni_2(PhPyF)_4$ formed in a week. Yield: 52 %.

Preparation of $Ni_3(PhPyF)_4(MeCN)_2(BF_4)_2$, 21 and $[Ni(HPhPyF)_2(MeCN)_2](BF_4)_2$, 22. The ligand HPhPyF (396 mg, 2.00 mmol) was dissolved in 15 ml of THF and deprotonated with 1 equiv of MeLi at -78 °C. After the temperature of the solution had slowly risen to room

temperature, the THF was removed under vacuum. Then, 40 ml of MeCN was used to dissolve the residue and the solution was transferred to a flask containing $NiBr_2$ (378 mg, 1.50 mmol). The yellow mixture was stirred for 3 h at room temperature. To this mixture $AgBF_4$ (584 mg, 3.00 mmol) was added, and the mixture was refluxed for 12 h, and then filtered. The filtrate was reduced to half of its original volume and 60 ml of Et_2O was added. A black-brown solid formed. This was collected by filtration, washed twice with 20 ml of Et_2O, and then dried briefly under vacuum. Finally, the solid was dissolved in 20 ml of MeCN, and the solution was layered with ether (40 ml). Three weeks later, several dark-red, block-shaped crystals of $Ni_3(PhPyF)_4(MeCN)_2(BF_4)_2$ (**21**) were obtained along with some blue needle-like crystals of $[Ni(HPhPyF)_2(MeCN)_2](BF_4)_2$(**22**). The crystals were separated manually. The yield for compound **21** was about 2% and that of **22** was 40%.

Preparation of $[Ni_3(PhPyF)_4Cl]Cl$, 23. To the ligand HPhPyF (396 mg, 2.00 mmol) in 40 ml of THF was added 1 equiv of MeLi at -78 °C. The deprotonation was essentially complete when the temperature of the mixture rose to room temperature. The THF solution was transferred to a flask containing $Ni(py)_4Cl_2$ (1.34 g, 3.00 mmol). The reaction mixture was refluxed for 15 h and then filtered. The volume of the resulting solution was reduced to *ca.* 10 ml. Ether (50 ml) was added to this mixture. The solid was collected by filtration, washed with copious amounts of ether, and then dissolved in 15 ml of THF. Addition of hexanes produced a precipitate which was isolated by filtration. Finally, the solid was dissolved in 15 ml of CH_2Cl_2, and layered with 40 ml of hexanes. Black-red crystals of $[Ni_3(PhPyF)_4Cl]Cl$ formed within two weeks along with a lot of dark-blue crystals of **20**. The yield of the trinuclear compound **23** was ~8%. Magnetic susceptibility at room temperature: 3.08 μ_B.

Preparation of $Ni_3(PhPyF)_4Cl_2$, 24·CH_2Cl_2. The method of preparation was similar to that

of **23**, except that a 3 fold excess of $Ni(py)_4Cl_2$ was used. After three weeks, very dark red (almost black) crystals of $Ni_3(PhPyF)_4Cl_2$ formed along with the some dark-blue crystals of **20**. The yield for the trinickel compound **24** was ~5%.

Preparation of Ni(HPhPyF)Br_2, 25. To a flask charged with HPhPyF (396 mg, 2.00 mmol) and $Ni(PPh_3)_2Br_2$, 10 g of naphthalene was added. The mixture was quickly heated to 145 °C with gently stirring. A dark-purple, crystalline precipitate formed. After 10 min of stirring at 145 °C, the reaction mixture was allowed to cool to room temperature. The solid was washed with copious amounts of ether, then 2 × 10 ml of benzene. The remaining solid was dissolved in 20 ml of acetone, and an insoluble portion was removed by filtration. The resulting acetone solution was layered with 40 ml of hexanes. Dark-purple crystals formed in a week. Yield: 58%.

CRYSTALLOGRAPHIC STUDIES

Data were collected on a Bruker SMART 1000 CCD area detector system. In each case, a suitable crystal was attached to the tip of a quartz fiber with a small amount of grease and transferred to a goniometer, where the crystal was kept in a stream of cold nitrogen. Cell parameters were obtained using SMART software.[18] Data were corrected for Lorentz and polarization effects using the program SAINTPLUS.[19] Absorption corrections were applied using SADABS.[20]

The positions of heavy atoms were found by the direct methods programmed in SHELXS-97.[21] Subsequent cycles of least-square refinement followed by difference Fourier syntheses revealed the positions of the non-hydrogen atoms. All hydrogen atoms were placed in idealized positions.

Crystallographic data and structure refinement details for **20**, **21**, **22**, **23**, **24**·CH_2Cl_2 and **25** reported in this chapter are listed in Tables XXXI, XXXII, XXXIII, XXXIV, XXXV and XXXVI, repectively. Selected bond lengths and angles for **20**, **21**, **22**, **23**, **24**·CH_2Cl_2 and **25** are given in Tables XXXVII, XXXVIII, XXXIX, XL, XLI and XLII, repectively. All space groups were uniquely determined by systematic absences, and refinements proceeded straightforwardly.

RESULTS AND DISCUSSION

Synthetic considerations. We were surprised to encounter a great deal of difficulty in preparing trinickel compounds with the PhPyF ligand. What we report here is far from satisfactory from a purely preparative point of view, but the existence of these compounds of structural interest has been established.

A simple and commonly-used method to prepare linear trimetal chain complexes is to react the lithium salt of the ligand with a stoichiometric amount of the anhydrous metal halides.[3-6] However, we found anhydrous nickel halides (chloride and bromide) to be very unreactive toward the lithium salt of HPhPyF. No reaction takes place when LiPhPyF and NiX_2 (X = Cl, Br) are mixed in THF even during an extended period of reflux. It seemed clear that either some other source of nickel(II) was required, or more forcing conditions were needed if an anhydrous nickel halide was to be used as a starting material. When two equivalents of $AgBF_4$ were added to precipitate the bromide ions from $NiBr_2$ in an attempt to make the nickel(II) ion more readily accessible to LiPhPyF, the trinuclear complex, $Ni_3(PhPyF)_4(MeCN)_2(BF_4)_2$, **21**, was obtained but the isolated yield was minute. The major product of this reaction, **22**, was a mononuclear nickel

Table XXXI. Crystal Data and Structure Refinement for **20**

Empirical formula	$C_{48}H_{40}N_{12}Ni_2$
Formula weight	902.34
Temperature	213(2) K
Wavelength	0.71073 Å
Crystal system	Monoclinic
Space group	$P2_1/n$
Unit cell dimensions	a = 13.5762(7) Å α = 90˚
	b = 10.4773(5) Å β = 96.526(1)˚
	c = 29.800(2) Å γ = 90˚
Volume	4211.4(4) $Å^3$
Z	4
Density (calculated)	1.423 g/mm^3
Absorption coefficient	0.945 mm^{-1}
Crystal size	0.54 x 0.48 x 0.42 mm
Instrument for data collections	Bruker SMART 1000
Theta range for data collection	2.06 to 27.51˚
Reflections collected	26008
Independent reflections	9640 [R(int) = 0.0162]
Scan Method	ω-scan
Refinement method	Full-matrix least-squares on F^2
Data / restraints / parameters	9640 / 0 / 559
Goodness-of-fit on F^2	1.034
Final R indices [$I > 2\sigma(I)$]	$R1$ = 0.0276, $wR2$ = 0.0693
R indices (all data)	$R1$ = 0.0338, $wR2$ = 0.0727
Largest Shift / esd, final cycle	0.002
Largest diff. peak and hole	0.244 and -0.303 e/$Å^3$

Table XXXII. Crystal Data and Structure Refinement for **21**

Empirical formula	$C_{52}H_{46}B_2F_8N_{14}Ni_3$
Formula weight	1216.78
Temperature	213(2) K
Wavelength	0.71073 Å
Crystal system	Tetragonal
Space group	$I4_1/a$
Unit cell dimensions	a = 18.7409(7)Å α = 90˚
	b = 18.7409(7) Å β = 90˚
	c = 29.8937(15) Å γ = 90˚
Volume	10499.3(8) Å^3
Z	8
Density (calculated)	1.540 g/mm^3
Absorption coefficient	1.146 mm^{-1}
Crystal size	0.45 x 0.44 x 0.40 mm
Theta range for data collection	2.05 to 27.53˚
Instrument for data collections	Bruker SMART 1000
Reflections collected	33065
Independent reflections	6034 [R(int) = 0.0246]
Scan Method	ω-scan
Refinement method	Full-matrix least-squares on F^2
Data / restraints / parameters	6027 / 0 / 398
Goodness-of-fit on F^2	1.177
Final R indices [I >2σ(I)]	R1 = 0.0539, wR2 = 0.1294
R indices (all data)	R1 = 0.0683, wR2 = 0.1411
Largest Shift / esd, final cycle	-0.044
Largest diff. peak and hole	0.740 and -0.467 e/Å^3

Table XXXIII. Crystal Data and Structure Refinement for **22**

Empirical formula	$C_{28}H_{28}B_2F_8N_8Ni$	
Formula weight	708.91	
Temperature	213(2) K	
Wavelength	0.71073 Å	
Crystal system	Orthorhombic	
Space group	*Pbcn*	
Unit cell dimensions	a = 20.911(2) Å	α = 90˚
	b = 10.5688(9) Å	β = 90˚
	c = 14.0333(11) Å	γ = 90˚
Volume	3101.4(4) Å^3	
Z	4	
Density (calculated)	1.518 g/mm^3	
Absorption coefficient	0.708 mm^{-1}	
Crystal size	0.66 x 0.50 x 0.40 mm	
Theta range for data collection	1.95 to 27.57˚	
Instrument for data collections	Bruker SMART 1000	
Reflections collected	18245	
Independent reflections	3573 [R(int) = 0.0237]	
Scan Method	ω-scan	
Refinement method	Full-matrix least-squares on F^2	
Data / restraints / parameters	3566 / 0 / 234	
Goodness-of-fit on F^2	1.065	
Final R indices [$I > 2\sigma(I)$]	$R1$ = 0.0464, $wR2$ = 0.1299	
R indices (all data)	$R1$ = 0.0552, $wR2$ = 0.1441	
Largest Shift / esd, final cycle	-0.072	
Largest diff. peak and hole	0.746 and -0.534 e/Å^{-3}	

Table XXXIV. Crystal Data and Structure Refinement for **23**

Empirical formula	$C_{48}H_{40}Cl_2N_{12}Ni_3$	
Formula weight	1031.95	
Temperature	213(2) K	
Wavelength	0.71073 Å	
Crystal system	Tetragonal	
Space group	*P4/ncc*	
Unit cell dimensions	a = 13.461(2) Å	α = 90˚
	b = 13.461(2) Å	β = 90˚
	c = 24.334(7) Å	γ = 90˚
Volume	4409.5(16) $Å^3$	
Z	4	
Density (calculated)	1.554 g/mm^3	
Absorption coefficient	1.440 mm^{-1}	
Crystal size	0.15 x 0.14 x 0.09 mm	
Instrument for data collections	Bruker SMART 1000	
Theta range for data collection	2.14 to 25.10˚	
Reflections collected	11474	
Independent reflections	1947 [*R*(int) = 0.1254]	
Scan Method	ω-scan	
Refinement method	Full-matrix least-squares on F^2	
Data / restraints / parameters	1946 / 0 / 152	
Goodness-of-fit on F^2	1.094	
Final *R* indices [$I > 2\sigma(I)$]	*R*1 = 0.0706, *wR*2 = 0.1544	
R indices (all data)	*R*1 = 0.1513, *wR*2 = 0.2006	
Largest Shift / esd, final cycle	-0.072	
Largest diff. peak and hole	0.832 and -0.859 e/$Å^3$	

Table XXXV. Crystal Data and Structure Refinement for **24**·CH_2Cl_2

Empirical formula	$C_{49}H_{42}Cl_4N_{12}Ni_3$	
Formula weight	1116.88	
Temperature	213(2) K	
Wavelength	0.71073 Å	
Crystal system	Tetragnal	
Space group	*P* $4_3 2_1 2$	
Unit cell dimensions	a = 14.8822(6) Å	α = 90˚
	b = 14.8822(6) Å	β = 90˚
	c = 43.382(4) Å	γ = 90˚
Volume	9608.4(9) $Å^3$	
Z	8	
Density (calculated)	1.544 g/mm^3	
Absorption coefficient	1.436 mm^{-1}	
Crystal size	0.44 x 0.34 x 0.34 mm	
Instrument for data collections	Bruker SMART 1000	
Theta range for data collection	1.66 to 27.51˚	
Reflections collected	59477	
Independent reflections	11021 [*R*(int) = 0.0418]	
Scan Method	ω-scan	
Refinement method	Full-matrix least-squares on F^2	
Data / restraints / parameters	11021 / 2 / 608	
Goodness-of-fit on F^2	1.152	
Final *R* indices [I> 2σ(*I*)]	*R*1 = 0.0639, *wR*2 = 0.1539	
R indices (all data)	*R*1 = 0.0766, *wR*2 = 0.1636	
Absolute structure parameter	0.04(2)	
Largest Shift / esd, final cycle	0.016	
Largest diff. peak and hole	0.937 and -0.968 e/$Å^3$	

Table XXXVI. Crystal Data and Structure Refinement for **25**

Empirical formula	$C_{12}H_{11}Br_2N_3Ni$	
Formula weight	415.77	
Temperature	213(2) K	
Wavelength	0.71073 Å	
Crystal system	Monoclinic	
Space group	$P2_1/c$	
Unit cell dimensions	a = 13.3441(11) Å	α = 90˚
	b = 13.3396(11) Å	β = 96.556(2)˚
	c = 8.1227(6) Å	γ = 90˚
Volume	1436.4(2) $Å^3$	
Z	4	
Density (calculated)	1.923 g/mm^3	
Absorption coefficient	6.899 mm^{-1}	
Crystal size	0.44 x 0.09 x 0.04 mm	
Instrument for data collections	Bruker SMART 1000	
Theta range for data collection	1.54 to 27.49˚	
Reflections collected	8927	
Independent reflections	3286 [R(int) = 0.0261]	
Scan Method	ω-scan	
Refinement method	Full-matrix least-squares on F^2	
Data / restraints / parameters	3286 / 0 / 163	
Goodness-of-fit on F^2	1.009	
Final R indices [$I > 2\sigma(I)$]	$R1$ = 0.0273, $wR2$ = 0.0658	
R indices (all data)	$R1$ = 0.0416, $wR2$ = 0.0725	
Largest Shift / esd, final cycle	0.001	
Largest diff. peak and hole	0.510 and -0.408 e/$Å^3$	

Table XXXVII. Selected Bond Lengths (Å) and Angles (˚) for **20**

Ni(1)—N(3)	2.091(1)	Ni(2)—N(6)	2.065(1)
Ni(1)—N(12)	2.094(1)	Ni(2)—N(9)	2.085(1)
Ni(1)—N(7)	2.097(1)	Ni(2)—N(10)	2.087(1)
Ni(1)—N(4)	2.116(1)	Ni(2)—N(1)	2.115(1)
Ni(1)—N(5)	2.181(1)	Ni(2)—N(2)	2.157(1)
Ni(1)—N(8)	2.185(1)	Ni(2)—N(11)	2.191(1)
N(3)—Ni(1)—N(12)	172.62(5)	N(5)—Ni(1)—N(8)	127.49(5)
N(3)—Ni(1)—N(7)	94.75(5)	N(6)—Ni(2)—N(9)	172.84(5)
N(12)—Ni(1)—N(7)	88.16(5)	N(6)—Ni(2)—N(10)	95.38(5)
N(3)—Ni(1)—N(4)	87.37(5)	N(9)—Ni(2)—N(10)	89.35(5)
N(12)—Ni(1)—N(4)	98.22(5)	N(6)—Ni(2)—N(1)	91.44(5)
N(7)—Ni(1)—N(4)	107.66(5)	N(9)—Ni(2)—N(1)	92.30(5)
N(3)—Ni(1)—N(5)	86.24(5)	N(10)—Ni(2)—N(1)	107.09(5)
N(12)—Ni(1)—N(5)	92.09(5)	N(6)—Ni(2)—N(2)	90.25(5)
N(7)—Ni(1)—N(5)	169.89(5)	N(9)—Ni(2)—N(2)	86.04(5)
N(4)—Ni(1)—N(5)	62.30(5)	N(10)—Ni(2)—N(2)	168.62(5)
N(3)—Ni(1)—N(8)	88.50(5)	N(1)—Ni(2)—N(2)	62.79(5)
N(12)—Ni(1)—N(8)	86.82(5)	N(6)—Ni(2)—N(11)	91.86(5)
N(7)—Ni(1)—N(8)	62.61(5)	N(9)—Ni(2)—N(11)	85.52(5)

Table XXXVIII. Selected Bond Lengths (Å) and Angles (˚) for **21**

Ni(1)—Ni(2)#1	2.4695(5)	Ni(1)—Ni(2)	2.4695(5)
Ni(2)—N(7)	2.028(4)	Ni(1)—N(4)#1	1.886(3)
Ni(2)—N(2)	2.081(3)	Ni(1)—N(4)	1.886(3)
Ni(2)—N(5)	2.084(3)	Ni(1)—N(1)	1.891(3)
Ni(2)—N(6)	2.095(3)	Ni(1)—N(1)#1	1.891(3)
Ni(2)—N(3)	2.097(3)		
N(4)#1—Ni(1)—N(4)	89.5(2)	N(1)#1—Ni(1)—Ni(2)#1	89.4(1)
N(4)#1—Ni(1)—N(1)	90.8(1)	N(7)—Ni(2)—N(2)	96.9(2)
N(4)—Ni(1)—N(1)	178.6(1)	N(7)—Ni(2)—N(5)	95.9(2)
N(4)#1—Ni(1)—N(1)#1	178.6(2)	N(2)—Ni(2)—N(5)	167.2(1)
N(4)—Ni(1)—N(1)#1	90.8(1)	N(7)—Ni(2)—N(6)	102.0(2)
N(1)—Ni(1)—N(1)#1	89.0(2)	N(2)—Ni(2)—N(6)	89.3(1)
N(4)#1—Ni(1)—Ni(2)	90.0(1)	N(5)—Ni(2)—N(6)	88.4(1)
N(4)—Ni(1)—Ni(2)	89.3(1)	N(7)—Ni(2)—N(3)	94.0(2)
N(1)—Ni(1)—Ni(2)	89.4(1)	N(2)—Ni(2)—N(3)	89.2(1)
N(1)#1—Ni(1)—Ni(2)	91.3(1)	N(5)—Ni(2)—N(3)	89.6(13)
N(4)#1—Ni(1)—Ni(2)#1	89.3(1)	N(6)—Ni(2)—N(3)	164.1(1)
N(4)—Ni(1)—Ni(2)#1	90.0(1)	N(1)—Ni(1)—Ni(2)#1	91.3(1)

Symmetry transformations used to generate equivalent atoms:
#1 -x+2,-y+3/2,z+0

Table XXXIX. Selected Bond Lengths (Å) and Angles (˚) for **22**

Ni(1)—N(3)	2.098(2)	N(3)—Ni(1)—N(3)#1	177.32(11)
Ni(1)—N(3)#1	2.099(2)	N(3)—Ni(1)—N(1)#1	91.27(8)
Ni(1)—N(1)#1	2.113(2)	N(3)#1—Ni(1)—N(1)#1	86.82(8)
Ni(1)—N(1)	2.113(2)	N(3)—Ni(1)—N(1)	86.83(8)
Ni(1)—N(4)#1	2.113(2)	N(3)#1—Ni(1)—N(1)	91.27(8)
Ni(1)—N(4)	2.113(2)	N(3)—Ni(1)—N(4)#1	93.23(8)
		N(3)#1—Ni(1)—N(4)#1	88.76(8)
		N(1)#1—Ni(1)—N(4)#1	93.33(8)
		N(3)—Ni(1)—N(4)	88.76(8)
		N(3)#1—Ni(1)—N(4)	93.23(8)
		N(1)#1—Ni(1)—N(4)	177.15(8)
		N(1)—Ni(1)—N(4)	93.33(8)

Symmetry transformations used to generate equivalent atoms:
#1 -x+1,y,-z+1/2

Table XL. Selected Bond Lengths (Å) and Angles (˚) for **23**

Ni(2)—Ni(3)	2.454(3)	Ni(1)—Ni(2)	2.443(3)
Ni(3)—Cl(2)	2.331(5)	Ni(1)—N(1)#1	1.921(6)
Ni(2)—N(2)#1	1.911(7)	Ni(1)—N(1)	1.921(6)
Ni(2)—N(2)	1.911(7)	Ni(1)—N(1)#2	1.921(6)
Ni(2)—N(2)#3	1.911(7)	Ni(1)—N(1)#3	1.921(6)
Ni(2)—N(2)#2	1.911(7)	Ni(3)—N(3)	2.129(7)
Ni(3)—N(3)#3	2.129(7)	Ni(3)—N(3)#1	2.129(7)
Ni(3)—N(3)#2	2.129(7)		
N(1)#1—Ni(1)—N(1)	89.80(2)	N(1)#2—Ni(1)—Ni(2)	86.6(2)
N(1)#1—Ni(1)—N(1)#2	89.80(2)	N(1)#3—Ni(1)—Ni(2)	86.6(2)
N(1)—Ni(1)—N(1)#2	173.3(3)	N(2)#1—Ni(2)—N(2)	89.943(12)
N(1)#1—Ni(1)—N(1)#3	173.3(3)	N(2)#1—Ni(2)—N(2)#3	176.4(4)
N(1)—Ni(1)—N(1)#3	89.80(2)	N(2)—Ni(2)—N(2)#3	89.945(12)
N(1)#2—Ni(1)—N(1)#3	89.80(2)	N(2)#1—Ni(2)—N(2)#2	89.943(13)
N(1)#1—Ni(1)—Ni(2)	86.6(2)	N(2)—Ni(2)—N(2)#2	176.4(4)
N(1)—Ni(1)—Ni(2)	86.6(2)	N(2)#3—Ni(2)—N(2)#2	89.941(13)
N(2)#1—Ni(2)—Ni(1)	88.2(2)	N(2)#2—Ni(2)—Ni(1)	88.2(2)
N(2)—Ni(2)—Ni(1)	88.2(2)	N(2)#1—Ni(2)—Ni(3)	91.8(2)
N(2)#3—Ni(2)—Ni(1)	88.2(2)	N(2)—Ni(2)—Ni(3)	91.8(2)

Symmetry transformations used to generate equivalent atoms:
#1 -y+1/2,x,z
#2 -x+1/2,—y+1/2,z
#3 y,-x+1/2,z

Table XLI. Selected Bond Lengths (Å) and Angles (˚) for **24**·CH_2Cl_2

Ni(2)—Ni(3)	2.503(1)	Ni(1)—Ni(2)	2.508(1)
Ni(3)—Cl(2)	2.310(2)	Ni(1)—Cl(1)	2.324(2)
Ni(2)—N(2)	1.884(4)	Ni(1)—N(12)	2.080(5)
Ni(2)—N(11)	1.887(5)	Ni(1)—N(4)	2.092(5)
Ni(2)—N(5)	1.896(5)	Ni(1)—N(7)	2.098(5)
Ni(2)—N(8)	1.904(5)	Ni(1)—N(3)	2.103(5)
Ni(3)—N(9)	2.088(6)	Ni(3)—N(6)	2.112(5)
Ni(3)—N(1)	2.100(5)	Ni(3)—N(10)	2.124(5)
N(12)—Ni(1)—N(4)	89.2(2)	N(7)—Ni(1)—Cl(1)	99.0(2)
N(12)—Ni(1)—N(7)	162.9(2)	N(3)—Ni(1)—Cl(1)	96.2(2)
N(4)—Ni(1)—N(7)	88.5(2)	N(12)—Ni(1)—Ni(2)	80.4(1)
N(12)—Ni(1)—N(3)	90.5(2)	N(2)—Ni(2)—N(11)	89.7(2)
N(4)—Ni(1)—N(3)	164.5(2)	N(11)—Ni(2)—N(5)	90.6(2)
N(7)—Ni(1)—N(3)	87.2(2)	N(2)—Ni(2)—N(8)	90.6(2)
N(12)—Ni(1)—Cl(1)	98.1(2)	N(5)—Ni(2)—N(8)	89.1(2)
N(4)—Ni(1)—Cl(1)	99.2(2)	N(5)—Ni(2)—Ni(3)	90.4(2)
N(9)—Ni(3)—Cl(2)	99.2(2)	N(8)—Ni(2)—Ni(3)	89.6(2)
N(1)—Ni(3)—Cl(2)	98.6(2)	N(5)—Ni(2)—Ni(1)	89.4(2)
N(6)—Ni(3)—Cl(2)	98.6(2)	N(8)—Ni(2)—Ni(1)	89.1(2)

Table XLII. Selected Bond Lengths (Å) and Angles (˚) for **25**

Ni(1)—N(3)	1.959(2)
Ni(1)—N(1)	1.982(2)
Ni(1)—Br(1)	2.3402(5)
Ni(1)—Br(2)	2.3719(5)
N(3)—Ni(1)—N(1)	93.28(9)
N(3)—Ni(1)—Br(1)	111.51(7)
N(1)—Ni(1)—Br(1)	106.37(6)
N(3)—Ni(1)—Br(2)	109.15(7)
N(1)—Ni(1)—Br(2)	107.18(6)
Br(1)—Ni(1)—Br(2)	124.59(2)
C(5)—N(1)—C(1)	118.4(2)
C(5)—N(1)—Ni(1)	123.6(2)
C(1)—N(1)—Ni(1)	117.9(2)
C(6)—N(2)—C(5)	129.2(2)
C(6)—N(3)—C(7)	118.6(2)
C(6)—N(3)—Ni(1)	121.5(2)
C(7)—N(3)—Ni(1)	119.9(2)

complex of octahedral structure[41] containing the neutral ligand, with the formula of $[Ni(HPhPyF)_2(MeCN)_2][BF_4]_2$.

In a search for other suitable Ni(II) sources to prepare trinickel complexes by reaction with the anion of HPhPyF, $Ni(py)_4Cl_2$ was examined. The reaction was carried out with $Ni(py)_4Cl_2$ and LiPhPyF in the stoichiometric ratio of 3:4 necessary to form a trinuclear compound. However, under such conditions only the dinuclear species $Ni_2(PhPyF)_4$, **20**, was obtained. This compound appears to be thermodynamically very stable. Since **20** is deficient in Ni, relative to the Ni_3^{6+} species, twice as much $Ni(py)_4Cl_2$ was used. In this way, a small amount of the trinickel complex $[Ni_3(PhPyF)_4Cl]Cl$ (**23**) was isolated, but a significant amount of the dinuclear compound **20** was again obtained. When a larger excess of $Ni(Py)_4Cl_2$ (*ca*. 3-fold) was used, a different trinickel species, $Ni_3(PhPyF)_4Cl_2$ (**24**), was isolated, but, again, **20** was present as the major product. The reactions of LiPhPyF and $Ni(py)_4Cl_2$ are summarized in Figure 26.

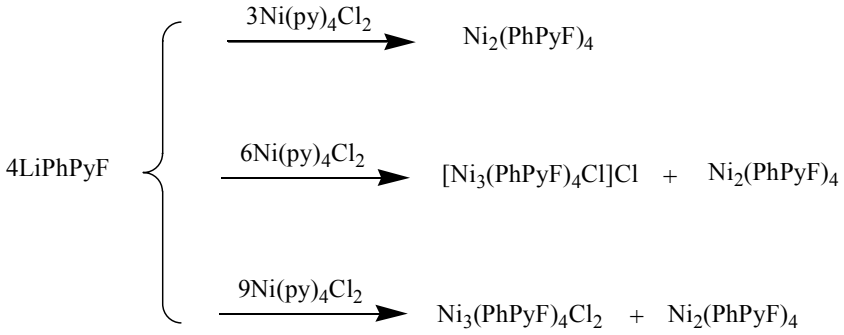

Figure 26. A summary of reactions of LiPhPyF and $Ni(py)_4Cl_2$.

Naphthalene has been proven to be a good reaction medium for the preparation of multinuclear metal chain complexes with the number of metal atoms extending from 3 to 9 as shown by Peng and coworkers.[12] In those reactions, naphthalene allows the reaction temperature to rise as high as about 185 °C, which is critical to generate the target compounds having many metal atoms in a linear array. However, the naphthalene reaction medium could not be used for the preparation of trinickel compounds with the anion PhPyF since a thermogravimetric analysis of HPhPyF showed that the ligand decomposes at *ca.* 153 °C. The reaction of HPhPyF with $NiCl_2$, $Ni(py)_4Cl_2$ and $Ni(PPh_3)_2Br_2$ in naphthalene using $KOBu^t$ as a base at 145 °C did not yield isolable products. When no base was added, the reaction of HPhPyF with $Ni(PPh_3)_2Br_2$ in naphthalene gave a mononickel species, $Ni(HPhPyF)Br_2$, in which a neutral ligand HPhPyF is found to be chelating the nickel atom, with the two bromide atoms filling the remaining two positions of a distorted tetrahedron.

The difficulty in preparing the Ni_3^{6+} chain compounds described here contrasts with the ease of preparing the Cr_3^{6+} analogs. Those have been synthesized relatively straightforwardly by reaction of $CrCl_2$ and unsymmetrical formamidinates. [42]

Table XLIII. Comparison of important parameters in the neutral linear trinickel compounds

mean values [a]	$Ni_3(dpa)_4Cl_2$	$(TBA)_2Ni_3(BPAP)_4$ (**4**)	$Ni_3(PhPyF)_4Cl_2$ (**25**)	$[Ni_3(PhPyF)_4Cl]Cl$ (**24**)	$Ni_3(PhPyF)_4(MeCN)_2(BF_4)_2$ (**22**)
Ni···Ni (Å)	2.43[8]	2.368[1]	2.5075(10) 2.5027(10)	2.443(3) 2.454(3)	2.469(5)
Ni–X, axial, (Å)	2.34[6]	-	2.317[2]	2.331(5)	2.0284(4)
Ni–N, central, (Å)	1.88[9]	1.906[7]	1.893[5]	1.911(7)	1.889[3]
Ni–N, outer, (Å)	2.10[7]	1.917[5]	2.100[5]	1.921(6) 2.129(7)	2.090[3]
Overall torsion angle (deg)	51.0	30	40.4	30	40.5
Ref.	5c	Chapter II	Chapter V	Chapter V	Chapter V

[a] Numbers within square brackets are e.s.d.s. of average values.

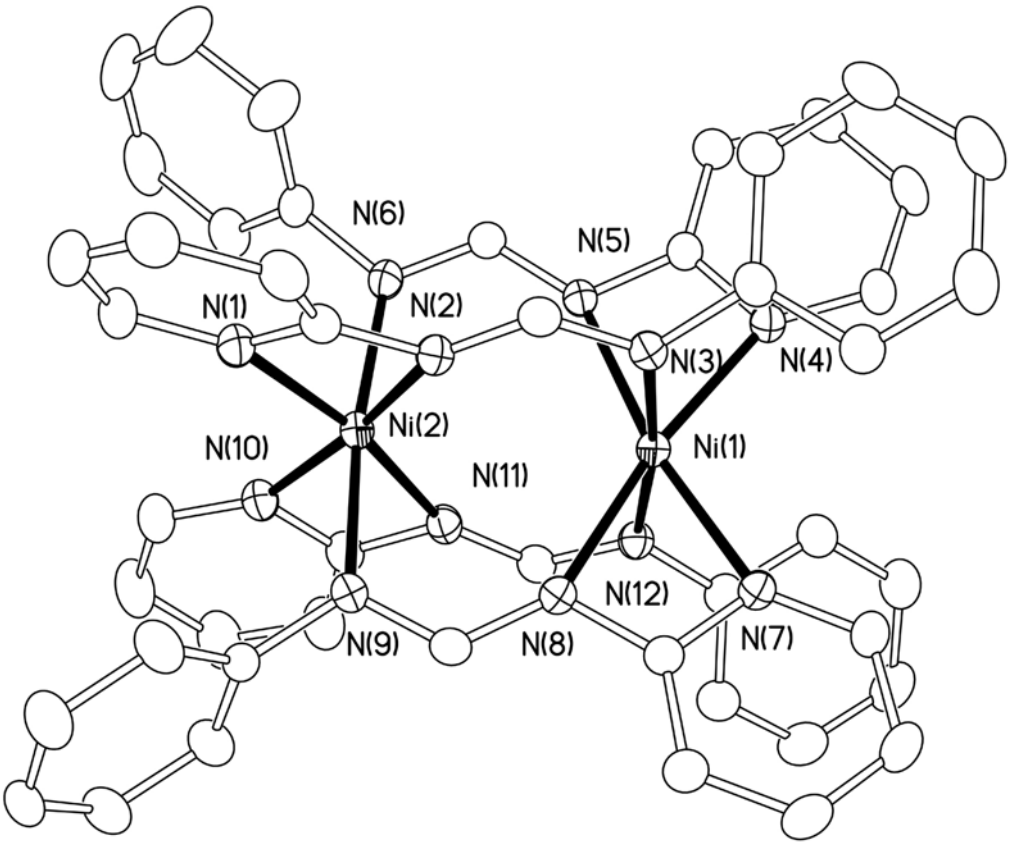

Figure 27. The molecular structure of $Ni_2(PhPyF)_4$ (**20**) with ellipsoids shown at the 45% probability level. Hydrogen atoms are omitted for clarity.

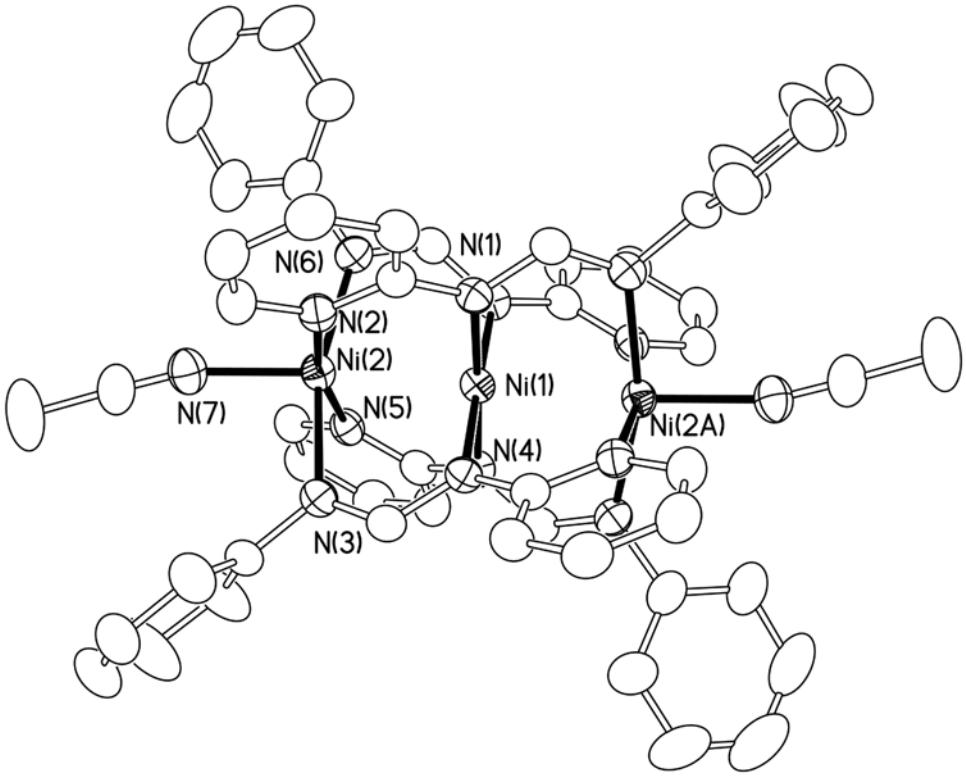

Figure 28. Perspective view of $Ni_3(PhPyF)_4(MeCN)_2^{2+}$ in **21**. Atoms are drawn at 45% probability level and hydrogen atoms are omitted for clarity.

Structural studies. The molecular structure of the dinuclear compound $Ni_2(PhPyF)_4$ is shown in Figure 27. It crystallizes in the space group $P2_1/n$ with all atoms of the molecule occupying general positions. Each ligand uses two nitrogen atoms to chelate one nickel atom while the third nitrogen atom spans to the other nickel atom. Each nickel atom has a very distorted octahedral geometry, and the nickel—nickel separation is long, about 3.41 Å, indicating there is no metal-metal bonding. There are two kinds of structural motifs commonly expected for dimetal complexes with four tridentate ligands and the general formula M_2L_4. In one type the two metal atoms form a direct bond and thus there is a short separation while the third donor atom on each L ligand is dangling as in $Cr_2(dpa)_4$.[3] The addition of a third metal atom to the dimetal unit is then possible by taking advantage of the third dangling nitrogen donor. In the second type, the structural motif for M_2L_4 is that seen here in the structure of $Ni_2(PhPyF)_4$. There is no dangling nitrogen donor as all of twelve nitrogen atoms in the four ligands coordinate to the metal atoms and two distorted octahedra are formed. Such a compound is thermodynamically very stable, and, it is very difficult to introduce an additional metal atom. This accounts for the low yield of trinickel complexes and the common presence of dinickel species in these reactions. This structural motif has been seen before in the compound $V_2(dpa)_4$ [43].

For the following discussion of trinickel complexes, it is important to compare some previously determined trinickel chain, Ni_3^{6+}, structures with those being reported here. For this purpose, critical dimensions for two such molecules are listed in Table XLIII along with those for the new compounds **21**, **23**, and **24**.

The molecular structure of $Ni_3(PhPyF)_4(MeCN)_2(BF_4)_2$ (**21**) is shown in Figure 28. The compound crystallizes in the $I4_1/a$ space group with a C_2 axis perpendicular to the linear trinickel chain and going through the central nickel atom. The chain is wrapped by four ligands in a

transoid relationship and two MeCN molecules occupying the axial positions. The counterions are BF_4^-. The distance from the terminal nickel atom to the nitrogen atom of MeCN is 2.028(4) Å. This is relatively short compared to the Ni—N_{MeCN} distance (*ca.* 2.11 Å) in the mononuclear compound *cis*-$Ni(PhPyF)_2(MeCN)_2(BF_4)_2$ (**22**), and is indicative of a strong metal-ligand interaction. The nickel···nickel separation is slightly longer (0.04 Å) than that in $Ni_3(dpa)_4Cl_2$, but the Ni—N distances follow the same trend as those in $Ni_3(dpa)_4Cl_2$. The Ni—N distances for the central nickel atoms are considerably shorter than those for the terminal ones with average values in $Ni_3(PhPyF)_4(MeCN)_2^{2+}$ being 1.888[3] Å and 2.089[3] Å, respectively. These values are almost identical to those in $Ni_3(dpa)_4Cl_2$. This strongly suggests that they may have a similar electronic structure. Based on the earlier results for $Ni_3(dpa)_4Cl_2$, the trinickel chain in $Ni_3(PhPyF)_4(MeCN)_2^{2+}$ can be interpreted as having two five-coordinate terminal nickel atoms, each possessing two unpaired electrons while the central nickel atom is d^8, square-planar, and diamagnetic. There is probably antiferromagnetic coupling between the terminal magnetic centers, but this has not been investigated because of the low yield of compound **21.**

The core structure of $[Ni_3(PhPyF)_4Cl]Cl$, **23**, (Figure 29) reveals a linear Ni_3^{6+} chain supported by a set of four PhPyF anions. The compound crystallizes in the space group *P4/ncc* with a C_4 axis passing through the trinickel chain. There is only one Cl anion in an axial position with the distance of 2.331(5) Å to the nickel atom; the other Cl anion, required to balance the charge, is not coordinated. The ligand arrangement is quite different from that in **21**, with the ligands all pointing in the same direction. Thus, all the pyridine rings are at one end of the molecule while all the phenyl groups are at other end. Despite this, the Ni—Ni distances of 2.443(3) Å and 2.454(3) Å are not significantly different and comparable to those in **21** and $Ni_3(dpa)_4Cl_2$, suggesting an absence of direct bonding between nickel atoms. Space-filling models

of the two ends of $[Ni_3(PhPyF)_4Cl]^+$ are shown in Figure 30. It is clear that the axial Cl anion fits on the end having pyridyl ring while there is not enough space for a Cl anion at the other end because of α hydrogen atoms on the phenyl rings.

The pattern of Ni—N distances in **23** is quite different from that in $Ni_3(dpa)_4Cl_2$, $Ni_3(PhPyF)_4Cl_2$ (**24**) and $[Ni_3(PhPyF)_4(CH_3CN)_2](BF_4)_2$ (**21**). In **23** there is only one outer nickel atom that is 5-coordinate, and for that one the Ni—N distances are 2.129(7) Å. The Ni—N distances for the other 4-coordinated outer nickel atom are 1.921(6) Å, and for the center 4-coordinated nickel atom the Ni—N distance are all 1.911(7) Å. The central and the outer nickel atom devoid of axial ligation are d^8 and square-planar, and would be expected to be diamagnetic while the other outer nickel atom attached to a Cl anion should possess two unpaired electrons. This is consistent with magnetic measurement of compound **23** at room temperature, which shows a magnetic moment of 3.08 μ_B.

Compound **24**, $Ni_3(PhPyF)_4Cl_2$, crystallizes in the space group $P4_32_12$ with the entire molecule on a general position. The structure (Fig. 31) consists of two square pyramidal Ni(II) atoms at each end of the trinickel chain and one square-planar, central Ni(II) atom. The ligands are *cisoid* to each other, whereas in **21** they are *transoid*. The Ni···Ni distances are 2.5075(10) Å and 2.5027(10) Å. These values are 0.07 Å longer than those in the $Ni_3(dpa)_4Cl_2$ analogue. The Ni—N distances are similar to those in $Ni_3(PhPyF)_4(MeCN)_2^{2+}$ and $Ni_3(dpa)_4Cl_2$. Once again, the central nickel atom can be regarded as having a low-spin, square-planar geometry; while the two outer nickel atoms are in a triplet state, but because of the low yield magnetic measurements have not been made.

In all three new trinickel compounds, the PhPyF ligands are twisted. The torsion angles from one terminal nickel atom to the other terminal nickel atom range from 30 ° to 40.5 °.

Individual values are given in Table XLIII. The compounds with the smaller torsion angles of 30° are $(TBA)_2Ni_3(BPAP)_4$[34] and **23**. The former does not show axial coordination while the latter has only one axial coordination site occupied. The others have two axially coordinated ligands. This is consistent with observations made on Cr_3^{6+} compounds in Chapter IV.

The structures of the mononuclear compounds **22** and **25** are given in Figure 32 and Figure 33, respectively. In the former, there are two neutral formamidines chelating the Ni atom which is also coordinated by two *cis* acetonitrile molecules. Compound **25** possesses one chelating formamidine and two Br anions creating a roughly tetrahedral environment around the nickel atom. This structure is reminiscent of that of $Co(Hdpa)Cl_2$.[44]

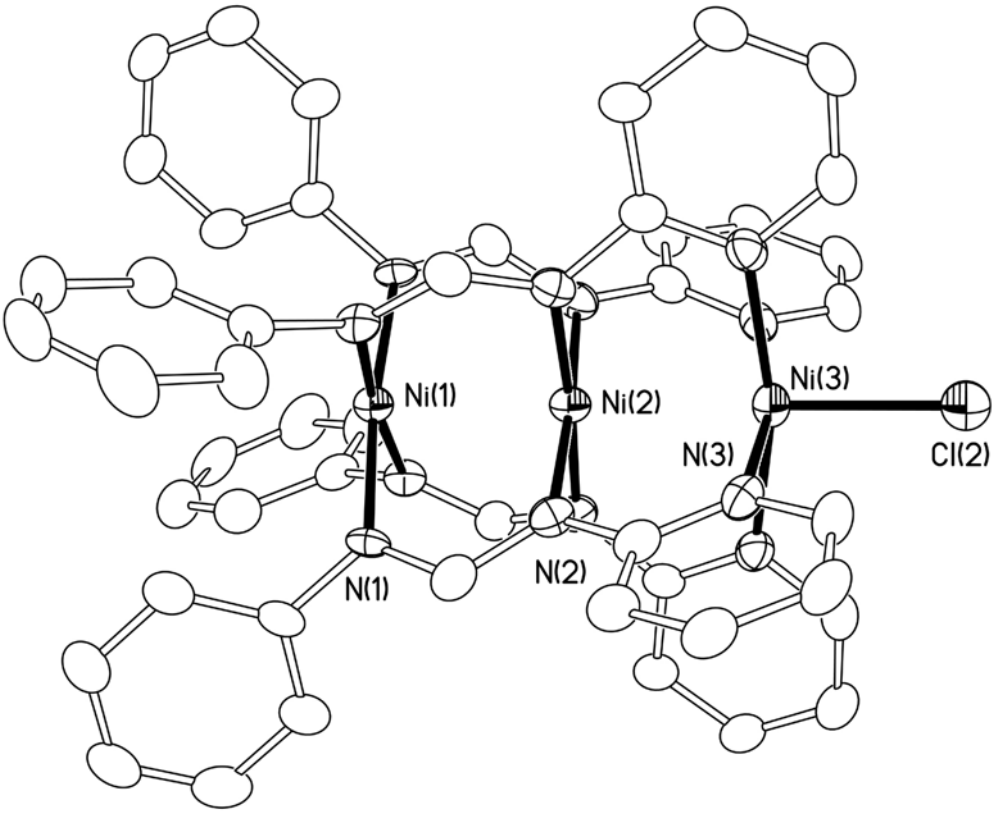

Figure 29. A drawing of the cation $Ni_3(PhPyF)_4Cl^+$ in **23** showing a vacant axial site. Ellipsoids are drawn at the 45% probability level and hydrogen atoms are omitted.

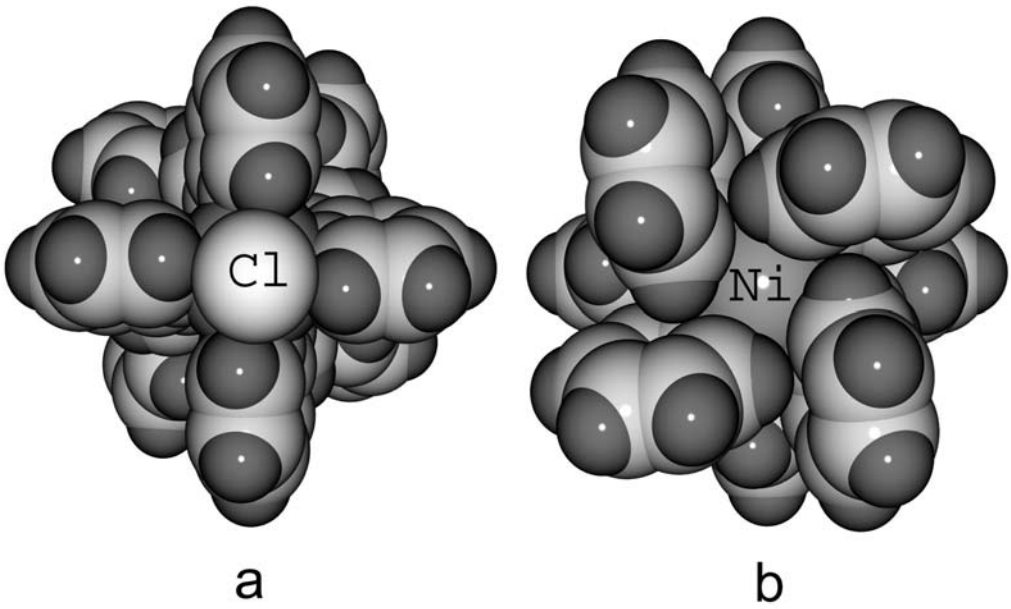

Figure 30. Space-filling models showing the two ends of $[Ni_3(PhPyF)_4Cl]^+$ in **23**. Note that the α-hydrogen atoms of the phenyl rings in **b** obstruct the possible approach of a Cl anion forcing an empty axial site.

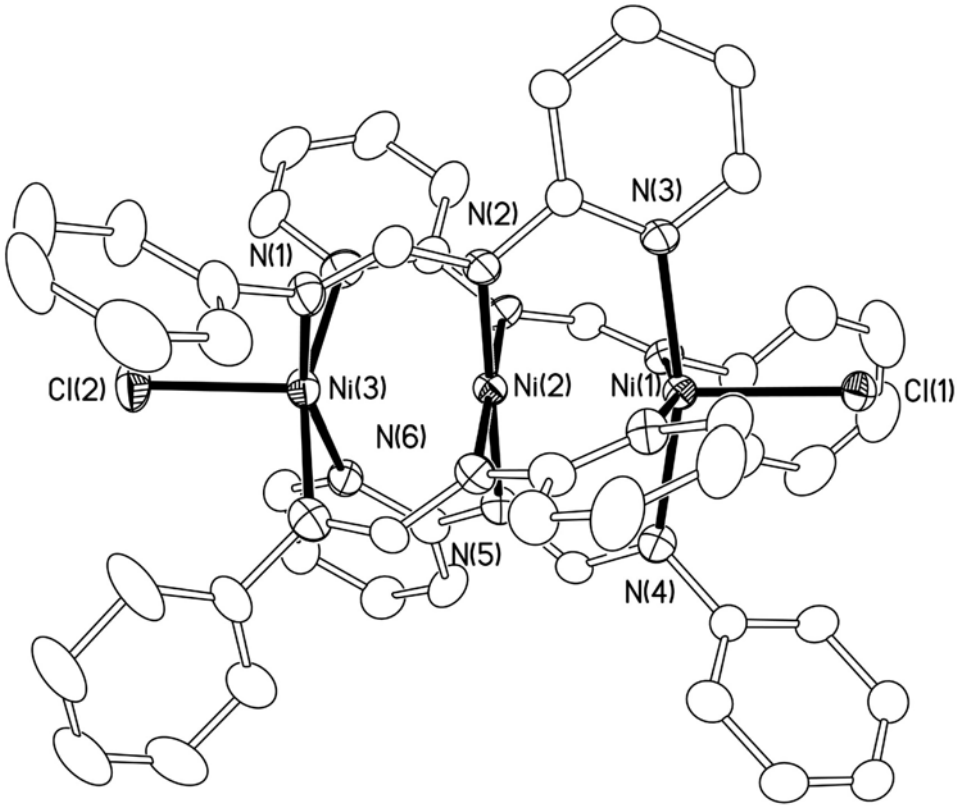

Figure 31. A drawing of the molecular structure of $Ni_3(PhPyF)_4Cl_2$ (**24**). Ellipsoids are drawn at 45% probability level with hydrogen atoms omitted for clarity.

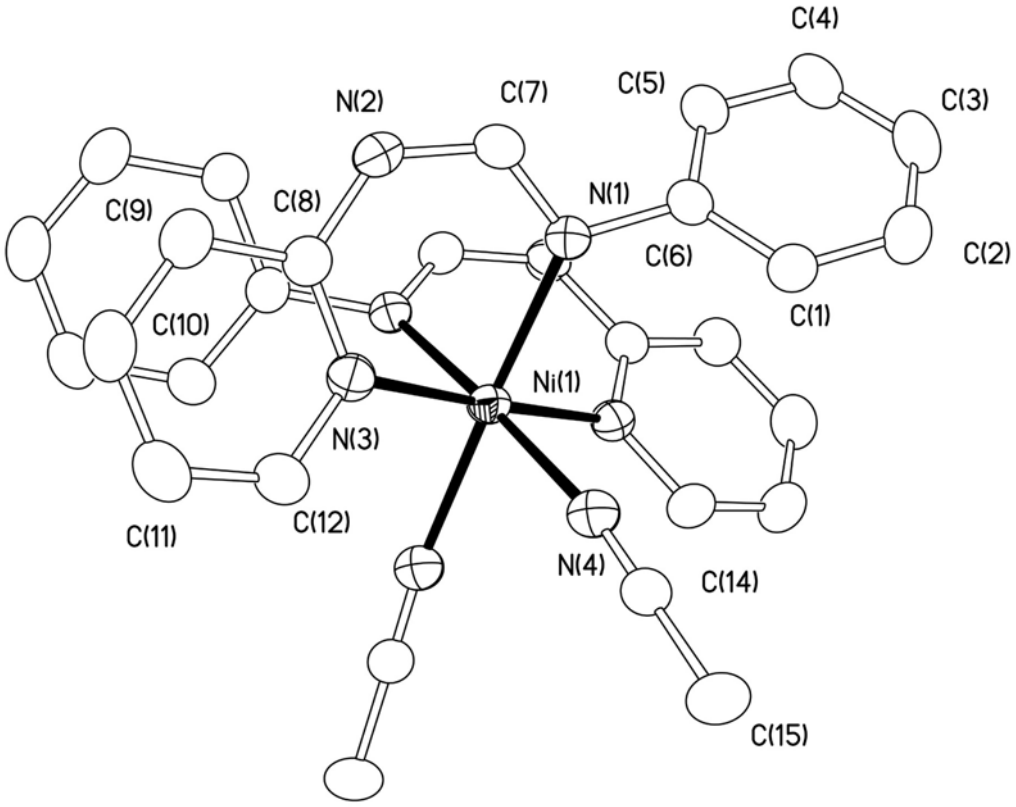

Figure 32. A drawing of the cation in **22** with ellipsoids drawn at the 45% probability level. Hydrogen atoms are omitted.

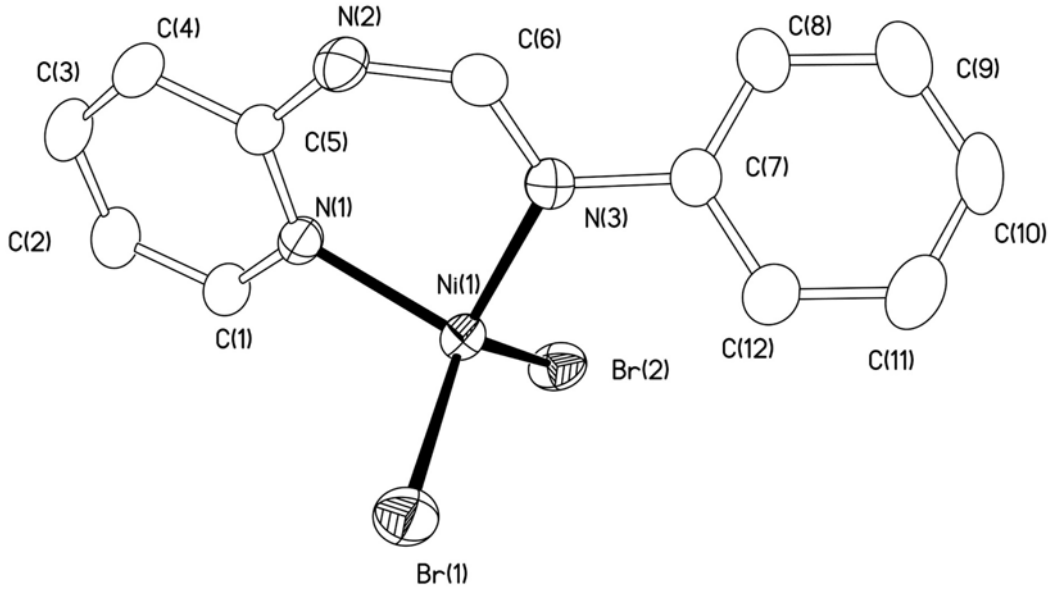

Figure 33. The molecular structure of Ni(HPhPyF)Br_2 (**25**) showing the pseudo tetrahedral environment. Ellipsoids are drawn at the 45% probability level with hydrogen atoms omitted.

CHAPTER VI

CONCLUSIONS

In this dissertation, we have presented an in depth exploration of syntheses and characterizations of a number of linear trimetal (chromium and nickel) complexes with different types of tridentate ligands. Those ligands include 2,6-bisphenylaminopyridine and a set of unsymmetrical formamidines with different organic substituents ranging from strong electron-donating groups, such as $-OCH_3$, to electron-withdrawing groups, e.g., F.

In case of 2,6-bisphenylaminopyridine, It has been shown that the potentially tridentate ligands, $BPAP^{2-}$, can do two things: (1) remain as $HBPAP^-$ and bind only a pair of metal ions (Cr_2^{4+}, Mo_2^{2+}) locked into a strong quadruply-bonded pair, or (2) support a chain of three metal ions (Cr_3^{6+}, Ni_3^{6+}). In the first case, what distinguishes $M_2(HBPAP)_4$ compounds from previous cases where potentially tridentate ligands have formed only binuclear compounds (for example $Cr_2(DPhIP)_4$ and $Cr_2(dpa)_4$) is that in the $M_2(HBPAP)_4$ compounds there are no significant axial interactions to cause lengthening of the M_2 bond. Importantly, an upfield displacement caused by the magnetic anisotropy of the quadruple bonds was observed for this first time in the NMR spectra of compounds **1** and **2**. In the case of the $M_3(BPAP)_4^{2-}$ ions, there are, again, no axial interactions because these anionic species do not attract ligands. This results in their having different properties from the $M_3(dpa)_4X_2$ molecules. Most notably, the $Ni_3(BPAP)_4^{2-}$ ion is diamagnetic and all three nickel ions can be described as square-planar, low-spin Ni^{II} centers.

In Chapter II, a reliable methodology to prepare unsymmetrical formamidines with excellent yields and easy separation has been established. This provides new opportunities for further investigation of the interesting behavior of linear trimetal chain complexes.

Results of a series of trichromium compounds with unsymmetrical formamidines shows that the unsymmetrical formamidines tend to support a symmetrical trichromium chain with Cr–Cr distances of *ca.* 2.46 Å and Cr–Cl distances of *ca.* 2.49 Å. Almost all other linear trichromium complexes with different wrapping ligands and various axial ligand are unsymmetrical. The bonding interactions in those unsymmetrical trichromium compounds can be regarded as having two of the chromium atoms paired by a quadruple bond with short distance while an isolated chromium center is at a longer distance from the central chromium atom. The most striking difference from the compounds reported earlier lies in that the separation between terminal chromium atoms in Cr_3(unsymmetrical-formamidine)$_4Cl_2$ is significantly longer (*ca.* 0.15 - 0.25 Å). Moreover, different substituents have no noticeable influence on Cr–Cr distances in the symmetrical chain, neither shorting nor elongating the distances.

Where the magnetic measurements have been made, it can also be concluded that the molecules with a linear trichromium chain have four unpaired electrons, whether the Cr_3^{6+} chain is symmetrical or unsymmetrical and regardless of any other molecular dimensions.

The selection of the new tridentate ligands in this dissertation was originally made to to address the issue of the existence of torsion angles observed in all known $M_3(dpa)_4X_2$ complexes, which is believed to be a result of the repulsion between two β-hydrogen atoms on the pyridine rings (shown in Figure 2, Chapter I). Structural studies of all the trichromium complexes reported here suggest that the torsion angle are not simply driven by the H···H repulsion. A comparison between trichromium compounds with unsymmetrical formamidines and $[Cr_3(DpyF)_4](PF_6)_2$, which has not torsion angle at all, indicate that axial Cl anions make an important contribution toward torsion angle in Cr_3(unsymmetrical-formamidine)$_4Cl_2$, also contribute to the elongated $Cr_{terminal}\cdots Cr_{terminal}$ distance.

It was a surprise that preparation of trinickel compounds with unsymmetrical formamidines proved to be very difficult. Nevertheless, the existence of these compounds of structural interest has been established.

REFERENCES

(1) Cotton, F. A.; Walton, R. A. *Multiple Bonds Between Metal Atoms*, 2nd ed., Oxford University Press, Oxford, UK, 1993.

(2) See, for example: (a) Cotton, F. A.; Daniels, L. M.; Murillo, C. A.; Wang, X. *Chem. Commun.* **1998** 39. (b) Clérac, R.; Cotton, F. A.; Daniels, L. M.; Dunbar, K. R.; Murillo, C. A.; Pascual, I. *Inorg. Chem.* **2000** *39* 752. (c) Clérac, R.; Cotton, F. A.; Daniels, L. M.; Dunbar, K. R.; Lu, T.; Murillo, C. A.; Wang, X. *J. Am. Chem. Soc.* **2000** *122* 2272. (d) Clérac, R.; Cotton, F. A.; Daniels, L. M.; Dunbar, K. R.; Murillo, C. A.; Wang, X. *J. Chem. Soc., Dalton Trans.* **2001** 386. (e) Shieh, S. -J.; Chou, C. -C.; Lee, G. H.; Wang, C. -C.; Peng, S. -M. *Angew. Chem. Int. Ed. Engl.* **1997** *36* 56. (f) Lai, S. -Y.; Lin, W. -T.; Chen, Y. -H;.Wang, C. -C.; Lee, G. -H.; Yang, M. -H., Leung, M. -K., Peng, S. -M. *J. Am. Chem. Soc*. **1999** *121* 250.

(3) (a) Cotton, F. A.; Daniels, L. M.; Murillo, C. A.; Pascual, I. *J. Am. Chem. Soc.* **1997** *119* 10223. (b) Clérac, R.; Cotton, F. A.; Dunbar, K. R.; Murillo, C. A.; Pascual, I, *Inorg. Chem.* **2000** *39* 748.

(4) (a) Yang, E. -C.; Cheng, M. -C.; Tsai, M., Peng, S. -M. *J. Chem. Soc. Chem. Commun.* **1994** 2377. (b) Cotton, F. A.; Daniels, L. M.; Jordan IV, G. T.; Murillo, C. A. *J. Am. Chem. Soc.* **1997** *119* 10377. (c) Clérac, R.; Cotton, F. A. Daniels, L. M.; Dunbar, K. R.; Kirschbaum, K.; Murillo, C. A;. Pinkerton, A. A.; Schultz, A. J.; Wang, X. *J. Am. Chem. Soc.* **2000** *122* 6226.

(5) (a) Hurley, T. J.; Robinson, M. A. *Inorg. Chem*. **1968** *7* 33. (b) Adulchecha, S.; Hathaway, B. J. *J. Chem. Soc., Dalton Trans.* **1991** 993. (c) Clérac, R.; Cotton, F. A.; Daniels, L. M.; Dunbar, K. R.; Murillo, C. A.; Pascual, I.; Wang, X. *Inorg. Chem.* **1999** *38* 2655.

(6) (a) Wu, L. -P.; Field, P.; Morrissey, T.; Murphy, C.; Nagle, P.; Hathaway, B.; Simmons, C.; Thornton, P. J. *J. Chem. Soc., Dalton Trans.* **1990** 3835. (b) Berry, J. F.; Cotton, F. A.; Lei, P.; Murillo, C. A. *Inorg. Chem.* **2003** *42* 377.

(7) Sheu, J. -T.; Lin, C. -C.; Chao, I.; Wang, C. -C.; Peng, S. -M. *Chem. Commun.* **1996** 315.

(8) Clérac, R.; Cotton, F. A.; Jeffery, S. P.; Murillo, C. A.; Wang, X. *Inorg. Chem.* **2001,** *40*, 1265.

(9) Cotton, F.A.; Murillo, C.A.; Wang, X. *J. Chem. Soc., Dalton Trans.* **1999** 3327.

(10) Clérac, R; Cotton, F. A.; Dunbar, K. R.; Lu, T.; Murillo, C. A.; Wang, X. *Inorg. Chem.* **2000**, *39*, 3065.

(11) Okafor, C. O. *J. Heterocyl. Chem.* **1976**, *13*, 107.

(12) (a) Wang, C. -C.; Lo, W. -C.; Chou, C. -C.; Lee, G. H.; Chen, J. -M.; Peng, S. -M. *Inorg. Chem.* **1998,** *37* 4059. (b) Lai, S. -Y.; Wang, C. -C.; Chen, Y. H.; Lee, C. -C.; Liu, Y. -H.; Peng, S. -M.; *J. Chin. Chem. Soc. (Taipei)* **1999**,*46*, 477. (c) Peng, S. -M., Wang, C. -C.; Jang, Y. -L.; Chen, Y. -H.; Li, F. -Y.; Mou, C. -Y.; Leung, M. -K. *J. Magn. Magn. Mater.* **2000**, *209*, 80.

(13) Berry, J. F.; Cotton, F. A.; Daniels, L. M.; Murillo, C. A. *J. Am. Chem. Soc.* **2002**, *124* 3212.

(14) Cotton, F. A.; Daniels, L. M.; Murillo, C. A.; Pascual, I.; Zhou, H. *J. Am. Chem. Soc*. **1999**, *121*, 6856.

(15) Cotton, F. A.; Norman, Jr. J. G. *J. Coord. Chem.,* **1971**, *1*, 161.

(16) Klinga, M.; Polama M.; Leskela, M. *Acta Cryst*., **1994**, *C50*, 2051.

(17) Pflugrath, J.; Messerschmitt, A., *MADNES*, Munich Area Detecor (New EEC) System, Version EEC 11/1/89, with enhancement by Enraf-Nonius Corp.: Deft, The Netherlands. A description of MADNES appears in: Messerschmitt, A.; Pflugrath, J., *J. Appl. Crystallogr.* **1987**, *20*, 306.

(18) *SMART V5.05 Software for the CCD Detector System*; Bruker Analytical X-ray Systems, Inc.: Madison, WI, 1998.

(19) *SAINTPLUS V5.05 Software for the CCD Detector System*; Bruker Analytical X-ray Systems, Inc.: Madison, WI, 1998.

(20) *SADABS.* Program for absorption correction using SMART CCD based on the method of Blessing appears in: Blessing, R. H. *Acta Crystallogr.* **1995**, *A51*, 33.

(21) Sheldrick, G. M. *Acta Crystallogr.* **1990**, *A46*, 467.

(22) $R1 = \Sigma||F_o|-|F_c||/\Sigma|F_o|$; $wR2 = [\Sigma[w(F_o^2-F_c^2)^2]/\Sigma w(F_o^2)^2]^{1/2}$, $w = 1/[\sigma^2(F_o^2) + (aP)^2 + bP]$, where $P = [\max(0 \text{ or } F_o^2) + 2(F_c^2)]/3$.

(23) Cotton, F. A.; Niswander, R. H.; Sekutowski, J. C. *Inorg. Chem.* **1978**, *17*, 3541.

(24) Numbers within square brackets are associated with average values.

(25) Chakravarty, A. R.; Cotton, F. A.; Shamshoum, E. S. *Inorg. Chem.* **1984**, *23*, 4216.

(26) See for example: (a) Cotton, F. A.; Ren, T. *J. Am. Chem. Soc*. **1992**, *114*, 2237. (b) Lin, C.; Protasiewicz, J. D.; Smith, E. T.; Ren, T. *Inorg. Chem.* **1996**, *35*, 6422. (c) Cotton, F. A.; Daniels, L. M.; Murillo, C. A. *Angew. Chem. Int. Ed. Engl.* **1992**, *31*, 737.

(27) San Filippo, J. R. *Inorg. Chem.* **1972**, *11*, 3140.

(28) See for example: (a) Cotton, F. A.; Kitagawa, S. *Polyhedron,* **1988**, *18*, 1673. (b) Cotton, F. A.; Kitagawa, S. *Inorg. Chem.* **1987**, *26*, 3463.

(29) See for example: Chisholm, M. H.; Cotton, F. A.; Frenz, B. A.; Reichert, W. W.; Shive, L. W.; Stults, B. R. *J. Am. Chem. Soc.* **1976**, *98*, 4469.

(30) Silverstein, R. M.; Bassler, G. C.; Morrill, T. C. *Spectrometric Identification of Organic Compounds*, 4th ed. John Wiley & Sons: New York, *1981*.

(31) McConnell, H. N. *J. Chem. Phys.* **1957**, *27*, 226. See also references 17-20.

(32) Furthermore, the value of $\triangle\delta$ for M_2(formamidinate)$_4$ complexes is typically obtained from the chemical shifts of the metal-metal bound complex and the analogous non-metal-metal bound Ni_2(formamidinate)$_4$ complex. So far we have been unable to prepare a nickel analog of the M_2(HBPAP)$_4$, M = Cr and Mo.

(33) Clérac, R.; Cotton, F.A.; Daniels, L.M.; Dunbar, K. R.; Murillo, C.A.; Zhou, H-C. *Inorg. Chem.* **2000**, *39,* 3414.

(34) Cotton, F.A.; Daniels, L.M.; Lei, P.; Murillo, C.A.; Wang, X. *Inorg. Chem*. **2001**, *40*, 2778.

(35) (a) Roberts, R. M. *J. Org. Chem.***1949**, 14, 277. (b) Barker, J.; Kilner, M.; *Coord. Chem. Rev.* **1994**, *133*, 219.

(36) Cotton. F.A.; Daniels, L.M.; Jordan, IV, G.T.; Murillo, C.A. *Polyhedron* **1998**, *17*, 589.

(37) Blake, A. J.; Parsons, S.; Rawson, J. M.; Winpenny, R. E. *Polyhedron* **1995**, *14*, 1895.

(38) Cotton, F. A.; Lei, P.; Murillo, C. A., Wang, L-S. *Inorg. Chim Acta.* In press.

(39) Long, G. T.; Clarke, P. J. *Inorg. Chem.* **1978**, *17*, 1394.

(40) Jarris, J. A. J.; Mais, R. H. B.; Owston, P. G. *J. Chem. Soc.* **1968,** 1473.

(41) The crystal structure of this compound showed an octahedral arrangment with two neutral HPhPyF ligands chelating to the nickel atom and two MeCN molecules *cis* to each other.

(42) Cotton, F. A.; Lei, P.; Murillo, C. A. *Inorg. Chim. Acta*. In press.

(43) Cotton, F. A.; Daniels, L. M.; Murillo, C. A.; Zhou, H. -C. *Inorg. Chim. Acta* **2000**, *305*, 69.

(44) Cotton, F. A.; Daniels, L. M.; Jordan, IV, G. T.; Murillo, C. A. *Polyhedron* **1998**, *17* 589.

APPENDIX I

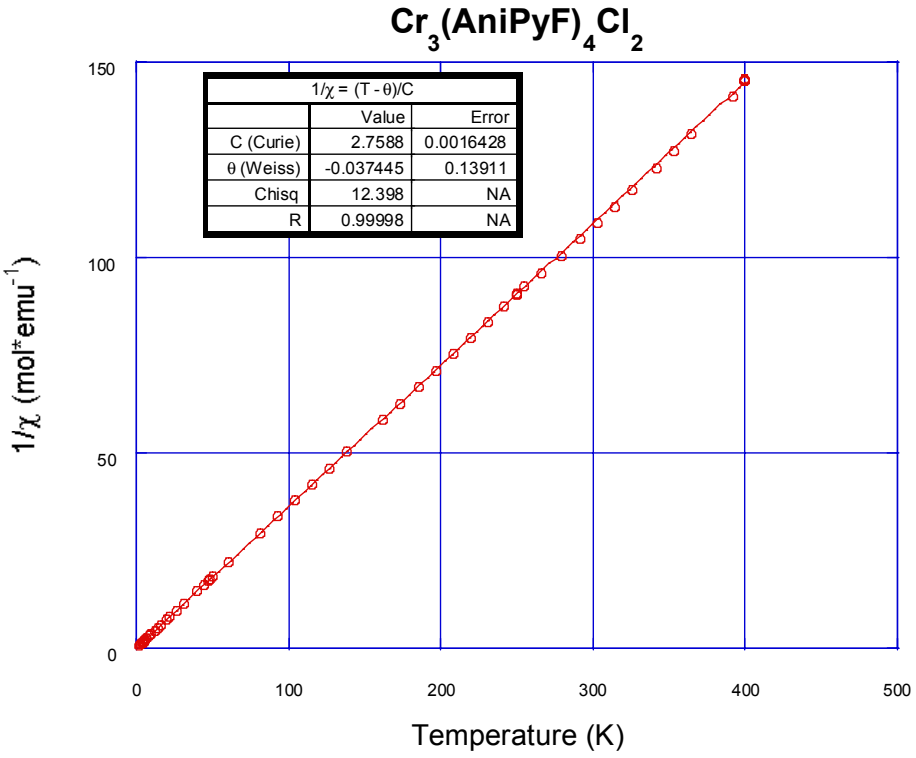
Cr3(AniPyF)4Cl2
1/χ = (T - θ)/C
Value
Error
C (Curie) 2.7588 0.0016428
θ (Weiss) -0.037445 0.13911
Chisq 12.398 NA
R 0.99998 NA
1/χ (mol*emu-1)
Temperature (K)
0
50
100
150
0
100
200
300
400
500

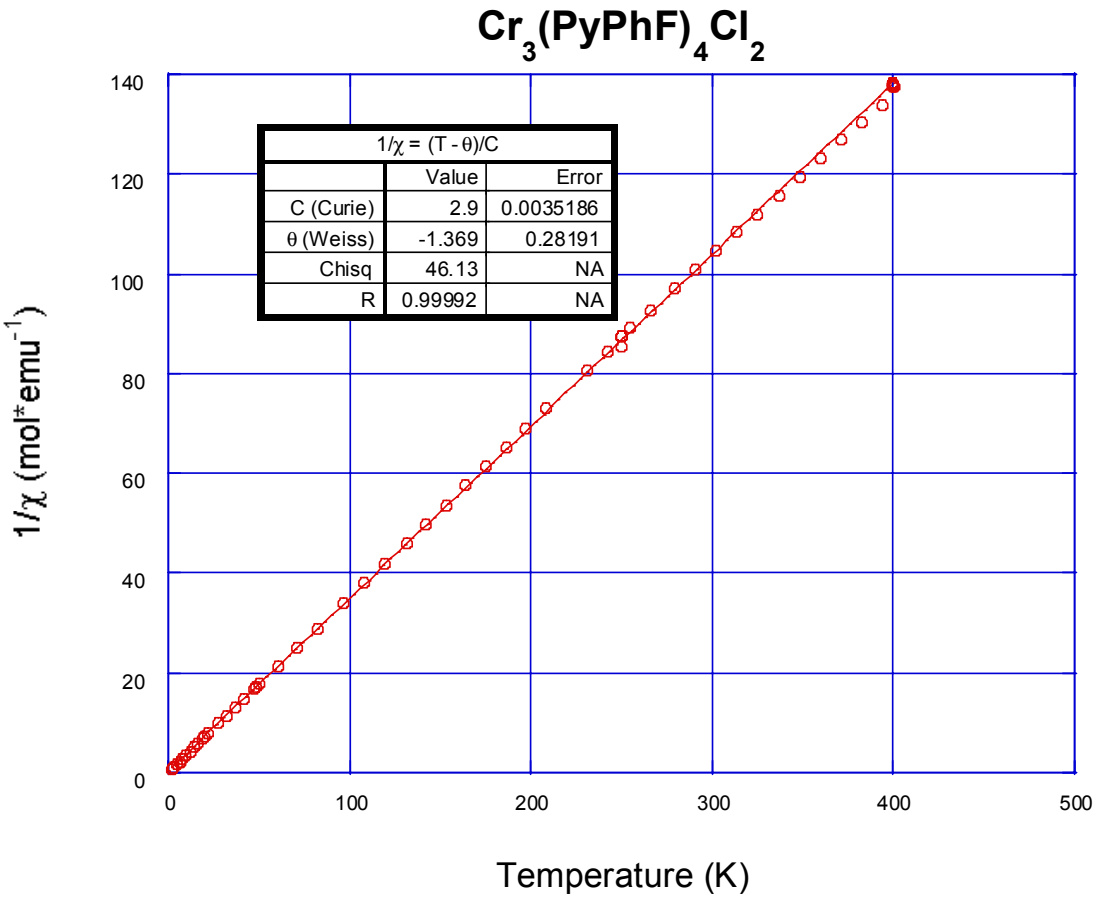
Cr3(PyPhF)4Cl2
1/χ = (T - θ)/C
Value
Error
C (Curie)
2.9
0.0035186
θ (Weiss)
-1.369
0.28191
Chisq
46.13
NA
R
0.99992
NA
1/χ (mol*emu-1)
Temperature (K)
0
20
40
60
80
100
120
140
0
100
200
300
400
500

APPENDIX II

MAGNETIC ANISOTROPY OF MULTIPLE BONDS

Circulation of electrons around a nucleus can be viewed as being similar to the flow of an electric current in an electric wire. From physics, we know that the flow of a current through a wire induces a magnetic field. In an atom, the local current generates a secondary, induced magnetic field which has a direction opposite to the applied magnetic field. The effect is called magnetic anisotropy. In multiple bonded systems, π-electrons are more polarizable than σ-bond electrons. Therefore, the field induced π-electron movement is capable of producing strong secondary fields that perturb nearby nuclei. The π-electrons associated with a benzene ring provide a striking example[1] of this phenomenon, as shown below. When benzene is placed in a magnetic field, the π electrons in the aromatic ring systems induce a magnetic field much like that generated in a loop of wire through which a current flows. This magnetic field, which is highly anisotropic, covers a spatial volume large enough that it influences the benzene hydrogen atoms as shown in Figure A-1.

The benzene hydrogen atoms are said to be **deshielded** by the magnetic anisotropy of π electrons. In the NMR spectrum, the signal of those hydrogen atoms appears at a lower field than would otherwise be expected. This kind of shift is called a **downfield** displacement. These hydrogen atoms just happen to lie in a deshielding region of the induced anisotropic field. If a hydrogen atom were placed in the center of the ring or directly above the center rather than on its periphery, it would be found to be **shielded**, since the field lines there would have the opposite

---

(1) Silverstein, R. M.; Bassler, G. C.; Morrill, T. C. *Spectrometric Identification of Organic Compounds*, 4th ed. John Wiley & Sons: New York, 1981.

direction from those at periphery. The signal of the hypothetical hydrogen atom would move to a higher field. This is called an **upfield** displacement.

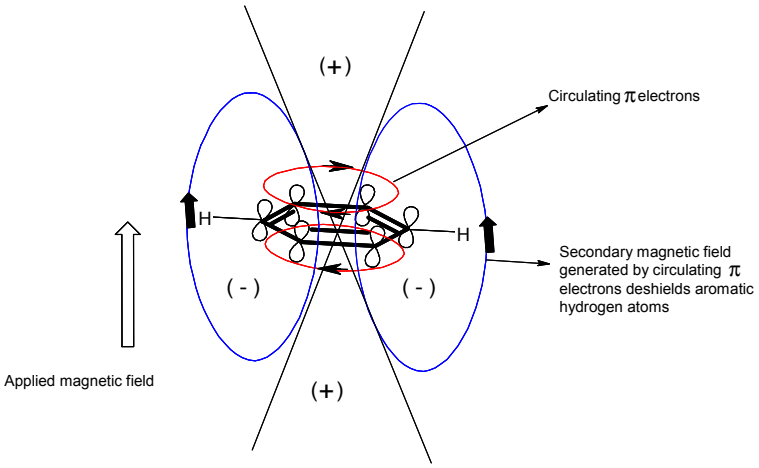

Figure A-1. Magnetic anisotrophy in benzene. Positive signs (+) indicate shielding zones; negative signs (-) indicating deshielding zones.

Another well understood example[1] is that of acetylene. In this molecule, the triple bond is along the molecular axis. When this axis is aligned with the applied magnetic field, the circulation of the π-electrons of the bond gives rise to an opposing magnetic field that has a geometry such that the acetylene hydrogen atoms are **shielded** (Figure A-2) and the NMR signal shifts **upfield**. Clearly, similar behavior should occur for quadruple bonds between metal atoms.

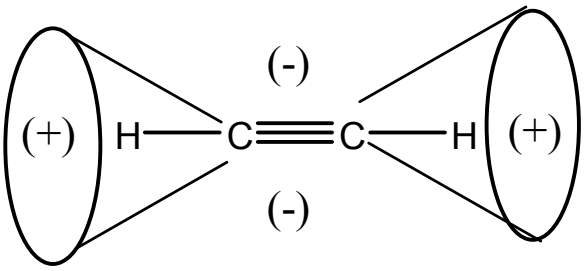

Figure A-2. Anisotropy caused by the π electrons in acetylene systems. Positive signs (+) indicate shielding zones; negative signs (-) indicating deshielding zones.

Thus one would expect hydrogen atoms above the M—M bond to be **deshielded** (e.g. the methine hydrogen atoms of a formamidinate ligand)[2] and thus shifted **downfield**, or **shielded** if they are more or less along the M—M axis, as shown schematically in Figure A-3 and thus shifted **upfield**. For $M_2(HBPAP)_4$ (Chapter II), the amine hydrogen atoms fall in the positive shielding zone, therefore, an **upfield** displacement is expected. Indeed, that is what is found.

(2) See for example: (a) Cotton, F. A.; Ren, T. *J. Am. Chem. Soc*. **1992**, *114*, 2237. (b) Lin, C.; Protasiewicz, J. D.; Smith, E. T.; Ren, T. *Inorg. Chem.* **1996**, *35*, 6422. (c) Cotton, F. A.; Daniels, L. M.; Murillo, C. A. *Angew. Chem. Int. Ed. Engl.* **1992**, *31*, 737.

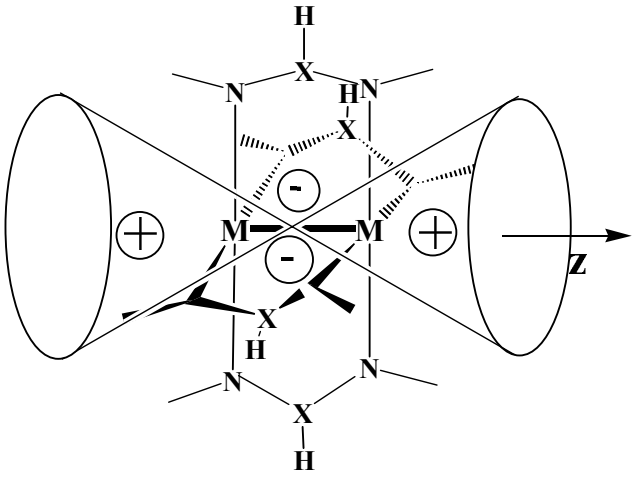

a

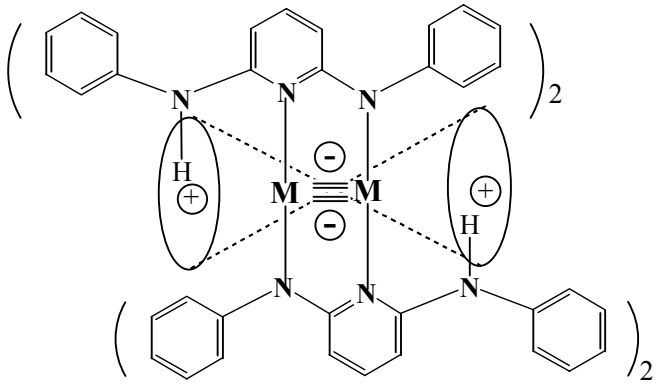

b

Figure A-3. Shielding and deshielding caused by magnetic anisotropy of the M—M multiple bond in dinuclear paddlewheel compounds. Positive signs (+) indicate shielding zones, while negative signs (-) represent deshielding zones.

APENDIX III

REASONABLE EXPLANATION FOR 4 UNPAIRED ELECTRONS IN SYMMETRICAL TRICHROMIUM

In Chapter IV, it was shown that symmetrical trichromium compounds containing unsymmetrical formamidinates have four unpaired electrons. This reason for this can be explained by a qualitative diagram of the molecular orbitals (MO) that could form in a symmetrical trichromium chain. For this situation, only the interactions of four d orbitals (d_z2, d_{xz}, d_{yz}, and d_{xy}) on each metal atom are relevant. σ MOs (bonding, nonbonding, antibonding) are formed from d_{z^2} orbitals; two mutually orthogonal sets of π MOs (bonding, nonbonding, antibonding) are formed from d_{yz}, and d_{xz}. Since the Cr—Cr distances are long, it is pretty reasonable to say there are no δ interactions between those chromium atoms. Therefore, the d_{xy} orbitals on each metal atom should give rise to three degenerate MOs, which should be at the same energy level as the π nonbonding MOs are. The interaction of axial chlorine atoms with trimetal chain is significant. The π interactions are probably less important than σ interaction. The lone pairs on Cl^- are of the proper symmetry to interact with the σ MOs, and make the σ nonbonding orbital higher in energy than the rest of the nonbonding sets (π and 3 d_{xy} orbitals). Thus, the qualitative MO diagram shown in Figure A-4 is obtained.

Totally there are 12 valence electrons on three Cr^{2+} ions. Six of them fill the σ and π bonding orbitals; the remaining six electrons have five orbitals to fill: three δ orbitals and two π nonbonding orbitals. Following Hund's rule, this leads to four unpaired electrons as shown in Figure A-4.

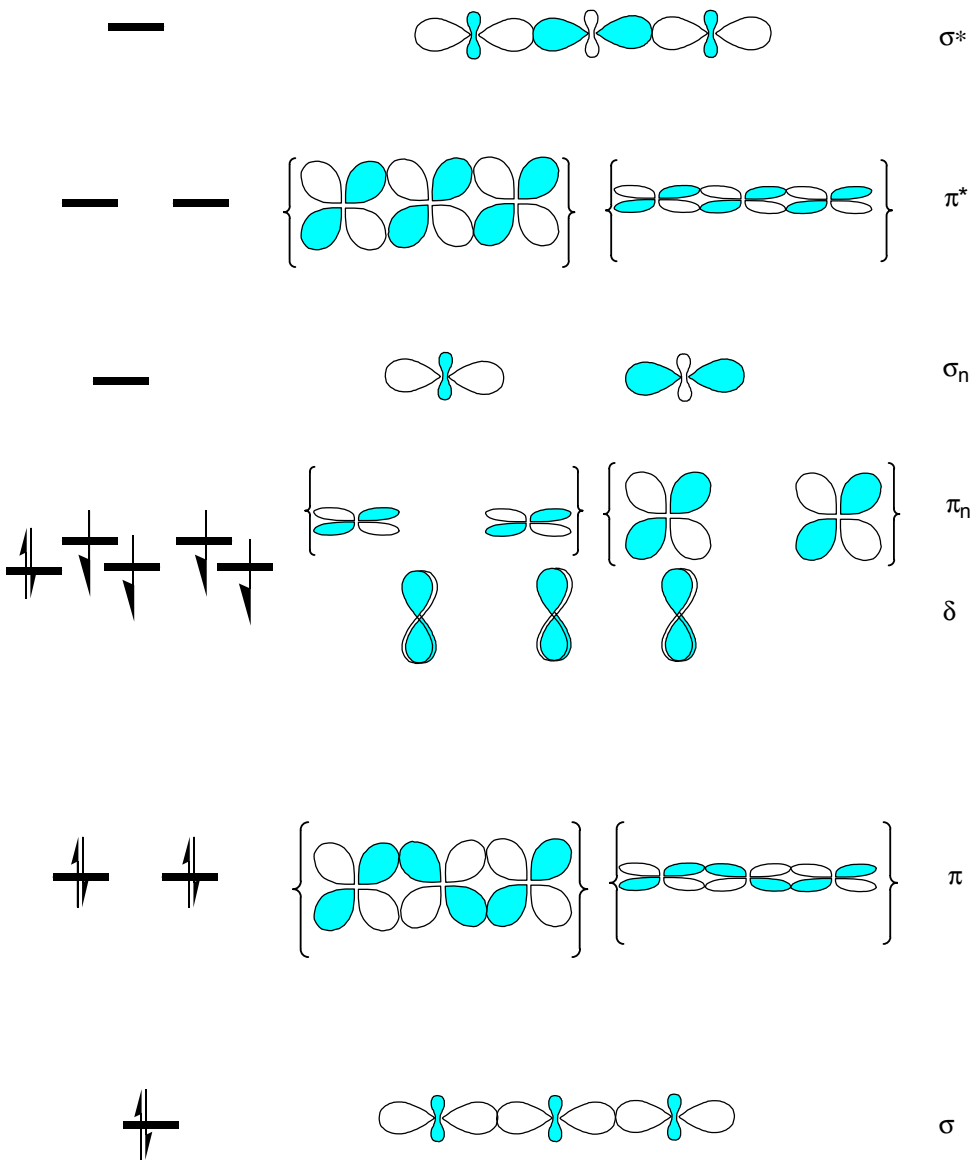

Figure A-4. A qualitative MO diagram that explains why there are four unpaired electrons in the symmetrical trichromium chains discussed in Chapter IV.

APPENDIX IV

REASON FOR THE SHRINKING OF Ni—Ni SEPARATION IN $Ni_3(dpa)_4(PF_6)_3$

It has been found that $Ni_3(dpa)_4Cl_2$ (**A**) can be oxidized by $AgPF_6$ to form $Ni_3(dpa)_4(PF_6)_3$ (**B**). In this process there is a significant change in metal—metal distances which change from 2.43 Å in **A** to 2.28 Å in **B**.[3] In general, when an electron is removed from two independent, positively charged units (e.g. Ni^{2+}), one would expect the separations of those two units (e.g. Ni—Ni distance) to become longer since electrostatic repulsions are greater because of the additional positive charge. This, however, is not what happens upon oxidation of **A** to **B**. The reason for the shorter Ni—Ni separations is the formation of three-center metal-metal bonding with a formal bond order of 0.5 in the oxidized species (**B**) while there is no bonding between metal atoms in **A**. Bonding between the metal atoms can arise only from the overlaps of symmetry-matched orbitals. Thus, the three d_{z^2} orbitals can combine to form the typical three-center pattern of bonding, nonbonding, and antibonding three-center molecular orbitals, somewhat perturbed by interaction with the σ lone pairs on the axial position. In a similar way the three d_{xz}, the three d_{yz}, and the three d_{xy} orbitals would all combine into bonding, nonbonding, and antibonding MOs. Overall there would be four bonding, four nonbonding, and four antibonding orbitals. Three Ni^{2+} ions in **A** have 24 electrons. Thus there are 12 electrons pairs to fill 12 MOs, and there would be no net bonding. This is consistent with the magnetic susceptibility at 5 K.[4] However, **A** has four unpaired electrons at room temperature.[4] The right way to view the electronic structure of **A**[4] is that the central

---

(3) Berry, J. F.; Cotton, F. A.; Daniels, L. M.; Murillo, C. A. *J. Am. Chem. Soc.* **2002**, *124* 3212.

(4) Clérac, R.; Cotton, F. A.; Daniels, L. M.; Dunbar, K. R.; Murillo, C. A.; Pascual, I.; Wang, X. Inorg. Chem. **1999** *38* 2655.

nickel(II) atom central nickel atoms is in a square planar ligand field that results in a low-spin state. Each of the two outer nickel(II) atoms has two unpaired electrons, and there is antiferromagnetic coupling between them that leads to a temperature-dependant magnetic moment. This formulation of the electronic structure leads to the conclusion that there is no net nickel-nickel bonding, consistent with the relatively long Ni—Ni separations of 2.43 Å. There is not believed to be any electron delocalization over the Ni_3 chain in **A**. In **B**, the Ni_3^{7+} unit possess a total of 23 valence electrons, and it is believed that there is now a delocalized electronic structure with 8 electrons filling bonding MOs, 8 electrons for the four nonbonding MOs, but only 7 electrons to fill antibonding orbitals. The result is the formation of three-center metal-metal bonding and a formal bond order of 0.5 as shown in Figure A-5.

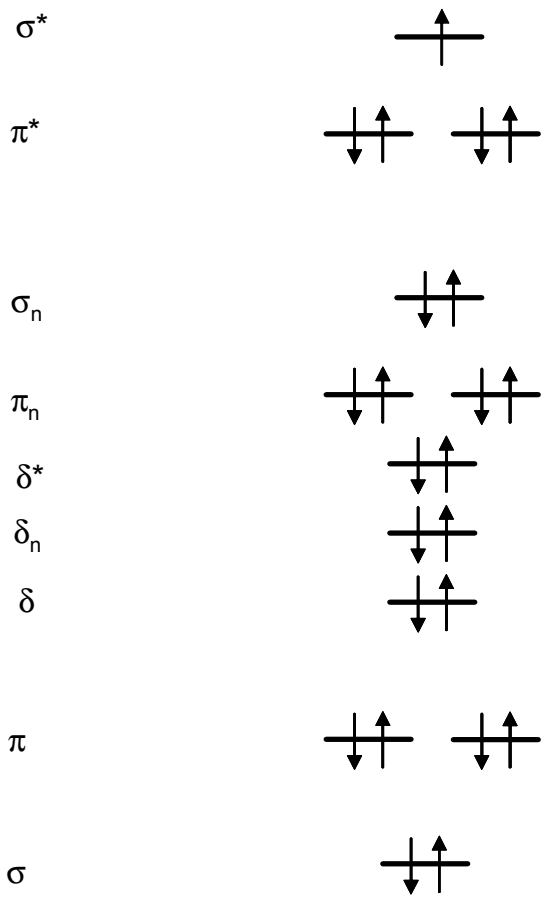

$Ni_3(dpa)_4(PF_6)_3$

Figure A-5. Qualitative MO diagram for **B**, $Ni_3(dpa)_4(PF_6)_3$, showing the absence of an electron from the σ antibonding orbital.

VITA

Peng Lei was born on October 30, 1971 in Hunan, China. He went to Central South University of Technology in Changsha to study chemistry in September, 1990. After receiving his B.S. degree in chemistry in July, 1994, he began work on his M.S. degree in September under the direction of Professor Xinlan Chen at Wuhan University.

He received his M.S. degree in chemistry in July, 1997, then he move back to Huan, and worked as a synthetic chemist at Hunan Chemical Research Institute. He synthesized 15 new compounds for bioassay for potential herbicides in his 10 months at that institute.

In 1998, he was accepted by Professor F. A. Cotton at Texas A&M University and started his Ph.D. studies in Inorganic Chemistry in June at College Station, TX. He received his Ph.D. degree in May, 2003. He can be reached at the following address:

399 Middle HuRong Road
Hunan Chemical Research Institute
Changsha, Hunan 410007
P. R. China